CONCEPTUAL DESIGN STUDIES OF A MONO TILTROTOR (MTR) ARCHITECTURE

J. Gordon Leishman* and Robin Preator†
Department of Aerospace Engineering
Glenn L. Martin Institute of Technology
University of Maryland
College Park
Maryland 20742

G. Douglas Baldwin‡
Baldwin Technology Company, LLC
Port Washington
New York 11050

Final Report under Contract:
Mono Tiltrotor (MTR) Studies
Contract Number N00014-03-C-0531
Office of Naval Research
Arlington, VA.

December 10, 2004.

*Principal Investigator. Martin Chair of Engineering and Professor of Aerospace Engineering.
†Graduate Research Assistant.
‡Managing Director.

REPORT DOCUMENTATION PAGE

Form Approved
OMB No. 0704-0188

Public reporting burden for this collection of information is estimated to average 1 hour per response, including the time for reviewing instructions, searching existing data sources, gathering and maintaining the data needed, and completing and reviewing this collection of information. Send comments regarding this burden estimate or any other aspect of this collection of information, including suggestions for reducing this burden to Department of Defense, Washington Headquarters Services, Directorate for Information Operations and Reports (0704-0188), 1215 Jefferson Davis Highway, Suite 1204, Arlington, VA 22202-4302. Respondents should be aware that notwithstanding any other provision of law, no person shall be subject to any penalty for failing to comply with a collection of information if it does not display a currently valid OMB control number. **PLEASE DO NOT RETURN YOUR FORM TO THE ABOVE ADDRESS.**

1. REPORT DATE *(DD-MM-YYYY)*
10-12-2004

2. REPORT TYPE
Final Scientific Report

3. DATES COVERED *(From - To)*
21 NOV 2003 - 10 DEC 2004

4. TITLE AND SUBTITLE

Conceptual Design Studies of a Mono Tiltrotor (MTR) Architecture

5a. CONTRACT NUMBER
N00014-03-C-0531

5b. GRANT NUMBER

5c. PROGRAM ELEMENT NUMBER

6. AUTHOR(S)

LEISHMAN, J. Gordon; PREATOR, Robin; BALDWIN, G. Douglas

5d. PROJECT NUMBER

5e. TASK NUMBER

5f. WORK UNIT NUMBER

7. PERFORMING ORGANIZATION NAME(S) AND ADDRESS(ES)

Department of Aerospace Engineering
Glenn L. Martin Institute of Technology
University of Maryland
College Park, MD 20742

Baldwin Technology Company, LLC
4 Harbor View Road
Port Washington, NY 11050

8. PERFORMING ORGANIZATION REPORT NUMBER

9. SPONSORING / MONITORING AGENCY NAME(S) AND ADDRESS(ES)
Office of Naval Research
ONR Code 36; ExLog FNC IPT
Ballston Centre Tower One
800 North Quincy Street
Arlington, VA 22217-5660

10. SPONSOR/MONITOR'S ACRONYM(S)
ONR

11. SPONSOR/MONITOR'S REPORT NUMBER(S)

12. DISTRIBUTION / AVAILABILITY STATEMENT

Approved for public release; distribution is unlimited.

13. SUPPLEMENTARY NOTES

14. ABSTRACT

The Mono Tiltrotor (MTR) is a proposed, innovative heavy-lift rotorcraft architecture. The emerging military strategies most suited to potential application of the MTR are Navy Sea Basing with Ship to Objective Maneuver, and Army Future Combat Systems with mounted maneuver and air mobility. The present work reports on a conceptual design study that has been conducted to predict the sizes and weights of the MTR architecture and to objectively examine its potential performance. A detailed weight budget has been determined based on historical component data for helicopters and airplanes. A thorough component drag breakdown has allowed for good estimates of the overall lift-to-drag ratio of the MTR concept in both the helicopter mode and airplane cruise conditions. A requirement was that the machine carry its payload over an unprecedented unrefueled distance of 1,000 nautical miles. It is shown that if technically realizable, the MTR architecture allows for a relatively compact and lightweight rotor design, with an accompanying lightweight airframe and relatively low fuel load compared to competing helicopter concepts.

15. SUBJECT TERMS
Helicopter; Rotorcraft; Tiltrotor; Seabasing; Aircraft; Innovation; Transportation; Mono Tiltrotor; MTR

16. SECURITY CLASSIFICATION OF:			17. LIMITATION OF ABSTRACT	18. NUMBER OF PAGES	19a. NAME OF RESPONSIBLE PERSON
					G. Douglas Baldwin
a. REPORT	b. ABSTRACT	c. THIS PAGE			19b. TELEPHONE NUMBER *(include area code)*
UNCLASSIFIED	UNCLASSIFIED	UNCLASSIFIED	UL	106	516-414-0700

Standard Form 298 (Rev. 8-98)
Prescribed by ANSI Std. Z39.18

Abstract

The Mono Tiltrotor (MTR) is a proposed, innovative heavy-lift rotorcraft architecture. The emerging military strategies most suited to potential application of the MTR are Navy Sea Basing with Ship to Objective Maneuver, and Army Future Combat Systems with mounted maneuver and air mobility. The capabilities of the MTR are predicated on the combination of an advanced coaxial rotor system and sophisticated kinematics that morph the aircraft topology for efficient flight over the entire operational envelope. The MTR rotorcraft integrates a coaxial rotor, a folding lifting wing system, a lightweight airframe and an efficient cargo handling system that is capable of rapidly and economically transporting different types of mission tailored payloads. The present work reports on a conceptual design study that has been conducted to predict the sizes and weights of the MTR architecture and to objectively examine its potential performance. A detailed weight budget has been determined based on historical component data for helicopters and airplanes. A thorough component drag breakdown has allowed for good estimates of the overall lift-to-drag ratio of the MTR concept in both the helicopter mode and airplane cruise conditions. Various sizes of MTR have been examined, ranging from small machines with relatively light payloads of less than 5 tons to large heavy-lifters with payloads of 20 tons or more. A requirement was that the machine carry its payload over an unprecedented unrefueled distance of 1,000 nautical miles. The ability to morph the MTR so that its lift is created by a fixed wing when in cruising flight gives the machine a relatively high lift-to-drag ratio of about 14, good specific fuel consumption, and excellent net vehicle transportation efficiency in terms of payload carried per unit of fuel expended. It is shown that if technically realizable, the MTR architecture allows for a relatively compact and lightweight rotor design, with an accompanying lightweight airframe and relatively low fuel load compared to competing helicopter concepts. The results also show that structural weight efficiency is one key to the potential value of the MTR vehicle.

Contents

Abstract **2**

List of Principal Symbols **9**

1 Introduction **13**

2 Development of Methodology **17**

2.1 General Performance & Sizing Analysis 19

2.1.1 Takeoff Weight & Energy Efficiency 20

2.1.2 Main Rotor Sizing Equations 23

2.1.3 Tail Rotor Sizing Equations 25

2.1.4 Power Requirements in Cruise Flight 26

2.1.5 MTR Specific Sizing Equations 28

2.2 Component Weights 29

2.2.1 Rotor Weights 30

2.2.2 Transmission Weights 32

2.2.3 Rotor Control Weights 33

2.2.4 Airframe Weights 34

2.2.5 Fuselage Weights 34

2.2.6 MTR Container Handling System Weight 35

2.2.7 Suspension Structure Weight 35

2.2.8 Crew Compartment and Furnishings Weight 35

2.2.9 MTR Tilt Boom & Actuator Weights 36

2.2.10 Empennage Weights 36

2.2.11 MTR Wing Weights 37

2.2.12 Power Plant & Fuel System Weights 37

2.2.13 Electrical System Weight 38

2.2.14 Landing Gear Weight 38

2.2.15 Ground Handling Equipment Weight 39

2.3 MTR Mission Model 39

2.3.1 Mission Profiles 39

2.3.2 Detailed Fuel Burn Calculation 41

3 Application of Methodology **47**
3.1 Single Rotor Helicopter 47
3.2 Coaxial Dual Rotor Helicopter 54
3.3 Ultra-Long Range Heavy-Lift Helicopter 60
3.4 Performance of MTR Architecture 62
3.5 Vehicle Efficiency 70
3.6 Payload–Range Performance 72

4 Refined Aerodynamic Analysis **75**
4.1 Component Drag Breakdown 75
4.2 Lift-to-Drag Ratio Estimation 78
4.3 Revised Wing Sizing Methodology 80
4.3.1 Determination of Wing Area 81
4.3.2 Determination of Wing Aspect Ratio 81

5 Mission Profile Trade Studies **83**
5.1 Destination Hover Time 84
5.2 Takeoff Density Altitude 85
5.3 Cruise Density Altitude 88

6 MTR Design Optimization & Performance **90**
6.1 Determination of Cruise Speed 92
6.2 Engine Selection 92
6.3 MTR Point Design Summary 93
6.4 MTR Performance 96

7 Conclusions **99**

8 Acknowledgements **101**

Appendix 1: Correlation Coefficients for Performance Equations **104**

Appendix 2: Correlation Coefficients for Weight Equations **105**

List of Figures

1 Conceptual sketch of the MTR transitioning from being at rest on the ground to hovering over a container, then morphing from helicopter mode to airplane mode. . 14
2 Conceptual sketch of the MTR operating in helicopter mode picking up a standardized cargo container. 15
3 Conceptual sketch of the MTR with payload operating in cruise mode with wing deployed. 15
4 Flowchart of the conceptual rotorcraft design analysis. 18
5 Empty weight fraction versus vehicle gross weight for helicopters and conventional tiltrotors. 20
6 Hovering figure of merit of coaxial rotor design showing the effect of rotor-on-rotor interference. 25
7 Component breakdown of the MTR architecture. 30
8 MTR Long-range cruise mission profile. 39
9 MTR radius of action mission profile. 40
10 MTR helicopter pickup mission profile. 40
11 Predicted main rotor diameter versus payload for single rotor helicopters. 48
12 Predicted gross takeoff weight versus payload for single rotor helicopters. 48
13 Predicted empty weight versus payload for single rotor helicopters. 49
14 Predicted power requirements versus payload for single rotor helicopters. 50
15 Predicted blade weights versus payload for single rotor helicopters. 51
16 Predicted hub weights versus payload for single rotor helicopters. 51
17 Predicted transmission weights versus payload for single rotor helicopters. 52
18 Predicted engine weights versus payload for the single rotor helicopters. 53
19 Predicted fuselage weight versus payload for single rotor helicopters. 53
20 Predicted rotor diameter versus payload for coaxial dual rotor helicopters. 55
21 Predicted gross takeoff weight versus payload for coaxial dual rotor helicopters. . . 56
22 Predicted empty weight versus payload for coaxial dual rotor helicopters. 57
23 Predicted power requirements versus payload for coaxial dual rotor helicopters. . . 57
24 Predicted blade weights versus payload for the coaxial dual rotor helicopters. . . . 58
25 Predicted hub weights versus payload for the coaxial dual rotor helicopters. 58
26 Predicted transmission weights versus payload for the coaxial dual rotor helicopters. 59

27 Predicted engine weights versus payload for the coaxial dual rotor helicopters. . . . 59
28 Predicted fuselage weight versus payload for coaxial dual rotor helicopters. 60
29 Predicted rotor size versus payload for a single rotor helicopter with ranges of 220 nm and 1,000 nm. 61
30 Predicted takeoff weight versus payload for a single rotor helicopter with ranges of 220 nm and 1,000 nm. 62
31 Predicted fuel weight versus payload for a single rotor helicopter with ranges of 220 nm and 1,000 nm. 63
32 Predicted power requirements versus payload for a single rotor helicopter with ranges of 220 nm and 1,000 nm. 63
33 Predicted rotor size (diameter) for the MTR architecture to meet a 1,000 nm range requirement versus hypothetical conventional (single) and coaxial rotor helicopters. 65
34 Predicted gross takeoff weight for the MTR architecture to meet a 1,000 nm range requirement versus payload compared with hypothetical conventional (single) and coaxial rotor helicopters. 66
35 Predicted empty weight for the MTR architecture to meet a 1,000 nm range requirement versus payload compared with hypothetical conventional (single) and coaxial rotor helicopters. 66
36 Predicted disk loading of the MTR architecture versus historical data for conventional (single) and coaxial rotor helicopters. 67
37 Predicted power requirements for the MTR architecture to meet a 1,000 nm range requirement versus payload compared with hypothetical conventional (single) and coaxial rotor helicopters. 68
38 Predicted fuselage weight for the MTR architecture to meet a 1,000 nm range requirement versus payload compared with hypothetical conventional (single) and coaxial rotor helicopters. 69
39 Predicted rotor system weight for the MTR architecture to meet a 1,000 nm range requirement versus payload compared with hypothetical conventional (single) and coaxial rotor helicopters. 69
40 Comparison of rotor diameters for the hypothetical conventional (single) and coaxial rotor helicopters versus the MTR to meet the 1,000 nm range and 20 ton payload requirement. 70

41 Predicted weight efficiency for the MTR architecture to meet a 1,000 nm range requirement versus payload compared with hypothetical conventional (single) and coaxial rotor helicopters. 71
42 Predicted Tishchenko et al. “energy efficiency” of the MTR versus payload compared with hypothetical conventional (single) and coaxial rotor helicopters. 72
43 Predicted fuel weight for the MTR architecture to meet a 1,000 nm range requirement versus payload compared with hypothetical conventional (single) and coaxial rotor helicopters. 73
44 Predicted specific transport efficiency of the MTR versus payload compared with hypothetical conventional (single) and coaxial rotor helicopters. 73
45 Predicted gross weight and fuel weight versus distance flown for 20 ton useful payload MTR concept versus a legacy helicopter design. 74
46 Predicted payload/range graph for the MTR concept when compared with a legacy helicopter design. 74
47 Conceptual design sketch of MTR flying in airplane mode. 76
48 The equivalent flat plate area of a helicopter tends to grow with the square-root of its gross weight. “Crane” and utility helicopters tend to have a much higher drag because of their typically non-streamlined airframe shapes. 79
49 Lift-to-drag ratio of the MTR in both helicopter and airplane modes. 80
50 Variation in gross takeoff weight of the MTR with changes in wing aspect ratio. . . 83
51 Variation in wing span of the MTR with changes in wing aspect ratio. 84
52 MTR takeoff weight versus payload and destination hover time. 85
53 MTR rotor diameter versus payload and destination hover time. 86
54 MTR required fuel weight versus payload and destination hover time. 86
55 MTR gross takeoff weight versus payload and takeoff density altitude. 87
56 MTR rotor diameter versus payload and takeoff density altitude. 87
57 MTR engine power required versus payload and takeoff density altitude. 88
58 MTR gross takeoff weight versus design cruise density altitude. 89
59 MTR rotor diameter versus design cruise density altitude. 90
60 MTR required fuel weight versus design cruise density altitude. 91
61 MTR wingspan versus design cruise density altitude. 91
62 MTR power required versus airspeed at 20,000 feet. 93

63 Engine power required versus airspeed at mean sea level conditions for both flight modes. 96
64 MTR rate of climb capability versus airspeed at mean sea level conditions for both flight modes. 97
65 Maximum rate of climb versus altitude for the MTR in airplane mode. 98

List of Tables

1 MTR component drag breakdown in airplane mode. 77
2 MTR component drag breakdown in helicopter mode. 77
3 Key design inputs for heavy-lift MTR point design. 94
4 MTR general sizing for heavy-lift point design. 94
5 MTR component weights for heavy-lift point design. 95

List of Principal Symbols

A	Area
AR	Aspect ratio
A_f	Projected area of component
b	Wing span
c	Chord
C_e	Specific fuel consumption coefficients
C	Tail volume coefficient
C_{d_0}	Profile drag coefficient of blade sections
C_{D_0}	Profile drag coefficient of component
$C_{L_{\mathrm{des}}}$	Wing design lift coefficient
$C_{\mathrm{L_{max}}}$	Maximum lift coefficient
C_T	Rotor thrust coefficient
C_{pow}	Power conversion factor
C_P	Rotor power coefficient
C_T/σ	Blade loading coefficient
d	Characteristic diameter
D	Rotor diameter
D_{off}	Offset distance
D_{TB}	Diameter of tail boom
DL	Disk loading
e_W	Oswald's wing span efficiency factor
E	Energy efficiency parameter
f_{eq}	Equivalent flat plate area
F	Fuel flow rate
F_{CF}	Centrifugal force
FM	Figure of merit
f_{SH}	Transmission shaft torque overload factor
g	Acceleration due to gravity
H_p	Pressure altitude
H_ρ	Density altitude
k	Component weight correlation coefficient
k_{alt}	Engine lapse factor
k_{EW}	Empty weight fraction
k_{WE}	Weight efficiency coefficient

l	Characteristic length
l_{sep}	Separation distance from wing to tail
l_{SS}	Length of suspension strut
L	Flight range of vehicle
L/D	Lift-to-drag ratio
N_b	Number of rotor blades
N_{ENG}	Number of engines
P	Power required
Q	Torque required
R	Rotor radius
Re	Reynolds number
S	Wing or tail area
SFC	Specific fuel consumption
t	Time
t_{MR}	Main rotor thrust recovery factor
t_{TR}	Tail rotor thrust recovery factor
t/c	thickness-to-chord ratio
T	Temperature
T	Rotor thrust
$V_{\mathrm{CR_{hel}}}$	Cruise speed in helicopter mode
$V_{\mathrm{CR_{air}}}$	Cruise speed in airplane mode
W_{CREW}	Crew weight
W_{DG}	Design gross weight for airplane mode
W_{EW}	Empty weight
W_{FUEL}	Fuel weight
W_{LG}	Landing gear weight
W_{MEP}	Mission equipment package weight
W_{PL}	Payload weight
W_{TB}	Tilt boom weight
W_{TO}	Takeoff weight
α_{TPP}	Tip path plane angle of attack
η_{PR}	Propulsive efficiency
η_{coax}	Coaxial rotor efficiency
η_{prop}	Rotor propulsive efficiency
ρ_0	Air density at sea level
ρ_{HOGE}	Air density at hover out of ground effect

ρ_{CR}	Air density at cruise condition
ΩR	Rotor tip speed
κ	Rotor induced power factor
Λ	Wing sweep angle
μ	Advance ratio of the main rotor
σ	Solidity
σ_p	Density ratio, σ/σ_0
ζ	Efficiency factor

Abbreviations

air	Airplane mode
ALT	At altitude performance
APU	Auxiliary power unit
CF	Centrifugal force
CHS	Container handling system
CON	Conversion flight mode
cr	Cruise condition
CREW	Crew
EMP	Empennage
ENG	Engine
eq	Equivalent conditions
ES	Electrical system
FS	Fuel system
FUEL	Fuel
FUSE	Fuselage
GB	Gear box
GHE	Ground handling equipment
hel	Helicopter mode
hov	Hovering flight condition
HT	Horizontal tail
HUB	Rotor hub
IGB	Intermediate gear box
INST	Cockpit instruments, avionics & sensors
MEP	Mission equipment package
MR	Main rotor
MTR	Mono Tiltrotor
nom	Nominal value

OGE	Out of ground effect
PIS	Power plant installation system
ref	Reference value
RES	Reserve
SH	Shaft
SP	Swashplate
SS	Suspension structure
TB	Tail boom
TM	Tilt mechanism
to	Takeoff condition
TR	Tail rotor
VT	Vertical tail
W	Wing
WTM	Wing tilt mechanism

1 Introduction

The work documented in this report considers the conceptual design process of a new and innovative vertical heavy-lift architecture called the Mono Tiltrotor (MTR). The interest in developing heavy-lift vertical lift rotorcraft concepts has spanned several decades (Refs. 1–5). Recently, the US Military has again outlined requirements for a new heavy-lift rotorcraft, with high payload and good range capability. It is generally accepted that the range of such a vehicle must exceed that possible with legacy helicopter designs. One proposed requirement for such an aircraft is that it must carry twenty or more tons of useful payload over an operational radius of action of at least 500 nm. This is equivalent to an unrefueled range of over 1,000 nm. These are extremely demanding requirements for a rotorcraft, and no vehicle has yet been designed that can meet these requirements.

To this end, the MTR has been proposed as an innovative and potentially revolutionary medium and heavy-lift aircraft architecture* to meet the demanding vertical-lift payload and range carrying requirements of a modern military. The capabilities of the MTR are predicated on the combination of an advanced coaxial contra-rotating rotor system and sophisticated kinematics that morph the aircraft topology for efficient operation according to a specific flight condition. This means that the aircraft can be aerodynamically optimized for high efficiency (and hence low fuel burn) in both hovering flight and cruise flight.

Suggested originally in concept by the Baldwin Technology Company (BTC) (Refs. 7, 8), the MTR concept examined in the present study integrates an efficient coaxial rotor, a lightweight airframe, a folding lifting wing system and a cargo container handling system. This system is capable of rapidly and economically transporting different types of mission tailored payloads, offering a modern military a vehicle with extremely high asset value. The MTR is shown in concept in Figs. 1, 2 and 3. After picking up the primary payload, which is suspended below the rotor, this unique machine morphs from helicopter to airplane mode and vice-versa by tilting the coaxial rotor (see Fig. 1). The folding wing is designed to be actuated primarily by dynamic pressure as the machine increases airspeed, which is lifted and locked into its airplane position. Because the primary payload is external to the main aircraft, the payload is enveloped in a drag

*An innovative product architecture consists of off-the-shelf component technologies organized into a new system, offering discontinuous value attributes relative to legacy systems (Ref. 6).

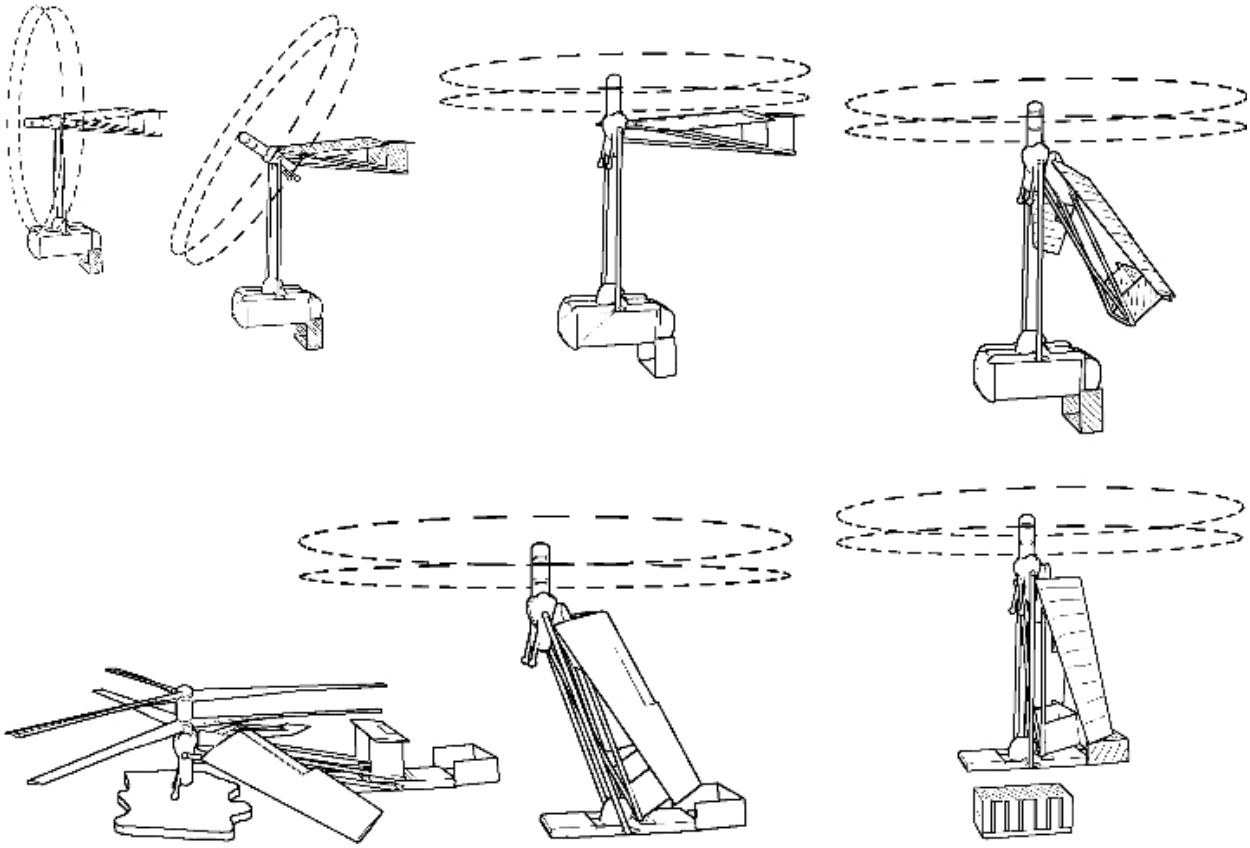

Figure 1: Conceptual sketch of the MTR transitioning from being at rest on the ground to hovering over a container, then morphing from helicopter mode to airplane mode.

reducing fairing. When transitioning from hover to an at-rest position on the ground, the tailboom is pinned parallel to the suspension structure for increased strength and stability.

Figures 2 and 3 show further details of the MTR in its helicopter mode and airplane (cruise) mode, respectively. While perhaps of a relatively unorthodox design, it will be shown in this report that the MTR architecture offers the potential of meeting large payload and long-range transportation goals that have previously eluded other vertical-lift aircraft concepts.

During the course of this work, various sizes of MTR have been considered, depending on the payload to be carried and also the detailed mission requirements. These vehicle sizes range from small-scale MTRs with relatively light payloads, to large heavy-lift MTRs with payloads of 20 tons or more. Of primary interest in the present study was the heavy-lift mission. The overall goals were to develop vehicle designs that could carry this payload efficiently with an operational radius of action (with full payload) of at least 500 nm.

Clearly, the emerging military strategies most suited to potential application of the MTR are

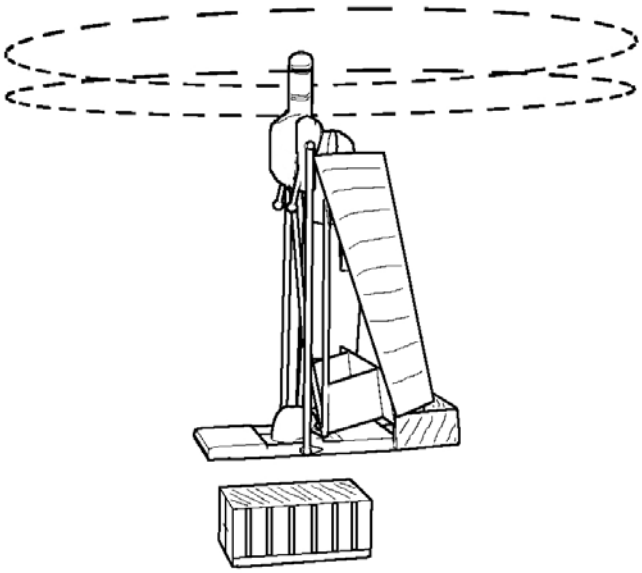

Figure 2: Conceptual sketch of the MTR operating in helicopter mode picking up a standardized cargo container.

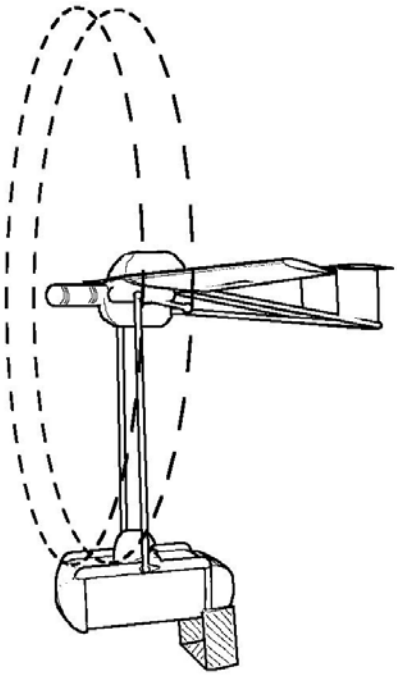

Figure 3: Conceptual sketch of the MTR with payload operating in cruise mode with wing deployed.

Navy Sea Basing with Ship to Objective Maneuver (STOM), and Army Future Combat Systems (FCS) with mounted maneuver and air mobility. Unforeseen breakthrough applications may also be discovered as a biproduct of the current study, such as having a single MTR platform capable of delivering fuel in vertical replenishment, in-flight refueling of airplanes and helicopters, and resupplying fuel to austere inland ground bases. A particularly important feature of the MTR concept is its rapid container capture and release capability. This capability significantly reduces overall system vulnerability to enemy fire when operated in military forcible entry roles, and also facilitates rapid reconfiguration for tailoring platform capabilities to the dynamic battle space.

The results documented in this report compare the MTR with conventional legacy helicopter designs. The results show that the contra-rotating coaxial rotor and external payload carrying capability of the MTR architecture allows for a relatively compact rotor and lightweight airframe design compared to an equivalent single rotor lifter. For example, the coaxial rotor diameter can be smaller in overall size compared to a single helicopter rotor of comparable lifting (hovering) efficiency. No anti-torque device (such as a tail rotor) is needed with a coaxial rotor configuration, which can be a source of significant power and weight savings. However, the inherent nonuniformities in the flow between the two contra-rotating rotors means that there can still be a small unbalanced torque. This may need to be removed by a fixed aerodynamic surface. Restricting the net size of the aircraft allows it to be better operated from existing land-based and sea-based assets, without any additional support infrastructure. However, the various aerodynamic performance and mechanical compromises associated with the use of coaxial rotors must be balanced against the advantages of a smaller, lighter rotor and the smaller overall size of the MTR, the better response to gusts from any direction, and potentially significantly lower acquisition costs.

A relatively large, high aspect ratio folding wing is used on the MTR for cruise flight operations. This gives the MTR the cruise efficiencies (i.e., high lift-to-drag ratios) necessary to achieve ranges and flight speeds significantly exceeding those possible by a conventional helicopter. The wing folds down to reduce vertical aerodynamic forces in hover, while still retaining the hovering and vertical-lift efficiency of conventional helicopters. Furthermore, the MTR is expected to be comparatively insensitive to gusts in hovering flight, a key issue in shipboard operations. The wing panels can freely pivot at their root about a coupling, which isolates most of the aerodynamic moments on the airframe from the wing panels themselves. As intended, transition of the wing

panels from their stowed position in hovering flight to their deployed configuration for airplane mode operation is powered mostly by aerodynamic forces with the wing panels lifting themselves into position.

The rotor of the MTR is designed to be relatively far away from the wing and payload, which offers several advantages in terms of minimizing rotor airframe interference effects and reducing groundwash velocities. For large rotorcraft, vertical download can approach or even exceed 5% of gross vehicle weight, negating substantially the resulting vertical lift payload. Advanced bearingless rotors may also be employed on the MTR, offering significant weight savings for increased payload capacity. Furthermore, the relatively large, lightly loaded, high inertia rotor of the MTR allows for sufficiently safe autorotational flight capability in the event of engine or transmission failure. The MTR's relatively low disk loading (it is comparable to a helicopter) is also a key to accomplishing successful rescue missions and for landing and takeoffs from unprepared runways.

The results documented in this report have been used to systematically examine the sizing and weight of the MTR concept, and help to properly quantify the value of the MTR aircraft architecture. While it must be recognized that there are many detailed design challenges and potentially several new technological developments that would be necessary to bring the MTR to final fruition, this conceptual design study assumes that such developments can, in fact, be ultimately realized. In this report, a conceptual aircraft design methodology is employed to calculate vehicle performance across important key metrics. This includes several types of mission profiles that are compatible with current military plans, including both Navy and Army missions. The quantifiable results from the work documented in this report will be useful in making policy and resource allocation decisions regarding science and technology investments that would be necessary to fully develop the MTR aircraft architecture into a useful and practical flight vehicle.

2 Development of Methodology

The present method of analysis follows, in part, a conceptual rotorcraft design analysis developed over several years at the University of Maryland. This analysis was originally based on the work of Tishchenko (Refs. 9–11). The parametric equations and algorithmic procedures have been used successfully by the University of Maryland over the past six years in the AHS's Student Design

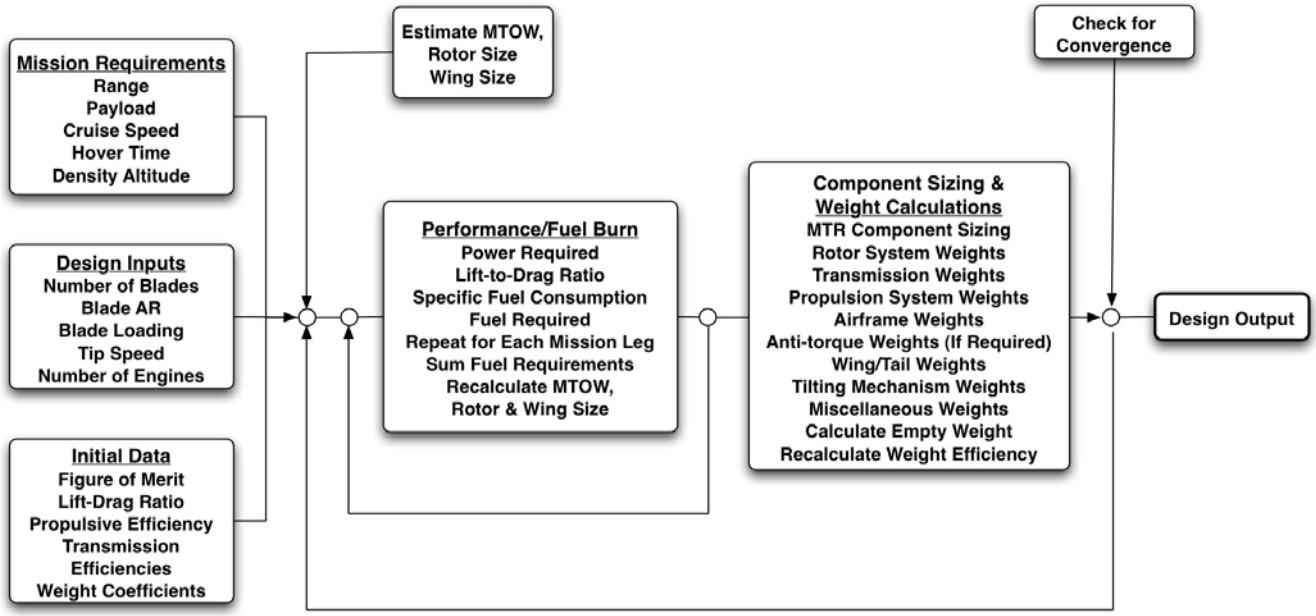

Figure 4: Flowchart of the conceptual rotorcraft design analysis.

Competition (Refs. 12–17). This analysis has been revised and updated to examine compound rotorcraft concepts and, in particular, the specific attributes of the MTR architecture. A flowchart outlining the general design process is shown in Fig. 4. The elements of the design model are based on a series of nonlinear equations describing both the performance and component weights of the candidate rotorcraft designs.

The calculation of the configuration and performance parameters of the candidate MTR concepts are based on the assumptions of certain payload weights carried over specified ranges (or an assumed mission radius of action) as primary operational inputs. In addition, hover time requirements can be specified for the mission profile, which can bias efficient hovering performance against efficient cruise performance. Of importance in this conceptual design study was the determination of the range specific transport efficiency, which is defined as the ratio of payload weight transported to fuel weight consumed for a specific transport range. This quantity is similar to a productivity index that is sometimes used in other types of rotorcraft design analyses. The transport efficiency calculation allows the effectiveness of various candidate vertical-lift designs to be objectively compared. Also of importance is the relationship between the range (or radius of action) and payload for a given candidate vehicle. To determine this, the vehicle weight efficiency (or empty weight fraction) is needed, along with other assumptions such as estimates of cruise flight

speed.

Because the MTR is a hybrid concept combining some of the attributes of a dual rotor coaxial helicopter and a fixed-wing aircraft, parametric equations describing the operation of the MTR both in helicopter and airplane mode have been developed. These equations are seamlessly integrated together in the design algorithms. Because the design proceeds as a highly nonlinear iterative process, these equations must be relatively parsimonious and robust but also highly representative of the underlying performance of the vehicle in each of its operational flight conditions.

The determination of the weight efficiency (or empty weight fraction) for the MTR concept is based, in part, on the use of historical data for both helicopters and fixed-wing aircraft, and also on a more detailed weights analysis for the MTR originally proposed by BTC. This initial design had an notional 80 ft diameter, coaxial rotor (Refs. 7, 8). A complicating factor in the overall design approach is that the MTR is a coaxial counter-rotating rotor configuration for which much more limited historical weight and performance data exists, especially for larger helicopters. The largest coaxial helicopters previously developed (by Kamov in Russia) have payload capabilities of less than 5 tons. This lack of historical data requires careful validation of the analysis for larger single rotor helicopters, and also for coaxial helicopters where data is available. Only then can the analysis be used with confidence in the conceptual design and sizing of the MTR architecture.

2.1 General Performance & Sizing Analysis

The sequence of performance calculations that follows has been outlined, in part, by Tishchenko et al. (Ref. 11) for the conceptual design of large transport helicopters (i.e., those with payloads of over 6 tons). However, the present design analysis has been developed in a much more general form to allow trade studies to be conducted for different types of mission profiles, especially over longer ranges less typical of a conventional helicopter, and also between different vertical flight vehicle configurations. The analysis was also developed to encompass conventional helicopters (with both single and dual coaxial rotors) that would carry smaller payloads of less than 6 tons. The analysis was further developed for the specific features of the MTR architecture, taking into consideration the unique morphing and external load carrying capabilities of the design, assuming these morphing capabilities could indeed be realized. A key part of the performance analysis is the accurate determination of component weights, which as previously mentioned, was based in part

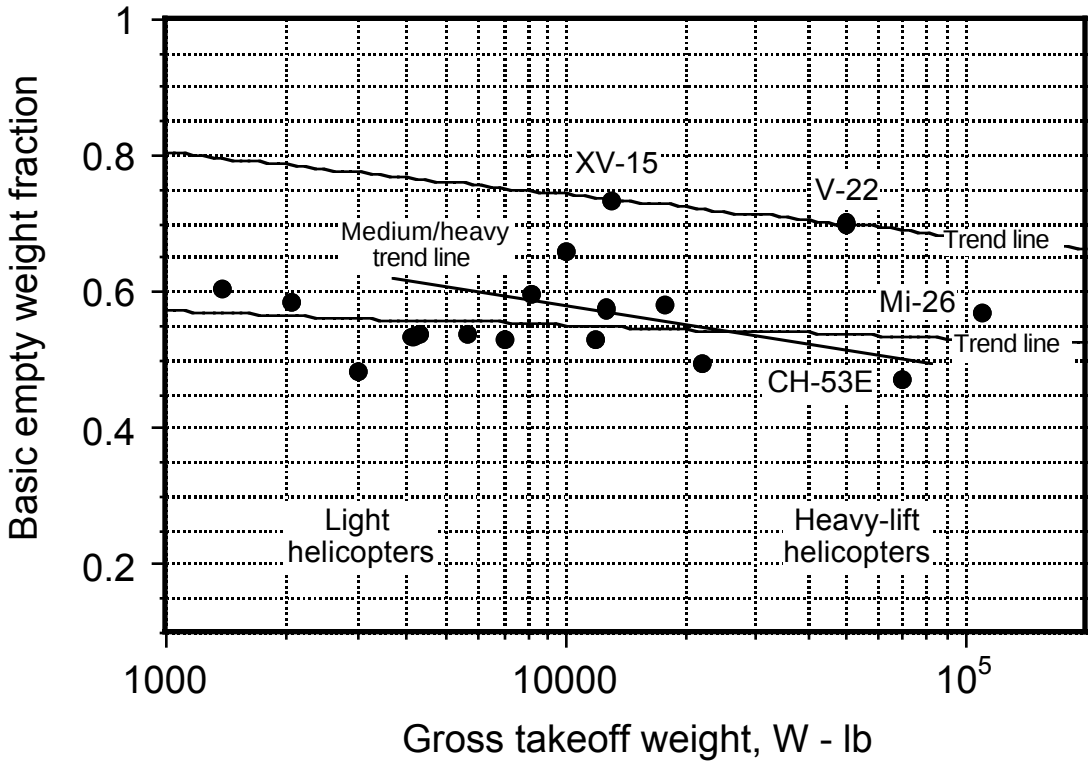

Figure 5: Empty weight fraction versus vehicle gross weight for helicopters and conventional tiltrotors.

on correlation studies against extensive historical data for existing helicopters. The correlation coefficients used in the performance studies are given in Appendix 1. Notice that the analysis performed on the legacy helicopter designs was based on the assumption that all of the payload was carried internally.

2.1.1 Takeoff Weight & Energy Efficiency

The takeoff weights of the vehicle depend on the structural efficiency (empty weight fraction) and the aerodynamic efficiency. Aircraft acquisition costs are approximately proportional to the empty weight of the aircraft, so structural efficiency is paramount for a heavy-lift rotorcraft design concept less it become prohibitably expensive. While the conventional tiltrotor concept is often viewed as being suitable for heavy-lift, the relatively efficient cruise speed efficiency of the conventional tiltrotor is offset by its higher empty weight fraction – see Fig. 5. The MTR is designed to have a structural efficiency that is much better than a conventional tiltrotor and is comparable to the best helicopters.

Aerodynamic efficiency, which is a function of both hovering efficiency and cruise (forward flight) efficiency, affects the fuel weight required. Fuel weight is a major factor in determining direct operating costs. A relatively small part of most mission time is spent in hover, therefore, the fuel weight is determined primarily by the cruise efficiency. The effect of hover time on the design metrics is considered later in this report.

Using the Bréguet range equation, the range L can be written as

$$L = \frac{(L/D)\,\eta_{\mathrm{PR}}\,\zeta_{\mathrm{CR}}}{C_e} \ln\left(\frac{W_{\mathrm{TO}}}{W_{\mathrm{TO}} - W_{\mathrm{FUEL}}}\right) \tag{1}$$

where C_e is the specific fuel consumption of the engines in cruise and L/D is the corresponding lift-to-drag ratio. The range can also be written as

$$L = E \ln\left(\frac{W_{\mathrm{TO}}}{W_{\mathrm{TO}} - W_{\mathrm{FUEL}}}\right) \tag{2}$$

where E has been referred to as an "energy efficiency" as defined by Tishchenko et al. (Ref. 11) as

$$E = \frac{(L/D)\,\eta_{\mathrm{PR}}\,\zeta_{\mathrm{CR}}}{C_e} \tag{3}$$

This index is useful as a comparative metric because it is a composite of aerodynamic, mechanical and fuel efficiency. It does not, however, provide a direct measure of the efficiency of the vehicle conveying payload. The weight of the fuel burnt is then

$$W_{\mathrm{FUEL}} = W_{\mathrm{TO}}\big(1 - \exp(-L/E)\big) \tag{4}$$

which comes from the Bréguet equation. For small ranges this is equivalent to

$$W_{\mathrm{FUEL}} = \frac{L\,W_{\mathrm{TO}}}{E} \tag{5}$$

Therefore, the determination of fuel required in cruise flight requires a determination of the cruise efficiency.

For small ranges the takeoff weight of the vehicle can now be determined according to the equation

$$W_{\mathrm{TO}} = \frac{W_{\mathrm{PL}} + W_{\mathrm{CREW}} + W_{\mathrm{MEP}} + W_{\mathrm{FUEL_{hov}}}}{k_{\mathrm{WE}} - k_{\mathrm{FW_1}} - k_{\mathrm{FW_2}} - 0.005} \tag{6}$$

where a fuel allowance of 0.5% of the total fuel has been made in the preceding equation to account for warm-up, taxi and takeoff. The consideration of flight operations in both helicopter and airplane mode have been separately considered using the fuel weight efficiency coefficients, namely:

$$k_{\mathrm{FW}_1} = \frac{L_{\mathrm{hel}} + V_{\mathrm{CR}_{\mathrm{hel}}}\, t_{\mathrm{RES}_{\mathrm{hel}}}}{E_{\mathrm{hel}}} \quad \text{(helicopter)} \tag{7}$$

and

$$k_{\mathrm{FW}_2} = \frac{L_{\mathrm{air}} + V_{\mathrm{CR}_{\mathrm{air}}}\, t_{\mathrm{RES}_{\mathrm{air}}}}{E_{\mathrm{air}}} \quad \text{(airplane)} \tag{8}$$

where t_{RES} is a specified reserve time in each flight mode. For long range vehicles the weight of fuel burned during the flight must be taken into account in the performance evaluation. The fuel weight efficiency coefficients in this case become

$$k_{\mathrm{FW}_1} = 1 - \exp\left(-\frac{L_{\mathrm{hel}} + V_{\mathrm{CR}_{\mathrm{hel}}}\, t_{\mathrm{RES}_{\mathrm{hel}}}}{E_{\mathrm{hel}}}\right) \quad \text{(helicopter)} \tag{9}$$

and

$$k_{\mathrm{FW}_2} = 1 - \exp\left(-\frac{L_{\mathrm{air}} + V_{\mathrm{CR}_{\mathrm{air}}}\, t_{\mathrm{RES}_{\mathrm{air}}}}{E_{\mathrm{air}}}\right) \quad \text{(airplane)} \tag{10}$$

For the MTR, both helicopter and airplane mode operations are possible, whereas for a pure helicopter all of the airplane terms are obviously zero.

The weight of fuel required for the mission, W_{FUEL} depends on that required for hovering flight plus that required in cruise flight. For the hovering portion of the flight, the fuel weight required is

$$W_{\mathrm{FUEL}_{\mathrm{hov}}} = C_{e_{\mathrm{hov}}} N_{\mathrm{ENG}} P_{\mathrm{ENG}}\, t_{\mathrm{hov}} \tag{11}$$

where $C_{e_{\mathrm{hov}}}$ is the specific fuel consumption of the engines in hovering flight and $N_{\mathrm{ENG}} P_{\mathrm{ENG}}$ is the total power required. Notice that the fuel weight is also affected by the part of the mission time that is required to hover, t_{hov}.

The specific fuel consumption can be defined as

$$C_e = \left(\frac{W_{\mathrm{FUEL}}}{P_{\mathrm{ENG}}\, N_{\mathrm{ENG}}}\right) \frac{1}{t_{\mathrm{flight}}} \tag{12}$$

Also, the flight time t_{flight} in the cruise condition is

$$t_{\mathrm{flight}} = \frac{L + t_{\mathrm{res}} V_{\mathrm{CR}}}{V_{\mathrm{CR}}} \tag{13}$$

where L is the range at the cruise speed V_{CR}, and t_{res} is the time reserve to meet various operational and/or certification requirements. This means that the total fuel weight W_{FUEL} is given by the equation

$$W_{\mathrm{FUEL}} = W_{\mathrm{TO}} \left(\frac{L_{\mathrm{hel}} + V_{\mathrm{CR}_{\mathrm{hel}}}\, t_{\mathrm{RES}_{\mathrm{hel}}}}{E_{\mathrm{hel}}} + \frac{L_{\mathrm{air}} + V_{\mathrm{CR}_{\mathrm{air}}}\, t_{\mathrm{RES}_{\mathrm{air}}}}{E_{\mathrm{air}}} + 0.005 \right) + W_{\mathrm{FUEL}_{\mathrm{hov}}} \tag{14}$$

Notice that the parameter k_{WE} in Eq. 6 is the net structural weight efficiency of the vehicle, which is defined by Tishchenko et al. (Ref. 11) as

$$k_{\mathrm{WE}} = \frac{W_{\mathrm{TO}} - W_{\mathrm{EW}}}{W_{\mathrm{TO}}} \tag{15}$$

This quantity is equivalent to using an empty weight fraction that is defined as

$$k_{\mathrm{EW}} = \frac{W_{\mathrm{EW}}}{W_{\mathrm{TO}}} = 1 - k_{\mathrm{WE}} \tag{16}$$

While weight efficiency has been used by default throughout the present work, they are easily related for other comparative purposes by using Eq. 16.

To proceed with the design process, it is apparent that both a component sizing and weight analysis of the MTR concept is required. These are considered in the following sections.

2.1.2 Main Rotor Sizing Equations

For a hovering vehicle, the solidity of the main rotor(s) σ_{MR} drives the rotor weight. The rotor solidity is

$$\sigma_{\mathrm{MR}} = \frac{N_{b_{\mathrm{MR}}} c}{\pi A_{\mathrm{MR}}} \tag{17}$$

which can be rewritten as

$$\sigma_{\mathrm{MR}} = \frac{N_{b_{\mathrm{MR}}}}{\pi AR_{b_{\mathrm{MR}}}} \tag{18}$$

where $N_{b_{\mathrm{MR}}}$ is the number of rotor blades per rotor and $AR_{b_{\mathrm{MR}}} = R/c$ is the aspect ratio of the main rotor blades. This leads to the effective disk loading DL of the rotor system as

$$DL = \left(\frac{C_T}{\sigma} \right)_{\mathrm{MR}} \sigma_{\mathrm{MR}}\, \rho_{\mathrm{HOGE}}\, (\Omega R)^2_{\mathrm{MR}} \tag{19}$$

where ρ_{HOGE} is the value of ambient air density for hovering out of ground effect (HOGE) conditions. Solving for the main rotor diameter D_{MR} using the latter equation gives

$$D_{\text{MR}} = \sqrt{\frac{4W_{\text{TO}}}{\pi DL}} \quad \text{for a conventional design} \tag{20}$$

where rotor thrust T is approximately equal to W_{TO} and

$$D_{\text{MR}} = \sqrt{\frac{2W_{\text{TO}}}{\pi DL}} \quad \text{for a coaxial design} \tag{21}$$

where it is assumed that for this conceptual design that each rotor of the coaxial carries one half of the total weight of the machine.

The power requirements for flight can now be established. The machine is assumed to have N_{ENG} engines that each deliver a power of P_{ENG}. In the case of the conventional (single rotor) design, the power required to hover is given by

$$N_{\text{ENG}} P_{\text{ENG}} = \frac{(W_{\text{TO}}\, t_{\text{MR}})^{3/2}}{\sqrt{\pi/2}\, FM_{\text{MR}}\, \zeta_{\text{MR}} D_{\text{MR}} \sqrt{\sigma_p}\sqrt{\rho_0}} \quad \text{(conventional)} \tag{22}$$

where FM is the figure of merit of the rotor system and t_{MR} is a thrust recovery factor that takes into account interference effects between the rotor and the airframe. For a coaxial rotor system the power required is

$$N_{\text{ENG}} P_{\text{ENG}} = \frac{(W_{\text{TO}}\, t_{\text{MR}})^{3/2}}{\sqrt{\pi/2}\, FM_{\text{MR}}\, \zeta_{\text{MR}} D_{\text{MR}}\, \eta_{\text{coax}} \sqrt{\sigma_p}\sqrt{\rho_0}} \quad \text{(coaxial)} \tag{23}$$

where η_{coax} represents a loss of net rotor aerodynamic efficiency because of rotor-on-rotor interference and the interacting flow fields between the two rotors. Based on NACA tests with coaxial rotors (Ref. 18) it would seem that on average $\eta_{\text{coax}} \approx 0.85$; that is, there is a loss of net rotor efficiency with a coaxial for rotors with the same equivalent disk loading and net solidity, i.e., at the same value of C_T/σ. This is equivalent to the use of a coaxial induced power factor, $\kappa_{\text{int}} \approx 1/\eta_{\text{coax}}$, which increases the induced power requirements over and above that required for two single (isolated) rotors. This is summarized in Fig. 6. The interference (efficiency) coefficient also depends on the relative thrust/torque balance between the rotors, although this is a secondary effect.

The nominal installed engine power is then

$$P_{\text{ENG}_{\text{nom}}} = P_{\text{ENG}}\, C_{\text{pow}} \tag{24}$$

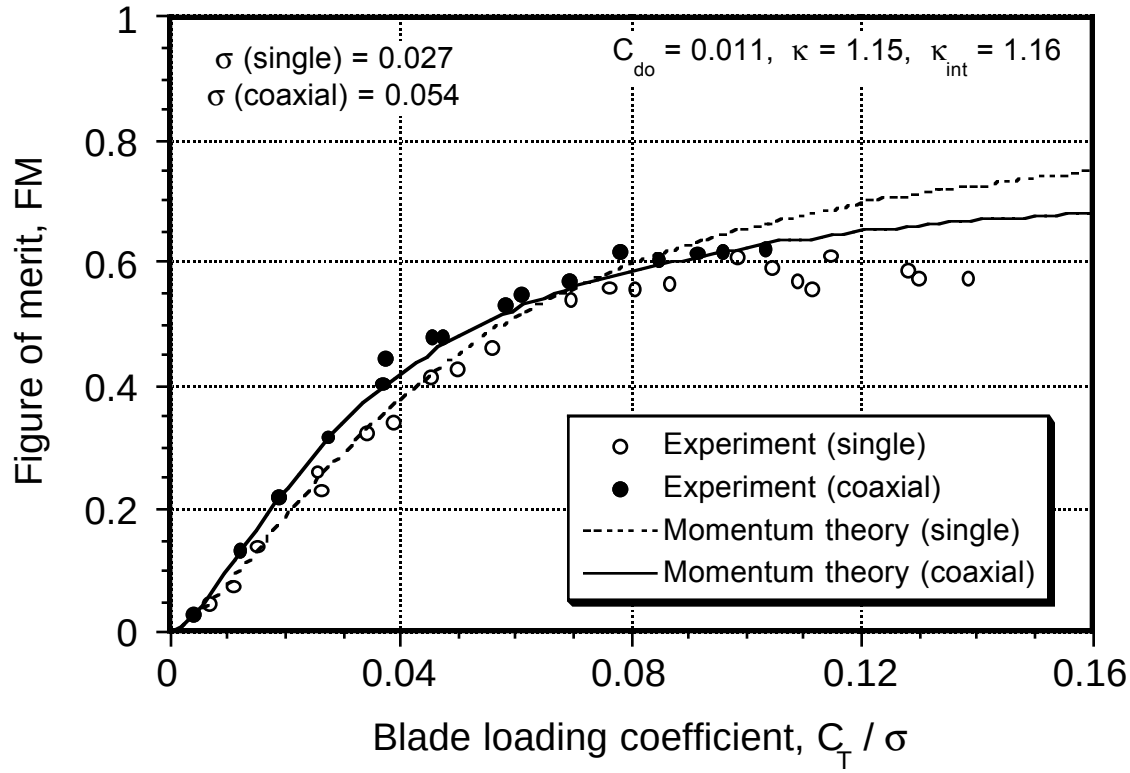

Figure 6: Hovering figure of merit of coaxial rotor design showing the effect of rotor-on-rotor interference.

where C_{pow} is an installation loss factor. The torque required for the main rotor system is then

$$Q_{\text{MR}} = \frac{(P_{\text{ENG}}\, N_{\text{ENG}})\, R_{\text{MR}}\, \zeta_{\text{MR}}}{(\Omega R)_{\text{MR}}} \tag{25}$$

The main rotor torque requirements define the transmission sizing requirements and other component weights for the aicraft. These weights are considered in the following sections.

2.1.3 Tail Rotor Sizing Equations

No tail rotor is required for either a coaxial machine or the MTR. However, the tail rotor performance must be accounted for in order to compare the MTR with a conventional single main rotor concept. The tail rotor thrust T_{TR} is

$$T_{\text{TR}} = \frac{2Q_{\text{MR}}}{(D_{\text{MR}} + D_{\text{TR}} + D_{\text{off}})} \tag{26}$$

where $D_{\text{off}} = 0.3$ meters and represents a minimum allowable spacing between the blade tips of the main rotor and the tail rotor. The tail rotor power required is then

$$P_{\text{TR}} = \frac{(T_{\text{TR}}\, t_{\text{TR}})^{3/2}}{\sqrt{\pi/2}\, FM_{\text{TR}}\, \zeta_{\text{TR}} D_{\text{TR}} \sqrt{\sigma_p} \sqrt{\rho_0}} \tag{27}$$

where t_{TR} is the thrust recovery factor for the tail rotor. This factor depends primarily on whether a tractor or pusher design is used. The corresponding tail rotor torque required is

$$Q_{\text{TR}} = \frac{P_{\text{TR}}\, R_{\text{TR}}\, \zeta_{\text{TR}}}{(\Omega R)_{\text{TR}}} \tag{28}$$

This allows the tail rotor shaft torque to be determined using

$$Q_{\text{TR}} = \frac{P_{\text{TR}}\, f_{\text{SH}}}{n_{\text{SH}}} \tag{29}$$

where f_{SH} is the transmission shaft torque overload factor and n_{SH} is the tail rotor shaft rpm.

The solidity of the tail rotor is given by

$$\sigma_{\text{TR}} = \frac{T_{\text{TR}}}{(C_T/\sigma)_{\text{TR}}\, \rho_0\, A_{\text{TR}}\, (\Omega R)^2_{\text{TR}}} \tag{30}$$

and the mean (average) chord of the tail rotor blades is then

$$c_{\text{TR}} = \frac{\pi R_{\text{TR}}\, \sigma_{\text{TR}}}{N_{b_{\text{TR}}}} \tag{31}$$

The blades have aspect ratio

$$AR_{b_{\text{TR}}} = \frac{R_{\text{TR}}}{c_{\text{TR}}} \tag{32}$$

The net main rotor efficiency is then updated using

$$\zeta_{\text{MR}} = \frac{P_{\text{ENG}}\, N_{\text{ENG}} - P_{\text{TR}} - P_{\text{DC}}}{P_{\text{ENG}}\, N_{\text{ENG}}} \tag{33}$$

where P_{DC} is an allowance for an auxiliary power drain for hydraulics and electrical systems. This is normally specified as a fixed amount independent of vehicle size.

2.1.4 Power Requirements in Cruise Flight

The power requirements in cruise flight must now be established. For a conventional (single rotor) helicopter configuration the power required is

$$P_{\text{CR}_{\text{hel}}} = \frac{W_{\text{TO}}\, V_{\text{CR}_{\text{hel}}}}{(L/D)_{\text{hel}}\, \eta_{\text{PR}}\, \zeta_{\text{cr}}} \quad \text{(conventional)} \tag{34}$$

and for a helicopter with a coaxial rotor system

$$P_{\mathrm{CR_{hel}}} = \frac{W_{\mathrm{TO}}\, V_{\mathrm{CR_{hel}}}}{(L/D)_{\mathrm{hel}}\, \eta_{\mathrm{PR}}\, \eta_{\mathrm{coax}} \zeta_{\mathrm{cr}}} \quad \text{(coaxial)} \tag{35}$$

where again, the rotor-on-rotor aerodynamic interference is accounted for through the term η_{coax}, which may be different from the value used in hover because it is a function of disk (and blade) loading – see Fig. 6. The net lift-to-drag ratios of the conventional and coaxial helicopters will be different, mainly because the coaxial rotor in edgewise flight experiences a higher parasitic loss from the larger exposed rotor hub and control system.

In the case of the MTR (which can cruise in airplane mode) the power required for the coaxial rotor in axial flight can be written as

$$P_{\mathrm{CR_{air}}} = \frac{W_{\mathrm{TO}}\, V_{\mathrm{CR_{air}}}}{(L/D)_{\mathrm{air}}\, \eta_{\mathrm{prop}} \zeta_{\mathrm{air}}} \quad \text{(MTR airplane mode)} \tag{36}$$

where η_{prop} is the propulsive efficiency of the MTR's coaxial rotor in the airplane mode. This efficiency depends on the specifics of the rotor and blade design.

The specific fuel consumption (SFC) in hovering flight can be determined from

$$C_{e_{\mathrm{hov}}} = C_{e_1} + C_{e_2} \left(\frac{P_{\mathrm{ENG_{nom}}}}{P_{\mathrm{ENG}}} \right) \quad \text{(hover SFC)} \tag{37}$$

where C_{e_1} and C_{e_2} are constants that depend on the characteristics of the type of engine being used. In helicopter cruise mode the specific fuel consumption is

$$C_{e_{CR_{\mathrm{hel}}}} = C_{e_1} + C_{e_2} \left(\frac{P_{\mathrm{ENG_{nom}}} N_{\mathrm{ENG}}}{P_{\mathrm{CR_{hel}}}} \right) \quad \text{(cruise SFC)} \tag{38}$$

and in MTR (airplane) cruise mode

$$C_{e_{CR_{\mathrm{air}}}} = C_{e_1} + C_{e_2} \left(\frac{P_{\mathrm{ENG_{nom}}}\, N_{\mathrm{ENG}}}{P_{\mathrm{CR_{air}}}} \right) \quad \text{(MTR cruise SFC)} \tag{39}$$

The fuel flows F can now be established. For the helicopter

$$F_{\mathrm{CR_{hel}}} = \frac{W_{\mathrm{TO}}}{E_{\mathrm{hel}}} \tag{40}$$

and for the MTR in airplane mode

$$F_{\mathrm{CR_{air}}} = \frac{W_{\mathrm{TO}}}{E_{\mathrm{air}}} \tag{41}$$

2.1.5 MTR Specific Sizing Equations

The specific equations used in the sizing of the MTR other than the rotor system must now be established. This includes the wing and tail groups, as well as the suspension structure and container handling system.

The wing span of the MTR is taken to be a fraction of the main rotor diameter, i.e.,

$$b_{\mathrm{w}} = k_{\mathrm{W}}\, D_{\mathrm{MR}} \tag{42}$$

where in the first instance $k_{\mathrm{W}} = 1$ has been used consistent with the conceptual design suggested in Ref. 8. The wing area S_{w} is

$$S_{\mathrm{w}} = \frac{W_{\mathrm{TO}}}{0.5\, \rho_{\mathrm{CR}}\, V^2_{\mathrm{CR_{air}}}\, C_{L_{\mathrm{des}}}} \tag{43}$$

where $C_{L_{\mathrm{des}}}$ is the design lift coefficient of the wing. To be efficient the wing must cruise at its best L/D ratio. Sizing the optimum wing in the case of the MTR may involve many factors, but the intent is to find a C_L that minimizes the sum of induced and profile losses. On average $C_{L_{\mathrm{des}}} \approx 0.5$ for a modest aspect ratio wing in subsonic flow, although it is expected that the MTR will cruise with a higher value of $C_{L_{\mathrm{des}}}$ to help minimize wing size and weight. This point is considered later in this report.

These assumptions lead to the determination of the mean aerodynamic chord of the wing $\bar{c}_{\mathrm{w}}$ as

$$\bar{c}_{\mathrm{w}} = \frac{S_{\mathrm{w}}}{b_{\mathrm{w}}} \tag{44}$$

and the aspect ratio of the wing AR_{W} is

$$AR_{\mathrm{W}} = \frac{b^2_{\mathrm{w}}}{S_{\mathrm{w}}} \tag{45}$$

The horizontal tail area S_{HT} of the MTR is defined as

$$S_{\mathrm{HT}} = \frac{C_{\mathrm{HT}}\, \bar{c}_{\mathrm{w}}\, S_{\mathrm{w}}}{l_{\mathrm{sep}}} \tag{46}$$

where C_{HT} is the horizontal tail volume coefficient. The corresponding vertical tail area S_{VT} is given by

$$S_{\mathrm{VT}} = \frac{C_{\mathrm{VT}}\, b_{\mathrm{w}} S_{\mathrm{w}}}{l_{\mathrm{sep}}} \tag{47}$$

where C_{VT} is the vertical tail volume coefficient.

The twin tail boom length (separation distance from wing to tail) of the MTR is written as a fraction of the main rotor diameter

$$l_{\mathrm{sep}} = k_{\mathrm{HT}}\, R_{\mathrm{MR}} \tag{48}$$

where in the first instance $k_{\mathrm{HT}} = 0.75$ has been used, which again is consistent with the conceptual design suggested in Ref. 7. With the assumption of a defined aspect ratio then the spans of the horizontal and vertical tails on the MTR are given by

$$b_{\mathrm{HT}} = \sqrt{AR_{\mathrm{HT}}\, S_{\mathrm{HT}}} \tag{49}$$

and

$$b_{\mathrm{VT}} = \sqrt{AR_{\mathrm{VT}}\, S_{\mathrm{VT}}} \tag{50}$$

respectively.

In keeping with the assumptions of geometric proportionality for different sizes of the MTR, the length of the suspension structure is defined as a fraction of the main rotor radius as

$$l_{\mathrm{SS}} = k_{\mathrm{SS}}\, R_{\mathrm{MR}} \tag{51}$$

where in the first instance it has been assumed that $k_{\mathrm{SS}} = 0.95$.

2.2 Component Weights

The parametric weight equations for the conventional helicopter configuration were developed following the work of Tishchenko et al. (Ref. 11). These equations were appropriately modified for a coaxial rotor system based on historical data (where available) and new sets of parametric equations were also developed for the MTR architecture. A component breakdown of the MTR architecture is shown in Fig. 7, which is used in the conceptual component weight analysis described in the following sections. The correlation coefficients used in the component weight studies are given in Appendix 2.

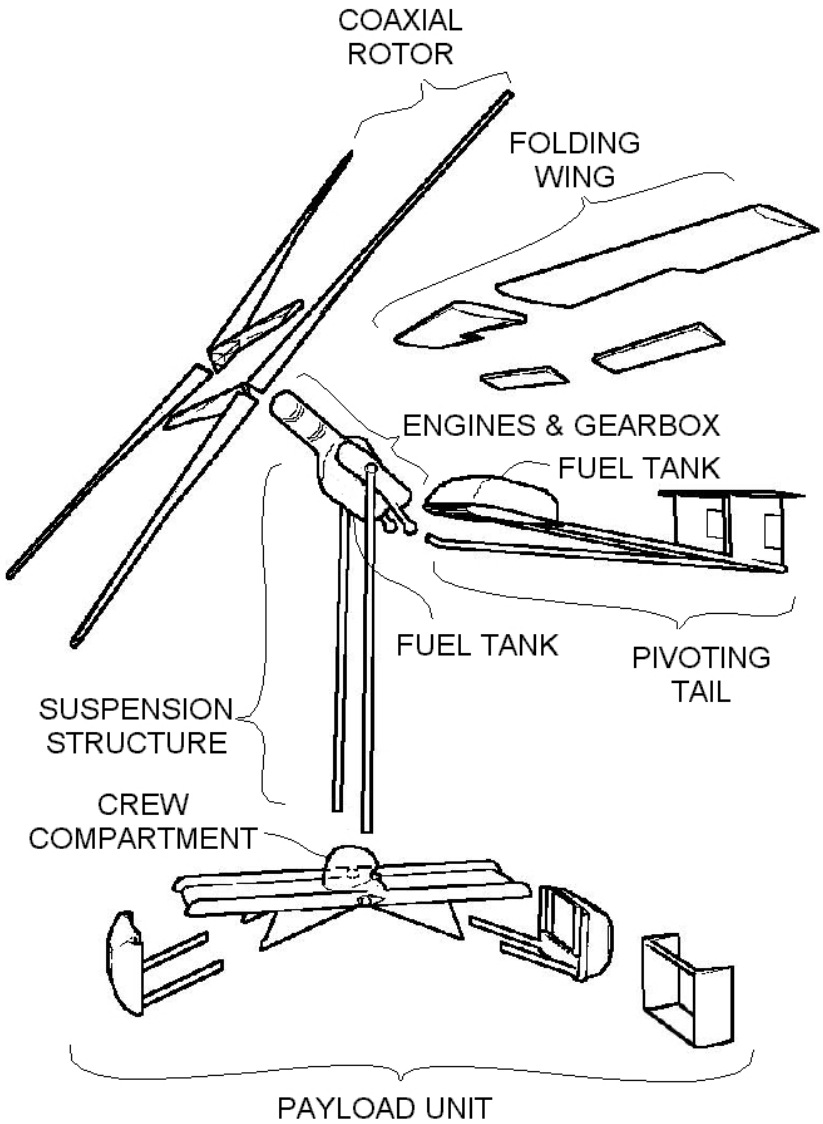

Figure 7: Component breakdown of the MTR architecture.

2.2.1 Rotor Weights

The weight of the main rotor blades $W_{\mathrm{MR_{BL}}}$ is defined based on their size and average weight per unit volume as

$$W_{\mathrm{MR_{BL}}} = k_{\mathrm{MR_{BL}}} \left(\frac{\sigma_{\mathrm{MR}} \, R_{\mathrm{MR}}^{2.7}}{\bar{AR}^{0.7}} \right) \tag{52}$$

where

$$\bar{AR} = \frac{AR_{\mathrm{MR_{BL}}}}{18} \tag{53}$$

For a coaxial rotor system the value of $W_{\mathrm{MR_{BL}}}$ would be doubled because of the two rotors, all other factors being equal. If a conventional single rotor configuration is being designed, then the accompanying weight of the tail rotor blades is

$$W_{\mathrm{TR_{BL}}} = k_{\mathrm{TR_{BL}}} \left(\frac{\sigma_{\mathrm{TR}}\, R_{\mathrm{TR}}^{2.7}}{\bar{AR}_{\mathrm{TR}}^{0.7}} \right) \tag{54}$$

where in this case

$$\bar{AR}_{\mathrm{TR}} = \frac{AR_{\mathrm{TR_{BL}}}}{18} \tag{55}$$

There is no tail rotor in the case of a coaxial machine or the MTR.

The weight of the main rotor hub is driven by the strength requirements, mostly to react centrifugal forces acting on the blades from their rotation. The hub weight $W_{\mathrm{MR_{HUB}}}$ is defined by the equation

$$W_{\mathrm{MR_{HUB}}} = k_{\mathrm{MR_{HUB}}} N_{\mathrm{MR_{BL}}}\, f_{z_{\mathrm{MR_{BL}}}} \left(10^{-4} F_{CF_{\mathrm{MR_{BL}}}} \right)^{N_{\mathrm{HUB}}} \tag{56}$$

where

$$N_{\mathrm{HUB}} = \begin{cases} 1.35 & \text{if } W_{\mathrm{PL}} \leq 6 \text{ tons} \\ 1.5 & \text{if } W_{\mathrm{PL}} > 6 \text{ tons} \end{cases} \tag{57}$$

and where

$$f_{z_{\mathrm{MR_{BL}}}} = \begin{cases} 1 & \text{if } N_{\mathrm{MR_{BL}}} \leq 4 \\ 1 + 0.05(N_{\mathrm{MR_{BL}}} - 4) & \text{if } N_{\mathrm{MR_{BL}}} > 4 \end{cases} \tag{58}$$

The centrifugal force acting on any one main rotor blade is given by

$$F_{CF_{\mathrm{MR_{BL}}}} = \left(\frac{W_{\mathrm{MR_{BL}}}}{N_{\mathrm{MR_{BL}}}} \right) \left(\frac{(\Omega R)_{\mathrm{MR}}}{R_{\mathrm{MR}}} \right)^2 \frac{R_{\mathrm{MR}}}{2g} \tag{59}$$

In the case of a conventional helicopter the tail rotor hub weight is given by the equation

$$W_{\mathrm{TR_{HUB}}} = k_{\mathrm{TR_{HUB}}}\, N_{\mathrm{TR_{BL}}}\, f_{z_{\mathrm{TR_{BL}}}} \left(10^{-4} F_{CF_{\mathrm{TR_{BL}}}} \right)^{1.35} \tag{60}$$

where

$$f_{z_{\mathrm{TR_{BL}}}} \begin{cases} 1 & \text{if } N_{\mathrm{TR_{BL}}} \leq 4 \\ 1 + 0.05(N_{\mathrm{TR_{BL}}} - 4) & \text{if } N_{\mathrm{TR_{BL}}} > 4 \end{cases} \tag{61}$$

and the centrifugal force acting on any one tail rotor blade is given by

$$F_{CF_{\mathrm{TR_{BL}}}} = \left(\frac{W_{\mathrm{TR_{BL}}}}{N_{\mathrm{TR_{BL}}}}\right)\left(\frac{(\Omega R)_{\mathrm{TR}}}{R_{\mathrm{TR}}}\right)^2 \frac{R_{\mathrm{TR}}}{2} \tag{62}$$

In the case of a coaxial rotor system then the weight of the hub will be doubled (if all other factors were held constant) giving an equation for the hub weight as

$$W_{\mathrm{MR_{HUB}}} = 2.25\, k_{\mathrm{MR_{HUB}}}\, N_{\mathrm{MR_{BL}}}\; f_{z_{\mathrm{MR_{BL}}}} \left(10^{-4} F_{CF_{\mathrm{MR_{BL}}}}\right)^{N_{\mathrm{hub}}} \tag{63}$$

where there is a penalty factor of 25% imposed on the net hub weight that accounts for structural redundancy and the typically longer shaft length that would be needed with a coaxial rotor design. This penalty factor is also used for the MTR design.

2.2.2 Transmission Weights

The weight of the main rotor transmission is defined in terms of the shaft torques required on the basis of Eq. 25. In the case of a conventional design, then the weight of the main rotor gearbox $W_{\mathrm{MR_{GB}}}$ is defined using

$$W_{\mathrm{MR_{GB}}} = k_{\mathrm{MR_{GB}}} (Q_{\mathrm{MR}})^{0.8} \tag{64}$$

The conventional helicopter design also requires a drive for the tail rotor, which comprises an intermediate gearbox off the main transmission, a transmission shaft and a tail rotor gearbox. The intermediate gear box weight W_{IGB} is given in terms of the tail rotor shaft torque required as

$$W_{\mathrm{IGB}} = k_{\mathrm{IGB}} (Q_{\mathrm{TR_{SH}}})^{0.8} \tag{65}$$

The tail rotor gearbox weight $W_{\mathrm{TR_{GB}}}$ is

$$W_{\mathrm{TR_{GB}}} = k_{\mathrm{TR_{GB}}} (Q_{\mathrm{TR}})^{0.8} \tag{66}$$

and finally the transmission shaft weight W_{SH} is

$$W_{\mathrm{SH}} = k_{\mathrm{SH}}\, C_{\mathrm{SH_G}}\, Q_{\mathrm{TR_{SH}}}^{0.8}\, l_{\mathrm{SH}} \tag{67}$$

where $C_{\mathrm{SH_G}}$ is a penalty factor to allow for future helicopter weight growth and l_{SH} is the tail rotor shaft length as given by

$$l_{\mathrm{SH}} = \frac{(D_{\mathrm{MR}} + D_{\mathrm{TR}} + D_{\mathrm{off}})}{2} \tag{68}$$

For the coaxial rotor system, the rotor gearbox weight is assumed to vary according to the equation

$$W_{\mathrm{MR_{GB}}} = 1.3\, k_{\mathrm{MR_{GB}}} (Q_{\mathrm{MR}})^{0.8} \tag{69}$$

where the factor of 1.3 accounts mostly for the additional planetary gearing required to produce two concentric output shafts.

2.2.3 Rotor Control Weights

The rotor control mechanism comprises the swashplate and pitch links (assuming a swashplate is used), the booster servo hydraulics and the automatic flight control system. The weight of the swashplate and control linkages depends on the blade loads, which depend in turn on the blade area and forward speed. The swashplate and control linkage weight is found to correlate with the equation

$$W_{\mathrm{SP}} = k_{1_{\mathrm{SP}}}\, c^2 R_{\mathrm{MR}}\, \mu + k_{2_{\mathrm{SP}}} \tag{70}$$

where $k_{1_{\mathrm{SP}}}$ and $k_{2_{\mathrm{SP}}}$ are constants and μ is the main rotor advance ratio which is defined as

$$\mu = \frac{V_{\mathrm{CR_{hel}}}\, \cos\alpha_{\mathrm{TPP}}}{(\Omega R)_{\mathrm{MR}}} \tag{71}$$

In the case of a coaxial rotor the weight of the swashplate and control system is higher and a parametric equation was developed in the form

$$W_{\mathrm{SP}} = 1.75 \left(k_{1_{\mathrm{SP}}}\, c^2\, R_{\mathrm{MR}}\, \mu + k_{2_{\mathrm{SP}}}\right) \tag{72}$$

The weight of the servo or hydraulic booster control system W_{BCS} is proportional to the size and weight of the swashplate and is defined as

$$W_{\mathrm{BCS}} = k_{1_{\mathrm{BCS}}}\, c^2\, R_{\mathrm{MR}}\, \mu + k_{2_{\mathrm{BCS}}} \tag{73}$$

Finally, the weight of the automatic flight control system W_{AFCS} is assumed to be a binary value that depends on the payload of the machine, i.e.,

$$W_{\mathrm{AFCS}} \begin{cases} 165 \text{ lb} & \text{if } W_{\mathrm{TO}} \leq 6 \text{ tons} \\ 330 \text{ lb} & \text{if } W_{\mathrm{TO}} > 6 \text{ tons} \end{cases} \tag{74}$$

2.2.4 Airframe Weights

On one hand, in the case of a conventional helicopter design, the fuselage weight depends on the takeoff weight, the weight of the payload and the size of the rotor. With an internally carried payload the fuselage weight is typically a function of the size and weight of the payload. On the other hand, the MTR is essentially an unmanned lifter with a suspended load, where the load includes a container handling system topped by a manned crew compartment. The rotating-wing portion of the unmanned lifter consists of engines, gearbox, rotor, fuel tank, and biped landing struts all connected together as a single unit having no conventional fuselage. The fixed-wing portion of the MTR also has no fuselage, but consists of a pivoting tailboom with tilt actuator, fuel tank and empennage, and folding wing panels pinned at their root to the tailboom. The load bearing members of the suspension structure and the container handling system carry tensile loads only to minimize structural weight. The container itself provides structural support for enveloping and streamlining fairings.

In all comparative studies, empty container weight of 5,000 lb was accounted for as included in payload weight, and a two person crew weight of 400 lb was assumed.

2.2.5 Fuselage Weights

For a conventional helicopter, Tishchenko et al. (Ref. 11) suggest that its fuselage weight W_{FUS} can be approximated by the parametric equation

$$W_{\mathrm{FUS}} = k_{1_{\mathrm{FUS}}} W_{\mathrm{TO}} + k_{2_{\mathrm{FUS}}} W_{\mathrm{PL}} + k_{3_{\mathrm{FUS}}} \left(D_{\mathrm{MR}} - D_{\mathrm{ref}}\right) \tag{75}$$

where the last term in this equation reflects the size of the main rotor relative to the nominal reference value used to determine the correlation coefficients.

The functional equivalent of a fuselage for the MTR is its combination of suspension structure, container handling system topped by a crew compartment, and the container itself. While the container provides some structural support, it is not included in airframe weight calculation for either the conventional helicopter or the MTR. Thus, the equation for MTR fuselage weight is

$$W_{\mathrm{FUS}} = W_{\mathrm{CHS}} + W_{\mathrm{SS}} + W_{\mathrm{CC}} \tag{76}$$

where W_{CHS}, W_{SS} and W_{CC} are defined in the following sections.

2.2.6 MTR Container Handling System Weight

Because the MTR carries an external load, the weight of the cargo handling system is an integral part of the overall design and not necessarily a function of payload weight. In this regard a structural analysis was performed to calculate the weight required to support a 20 foot long MILVAN container with cargo giving a 20 ton payload. This container will be used for payloads ranging from 10 to 32.5 tons. Therefore over this range, the size and weight of the payload handling unit will be constant. The weight of the cargo handling system is varied proportionally to the payload weight using

$$W_{\mathrm{CHS}} = k_{\mathrm{CHS}}\, W_{\mathrm{PL}} \tag{77}$$

with $k_{\mathrm{CHS}} = 0.050$, which means W_{CHS} = 2,000 lb for a 20 ton payload. The cargo handling system weight includes the tail capture mechanism.

2.2.7 Suspension Structure Weight

The weight of the trapeze struts of the suspension structure was estimated using

$$W_{\mathrm{SS}} = 2\, k_{\mathrm{SS}}\, l_{\mathrm{SS}} \left(\frac{P_{\mathrm{crit}} - k_{2_{\mathrm{SS}}}}{k_{1_{\mathrm{SS}}}} \right) \tag{78}$$

where k_{SS} is the mass density of the struts. The parameter P_{crit} represents a critical load for the trapeze design and is defined as a fraction of the vehicle weight.

2.2.8 Crew Compartment and Furnishings Weight

The MTR crew compartment is simply a canopy installed atop the container handling system and supported through the suspension structure. For this conceptual design, the weight of the structure of MTR crew compartment W_{CC} was assumed constant and respresented using

$$W_{\mathrm{CC}} = 500 \text{ lb} \tag{79}$$

For the conventional helicopter analysis, crew compartment weight is part of fuselage weight, so the above equation does not apply.

Cockpit instrumentation, avionics, sensors and cockpit furnishings is assumed to be given by the equation

$$W_{\mathrm{INST}} = 0.075 W_{\mathrm{PL}} \tag{80}$$

based on the work of Tishchenko et al. (Ref. 11).

2.2.9 MTR Tilt Boom & Actuator Weights

The weight of the tilt boom on the MTR is related to the vehicle size and its takeoff weight. From a more detailed design study the weight was determined to be approximately proportional to takeoff weight and in the conceptual design studies it was modeled using the equation

$$W_{\mathrm{TB}} = k_{\mathrm{TB}}\, W_{\mathrm{TO}} \tag{81}$$

Similarly, the tilt actuator was modeled using

$$W_{\mathrm{TM}} = k_{\mathrm{TM}}\, W_{\mathrm{TO}} \tag{82}$$

where the coefficient k_{TM} has been determined based on weight estimates that were conducted for the tilt actuators used on conventional tiltrotor aircraft such as the V-22 Osprey.

2.2.10 Empennage Weights

The empennage weight depends on the surface area of the horizontal and vertical tails. For a conventional single rotor helicopter, Tishchenko et al. (Ref. 11) suggest that the empennage area is approximately 2% of the main rotor disk area and its weight is given by

$$W_{\mathrm{EMP}} = k_{\mathrm{EMP}}\, A_{\mathrm{EMP}} = 0.005\pi\, k_{\mathrm{EMP}}\, D_{\mathrm{MR}}^2 \tag{83}$$

For a helicopter with a coaxial rotor the horizontal and vertical tails are considerably larger, at least twice that of a single rotor helicopter with its long tail boom. This is reflected by changing the weight equation for the empennage of a coaxial machine to

$$W_{\mathrm{EMP}} = k_{\mathrm{EMP}} A_{\mathrm{EMP}} = 0.015\pi\, k_{\mathrm{EMP}} D_{\mathrm{MR}}^2 \tag{84}$$

In the case of the MTR, the horizontal and vertical tails are sized differently to a helicopter, in part to meet stability and control requirements in airplane mode. Therefore, the empennage sizing proceeded using a different set of parametric equations developed for the design of a fixed-wing aircraft. In the case of the horizontal tail the equation for its weight, W_{HT}, (Ref. 19) is

$$W_{\mathrm{HT}} = 5.25\, S_{\mathrm{HT}} + 0.8 \times 10^{-6} \frac{n_{\mathrm{ult}}\, b_{\mathrm{H}}^3\, W_{\mathrm{TO}}\, \bar{c}_{\mathrm{w}}\, \sqrt{S_{\mathrm{HT}}}}{(t/c)_{\mathrm{HT}}\, \cos^2 \Lambda_{\mathrm{HT}}\, l_{\mathrm{sep}}\, S_{\mathrm{w}}^{3/2}} \tag{85}$$

where n_{ult} is the ultimate load factor. The weight of the vertical tail, W_{VT}, is given by

$$W_{\text{VT}} = 2.65\, S_{\text{VT}} + 0.8 \times 10^{-6} \frac{n_{\text{ult}}\, b_{\text{V}}^3 (8.04 + 0.44(W_{\text{TO}}/S_{\text{w}})}{(t/c)_{\text{VT}}\, \cos^2 \Lambda_{\text{VT}}} \tag{86}$$

Finally, the weight of the horizontal tail boom, W_{TB}, is estimated using

$$W_{\text{TB}} = 0.998\, W_{\text{DG}}^{0.35}\, n_{\text{ult}}\, l_{\text{TB}}^{0.5}\, D_{\text{TB}}^{1.534} \tag{87}$$

where the design gross weight is

$$W_{\text{DG}} = W_{\text{TO}} - 0.5 W_{\text{FUEL}} \tag{88}$$

2.2.11 MTR Wing Weights

The wings of the MTR comprise a significant part of the overall airframe weight. The wing center box is also used for fuel storage, although the wings themselves are designed to be as light as possible because they are primarily self-actuated by dynamic pressure as the MTR transitions to and from forward flight. The parametric equation used for the wing weight (Ref. 20) is

$$\begin{aligned} W_{\text{WING}} &= 0.0051\, (W_{\text{DG}}\, n_{\text{ult}})^{0.557}\, S_{\text{w}}^{0.649} AR^{0.5}\, (t/c)_{\text{W}})^{-0.4} \\ &\quad (1 + AR_{\text{W}})^{0.1} \cos^{-1} \Lambda_{\text{W}}\, (0.09 S_{\text{w}})^{0.1} \end{aligned} \tag{89}$$

where

$$W_{\text{DG}} = W_{\text{TO}} - 0.5 W_{\text{FUEL}} \tag{90}$$

An allowance was made for the wing pivot and wing actuator using

$$W_{\text{WTM}} = k_{\text{WTM}}\, W_{\text{WING}} \tag{91}$$

2.2.12 Power Plant & Fuel System Weights

The weight of the engine is essentially proportional to its power output. For a turboshaft engine the net uninstalled engine weight is given by the equation

$$W_{\text{ENG}} = N_{\text{ENG}}\, (k_{1_{\text{ENG}}} P_{\text{ENG}} + k_{2_{\text{ENG}}}) \tag{92}$$

To take account of the engine installation (intake, exhaust, mounts etc.) the power plant installation system (PIS) weight is assumed to be proportional to the engine weight, i.e.,

$$W_{\mathrm{PIS}} = k_{\mathrm{PIS}}\, W_{\mathrm{ENG}} \tag{93}$$

The weight of the engine fuel system is governed by the amount of fuel carried (i.e., by the size of the tanks) and by the lengths of the fuel lines and number of fuel pumps. The fuel system weight W_{FS} is assumed to be given by the equation

$$W_{\mathrm{FS}} = k_{\mathrm{FS}}\, W_{\mathrm{FUEL}} \tag{94}$$

In addition to the main engines, the weight of an auxiliary power unit (APU) for main engine starting and to power various electrical and hydraulic systems prior to engine start must be accounted for. The weight of the APU is essentially proportional to the power of one of the main engines and can be written as

$$W_{\mathrm{APU}} = k_{1_{\mathrm{APU}}} P_{\mathrm{ENG}} + k_{2_{\mathrm{APU}}} \tag{95}$$

2.2.13 Electrical System Weight

The weight of the electrical system is driven, on average, by the size of the machine and, in particular, the need for any anti-icing system. The parametric equation used for the electrical system weight was

$$W_{\mathrm{ES}} = k_{\mathrm{ES}}\,(1 + 0.08\, N_{b_{\mathrm{MR}}}\, c_{\mathrm{MR}}\, R_{\mathrm{MR}}) \tag{96}$$

where the second term accounts for the extra electrical power required for anti-icing, if included.

2.2.14 Landing Gear Weight

For a conventional helicopter the weight of the landing gear was assumed to be proportional to the maximum takeoff weight, i.e.,

$$W_{\mathrm{LG}} = k_{\mathrm{LG}}\, W_{\mathrm{TO}} \tag{97}$$

For the MTR with a self-supporting payload, landing gear weight was assumed to be proportional to the maximum takeoff weight less payload weight, i.e.,

$$W_{\mathrm{LG}} = k_{\mathrm{LG}}\,(W_{\mathrm{TO}} - W_{\mathrm{PL}}) \tag{98}$$

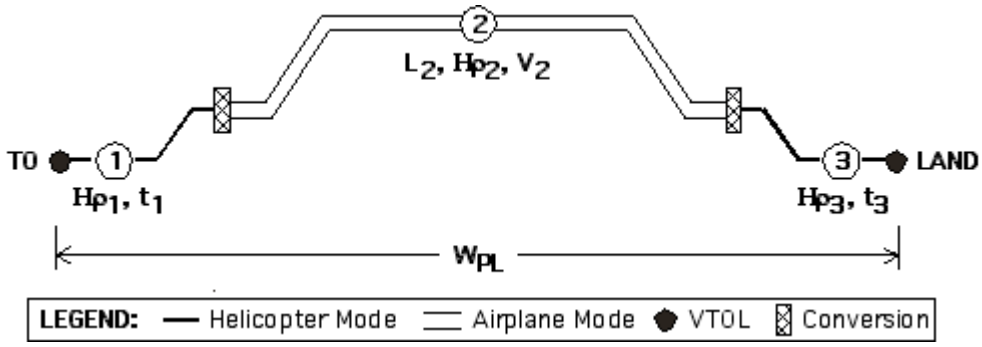

Figure 8: MTR Long-range cruise mission profile.

2.2.15 Ground Handling Equipment Weight

Ground handling equipment is required for the efficient loading and unloading of some types of payloads. This is carried with the aircraft. For a conventional helicopter, the equation for the ground handling equipment weight is assumed to be a fraction of the payload weight, as given by

$$W_{\mathrm{GHE}} = k_{\mathrm{GHE}}\, W_{\mathrm{PL}} \tag{99}$$

For the MTR, the foregoing equation is inapplicable as the MTR's container handling system provides this function.

2.3 MTR Mission Model

For an accurate assessment of mission perfromance, an analytical mission model was developed with consideration for mission profile, cruise altitude, and hover time.

2.3.1 Mission Profiles

To develop this capability, several mission profiles were created and implemented into the design code. The first of the three mission profiles considered was a long-range cruise mission, as depicted in Fig. 8. In this first mission profile, the aircraft takes off in helicopter mode with payload at a given density altitude H_{ρ_1}, hovers for some time t_1, converts to airplane mode and climbs to the design cruise density altitude, H_{ρ_2}. The MTR then cruises for a given range L_2, at cruise speed V_2. The aircraft then descends and converts back to helicopter mode, hovers for some time t_3 at density altitude H_{ρ_3}, and then lands at the destination.

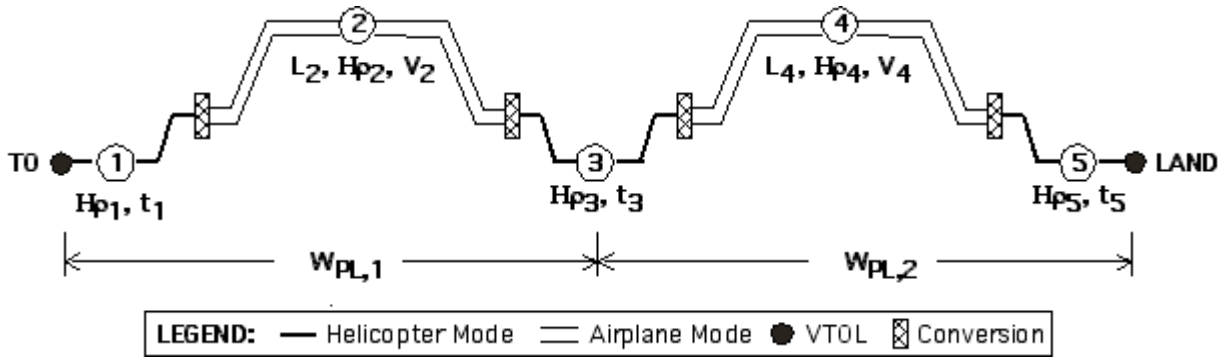

Figure 9: MTR radius of action mission profile.

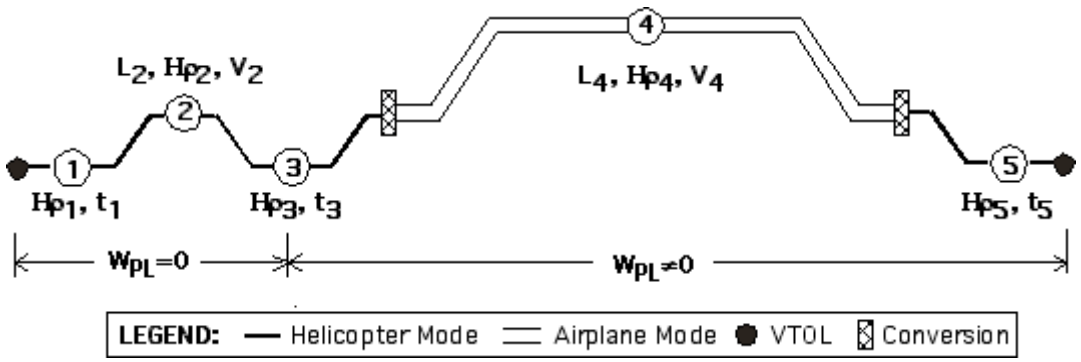

Figure 10: MTR helicopter pickup mission profile.

The second mission profile considered was a radius of action mission, as depicted in Fig. 9. In the radius of action mission profile, the aircraft takes off in helicopter mode, converts to airplane mode and cruises to a destination point where there is some hover time, t_3, allotted for dropping the payload (in helicopter mode) of weight, W_{PL_1}, and picking up an optional payload, W_{PL_2}. The aircraft then converts back to airplane mode, climbs, and either cruises back to the original takeoff point, or to some other specified destination.

The third mission profile considered was a helicopter pickup mission, as depicted in Fig. 10. This mission profile was designed for an operation in which the payload is not at the same location as the takeoff point, requiring the MTR to travel to the payload in helicopter cruise mode for some short distance, L_2. After collecting the payload in hover mode over some time, t_3, the aircraft converts to airplane mode and climbs to cruise altitude for some distance L_4 until the destination is reached.

2.3.2 Detailed Fuel Burn Calculation

These three mission profiles were integrated into the design code, incorporating appropriate subroutines that calculated iteratively the fuel requirements and overall size of the MTR. A flow chart diagram of the modified design analysis is shown in Fig. 4. After making estimates of the MTR takeoff weight, rotor size and wing size, a mission subroutine is called for the specified mission profile to which the MTR is to be designed. This mission profile subroutine calculates the power requirements for the vehicle, the lift-to-drag ratio, the specific fuel consumption and the fuel requirements for each mission leg based on the estimated size of the aircraft and the mission inputs. The fuel requirements for the mission legs were calculated in sequence, with the updated weight for each subsequent mission leg, thereby simulating the fuel being burnt during the appropriate portions of the flight.

To examine the performance of the MTR at altitude, the properties of the standard atmosphere were used along with inputs of an assumed pressure altitude, H_P, and the temperature above mean sea level, ΔT. These were used to calculate the air density, ρ, and engine lapse factor, k_{alt}. The density ratio, σ_{P}, as found in the standard atmosphere, can be found by the equation

$$\sigma_{\text{P}} = \frac{\rho}{\rho_0} = \left(1 - 6.873 \times 10^{-6} H_{\text{P}}\right)^{5.26} \left(\frac{T_0}{T_0 + \Delta T}\right) \tag{100}$$

where H_{P} is the pressure altitude and ΔT is the temperature above or below standard temperature at that altitude. The density of the air was then calculated from the standard sea level density ρ_0 using

$$\rho = \rho_0 \, \sigma_{\text{P}} \tag{101}$$

The engine lapse factor accounts for the degradation in performance of a turboshaft engine at altitudes above sea level conditions and temperatures above or below standard conditions. The engine lapse factor is based on the performance of an average modern turboshaft engine and was calculated as a function of the density altitude as

$$k_{\text{ALT}} = \left(1 - 2.23 \times 10^{-4} H_{\rho}\right)^{-1} \tag{102}$$

where the power at altitude P_{ALT} is given by

$$P_{\text{ALT}} = \frac{P_{\text{MSL}}}{k_{\text{ALT}}} \tag{103}$$

These values were calculated for each mission leg based on the design inputs before performing the mission calculation steps.

The following is a sequential list of calculations for the long-range mission profile with mission legs 1 through 3:

- **Mission Leg 1**

  As shown in Fig. 8, the first mission leg is hovering flight in helicopter mode just after takeoff. To calculate the fuel required to hover for a given time, the power required to hover out of ground effect, P_1, must be calculated using

$$P_1 = \frac{(W_{\mathrm{TO}}\, t_{\mathrm{MR}})^{3/2}}{\sqrt{\pi/2}\, FM_{\mathrm{MR}}\, \eta_{\mathrm{coax}}\, \zeta_{\mathrm{MR}}\, D_{\mathrm{MR}}\, \sqrt{\sigma_1}\, \sqrt{\rho_0}} \tag{104}$$

  This is also the power required for takeoff, which is used to set the overall engine requirements. The engine power required was calculated based on the power required to takeoff, P_1, the number of engines, and the takeoff density altitude, the latter which is represented by the engine lapse factor, k_{ALT_1}. Therefore, the engine power required is

$$P_{\mathrm{ENG}} = \frac{P_1\, k_{\mathrm{ALT}_1}}{N_{\mathrm{ENG}}} \tag{105}$$

  The engine power required will be higher if the takeoff density altitude is higher than mean sea level conditions, leading to a larger engine(s) and a heavier aircraft. The nominal engine power was then calculated using

$$P_{\mathrm{ENG}_{\mathrm{NOM}}} = P_{\mathrm{ENG}}\, C_{\mathrm{POW}} \tag{106}$$

  The specific fuel consumption, SFC, was calculated (as shown previously in the Methodology section) as a function of power required and the power available using

$$SFC_1 = Ce_1 + \frac{Ce_2}{P_1/(P_{\mathrm{ENG}}\, N_{\mathrm{ENG}})} \tag{107}$$

  The total fuel required for the first mission leg was then calculated as a function of the power required, the specific fuel consumption, and time required in the hover, t_1 using

$$W_{\mathrm{F}_1} = P_1\, SFC_1\, t_1 \tag{108}$$

- **Mission Leg 2**

The second mission leg is a long-range cruise in airplane mode, as shown in Fig. 9. The fuel requirements for this mission leg were calculated differently. The first step was to adjust the weight of the aircraft based on the fuel burnt in the previous mission leg by simply subtracting this weight from the initial takeoff weight using

$$W_2 = W_{\mathrm{TO}} - W_{\mathrm{F}_1} \tag{109}$$

The new aircraft gross weight, W_2, represents the weight of the aircraft at the beginning of the second mission leg, and this weight was then used for all of the subsequent calculations.

To calculate the power requirements and, ultimately, the lift-to-drag ratio of the MTR in airplane cruise, it is necessary to calculate the lift coefficient of the wing. This was calculated by using the definition of the lift coefficient and with the use of specific mission input values for the second mission leg, giving the following equation

$$C_{\mathrm{L}_2} = \frac{2W_2}{\rho_2\, V_2^2\, S_{\mathrm{W}}} \tag{110}$$

The lift coefficient in cruise was then used to calculate induced drag (drag resulting from lift), $C_{\mathrm{D_i}}$, of the MTR in cruise with the following standard equation

$$C_{\mathrm{D_i}} = \frac{C_{\mathrm{L}}^2}{\pi\, AR_{\mathrm{W}}\, e_{\mathrm{W}}} \tag{111}$$

The induced drag is used in combination with the mission inputs and equivalent flat plate parasitic drag of the MTR in airplane mode to calculate the net power requirements in cruise (as shown previously) using

$$P_2 = \frac{\rho_2 V_2^3\,(f_{\mathrm{air}} + S_{\mathrm{W}}\, C_{\mathrm{D_i}})}{2\eta_{\mathrm{prop}}\, \zeta_{\mathrm{air}}} \tag{112}$$

The power available in the second mission leg, P_{AV_2}, depends upon the total engine power and the engine power lapse with density altitude. This is represented in the equation

$$P_{\mathrm{AV}_2} = \frac{P_{\mathrm{ENG_{NOM}}}\, N_{\mathrm{ENG}}}{k_{\mathrm{ALT}_2}} \tag{113}$$

Power available will decrease with increases in density altitude. The specific fuel consumption for this mission leg was calculated again as a function of the ratio between required and

available power using

$$SFC_2 = Ce_1 + \frac{Ce_2}{(P_2/P_{\mathrm{AV}_2})} \tag{114}$$

The lift-to-drag ratio, which is a measure of aerodynamic efficiency, is required to calculate the fuel burnt during cruise. This was calculated (as shown previously) using

$$\left(\frac{L}{D}\right)_2 = \frac{W_2\, V_2}{P_2\, \eta_{\mathrm{prop}}\, \zeta_{\mathrm{air}}} \tag{115}$$

The vehicle energy efficiency, E_2, was calculated as a function of the aerodynamic, propulsive, mechanical and fuel efficiencies of the aircraft using

$$E_2 = \frac{(L/D)_2\, \eta_{\mathrm{prop}}\, \zeta_{\mathrm{air}}}{SFC_2} \tag{116}$$

The fuel requirements for the second mission leg are then calculated as a function of the vehicle energy efficiency, aircraft gross weight and the mission input range, L_2, using

$$W_{\mathrm{F}_2} = W_2\big(1 - \exp(-L_2/E_2)\big) \tag{117}$$

- **Mission Leg 3**

The third and final mission leg for this long-range haul profile is characterized by hovering flight in helicopter mode, as shown in Fig. 10. After the previous two mission legs, the gross weight of the aircraft should be much lower than at takeoff. Therefore, the aircraft weight at the start of this final mission leg is given by

$$W_3 = W_2 - W_{\mathrm{F}_2} \tag{118}$$

The greatly reduced gross weight of the MTR in the final mission leg leads to much lower power requirements and, therefore, the required fuel load. The power requirements were calculated in a manner similar to those of the first mission leg using

$$P_3 = \frac{(W_{\mathrm{TO}}\, t_{\mathrm{MR}})^{3/2}}{\sqrt{\pi/2}\, FM_{\mathrm{MR}}\, \eta_{\mathrm{coax}}\, \zeta_{\mathrm{MR}}\, D_{\mathrm{MR}}\, \sqrt{\sigma_3}\, \sqrt{\rho_0}} \tag{119}$$

As before, the power available in this mission leg was calculated based on the total engine power and the engine lapse from changes in density altitude using

$$P_{\mathrm{AV}_3} = \frac{P_{\mathrm{ENG}_{\mathrm{NOM}}}\, N_{\mathrm{ENG}}}{k_{\mathrm{ALT}_3}} \tag{120}$$

The specific fuel consumption was calculated similarly as

$$SFC_3 = Ce_1 + \frac{Ce_2}{(P_3/P_{\mathrm{AV}_3})} \tag{121}$$

Finally, the required fuel weight for the third and final mission leg was calculated as a function of the power requirements, specific fuel consumption and mission input hover time using

$$W_{\mathrm{F}_3} = P_3\, SFC_3\, t_3 \tag{122}$$

The total fuel weight for the mission is then taken as the sum of the individual mission leg fuel requirements with additional factors for takeoff, landing, climb, descent, conversion between flight modes and reserve fuel so that

$$W_{\mathrm{F_{TOT}}} = (1 + k_{\mathrm{F}})\,(W_{\mathrm{F}_1} + W_{\mathrm{F}_2} + W_{\mathrm{F}_3} + W_{\mathrm{F_{RES}}}) \tag{123}$$

The fuel reserve, $W_{\mathrm{F_{RES}}}$, was calculated as a function of the power requirements in cruise, the specific fuel consumption and the required reserve time (normally 20 minutes) as

$$W_{\mathrm{F_{RES}}} = P_2\, SFC_2\, t_{\mathrm{RES}} \tag{124}$$

The factor k_{F} accounts for takeoff, landing, climb and conversion, which is given as a function of the number of conversions between modes, N_{CONV}, and the number of full climbs and descents involved in a given mission profile, N_{CL}, i.e.,

$$k_{\mathrm{F}} = N_{\mathrm{CONV}}\, k_{\mathrm{CONV}} + N_{\mathrm{CL}}\, k_{\mathrm{CL}} \tag{125}$$

For the simple long-range haul mission profile, the values of N_{CONV} and N_{CL} are 2 and 1, respectively. For the radius of action mission profile, these values would be 4 and 2.

After the total fuel requirements were calculated, the takeoff weight is recalculated using this newly calculated fuel weight and the current values for the empty weight, payload and crew weight using

$$W_{\mathrm{TO}} = W_{\mathrm{EMPTY}} + W_{\mathrm{PL}} + W_{\mathrm{F_{TOT}}} + W_{\mathrm{CREW}} \tag{126}$$

The rotor size, D_{MR}, and wing area, S_{W}, are then recalculated, as discussed previously. The mission subroutine then iterates until a convergence threshold is reached, at which point the

proper fuel weight and aircraft size for the given empty weight is obtained. This process is implemented as a loop within the main design calculation loop, which uses the component weight equations to converge on the proper combination of empty weight and size, as shown in Fig. 4.

3 Application of Methodology

A significant number of calculations were conducted, both to validate the design analysis as well as to use the analysis as a predictive tool. In the first instance parametric validation studies for single and dual rotor (coaxial and tandem) helicopters were undertaken. This was followed by a design study for a helicopter to meet the requirements of a 20 ton useful payload carried over a 1,000 nm range mission. Comparative studies of the MTR against legacy helicopter designs was also considered, which show the substantial benefits of the MTR if it were to be technically realized.

3.1 Single Rotor Helicopter

Sizing estimates for the conventional single rotor helicopter are shown in Figs. 11 through 14 in terms of rotor size (rotor diameter), empty and maximum takeoff weights, and installed power requirements versus the net useful payload to be carried. Results are shown for unrefueled ranges of 110 to 330 nm (200 to 600 km), which would be typical for a conventional helicopter operating at or near maximum payload. Data points for several legacy helicopter designs are shown for reference and to help provide an appropriate validation of the design methodology.

Figure 11 shows predictions of the main rotor diameter versus payload (in tons). Notice that there is a break in the correlations near the 5 ton payload mark. The reasons for this were apparent from many of the subsystem weight correlation studies, where the correlation coefficients used to develop the parametric equations were found to be different for larger versus smaller helicopters. Another break in the correlation curves is shown near the 10 ton payload mark. This is because the design analysis predicts an increase in the number of rotor blades in an attempt to maintain a high blade aspect ratio (for efficiency) for a given rotor solidity and blade loading coefficient.

Notice also from Fig. 11, that the size of the rotor increases logarithmically with the payload required to be carried. This behavior is consistent with the well-known square-cube law, which predicts that the helicopter weight will grow much faster than the rotor size, the rotor size being determined based on the equations given previously. This point is made further in Fig. 12, which shows that takeoff weight is proportional to payload, so that the rotor radius is proportional to either $W_{\mathrm{PL}}^{1/3}$ or $W_{\mathrm{TO}}^{1/3}$. This means that for very large payloads (exceeding 25 tons) the size of the

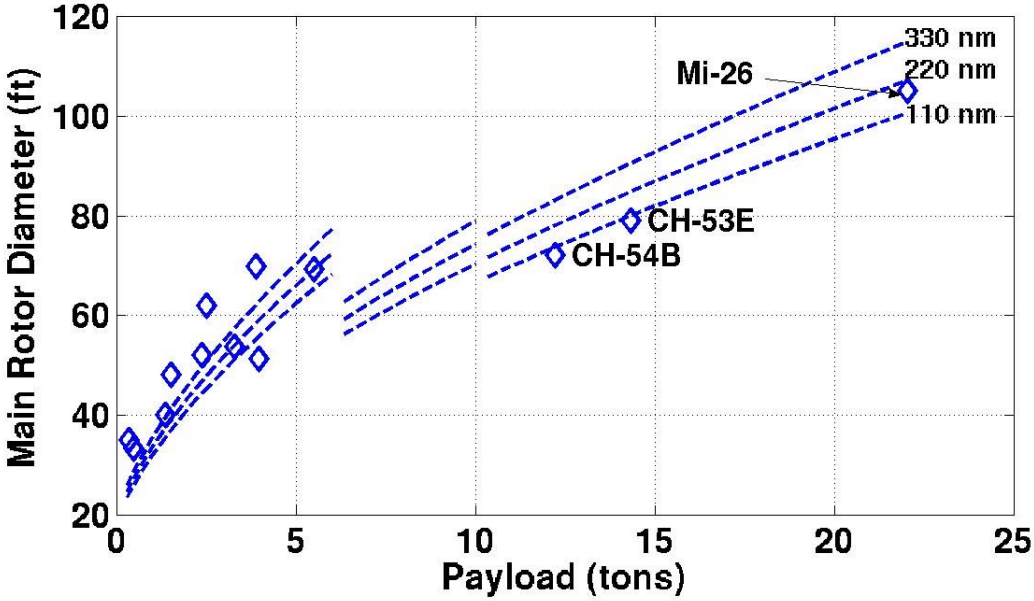

Figure 11: Predicted main rotor diameter versus payload for single rotor helicopters.

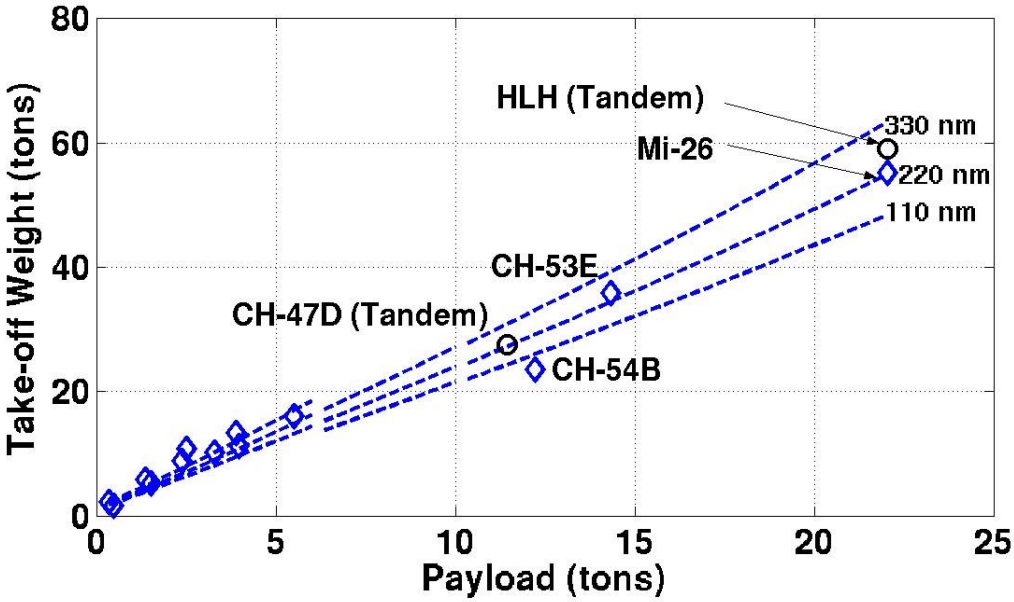

Figure 12: Predicted gross takeoff weight versus payload for single rotor helicopters.

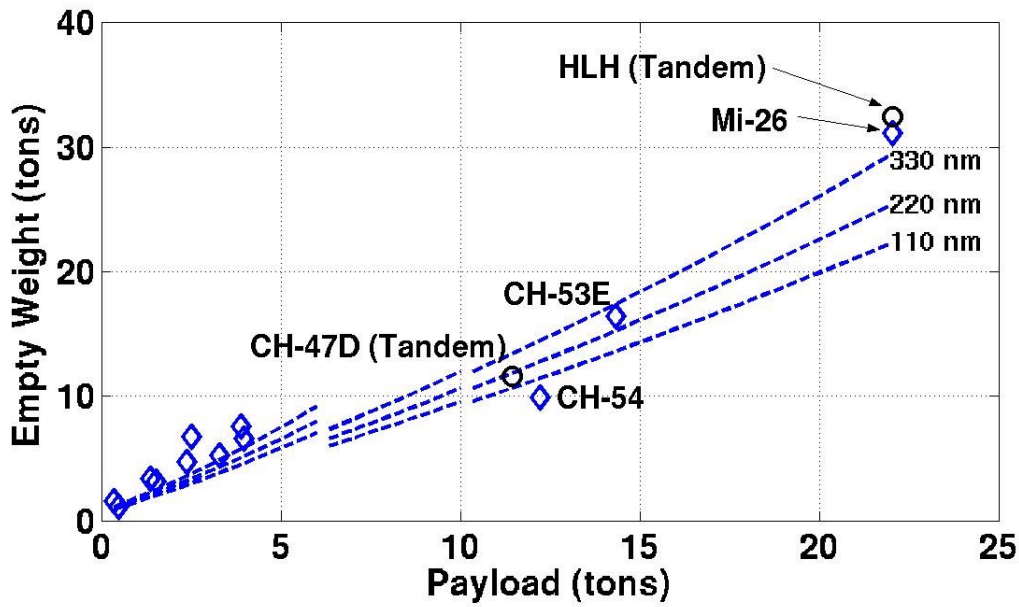

Figure 13: Predicted empty weight versus payload for single rotor helicopters.

rotor will become extremely large, and will become harder to build successfully. This immediately points to the possibilities of a coaxial rotor configuration (with its smaller rotor diameter) in better meeting heavy-lift requirements.

The predicted empty weight versus payload for the single rotor helicopter is shown in Fig. 13, and suggests a nearly linear relationship. Of particular interest are the results obtained for payloads of 10 tons and greater. Shown on the plots are data points for several "heavy-lift" helicopters, including the Sikorsky CH-53, CH-54 and Mil Mi-26, as well as the Boeing CH-47 and HLH, even though these are tandem machines.

Notice that the empty weight of the helicopter designs becomes very high for the larger payloads, with empty weights of between 20 and 25 tons for a 20 ton useful payload, which depends also on the range requirement. A further discussion of range issues on empty weight fraction for various vertical lift concepts is given later in this report.

The predicted installed power requirements for the single rotor helicopter are shown in Fig. 14 based on the performance equations laid down in the previous section. The agreement is considered acceptable. The predictions confirm that installed power requirements will become very large (approaching 20,000 hp) for the bigger machines that carry large payloads. Again, data points for

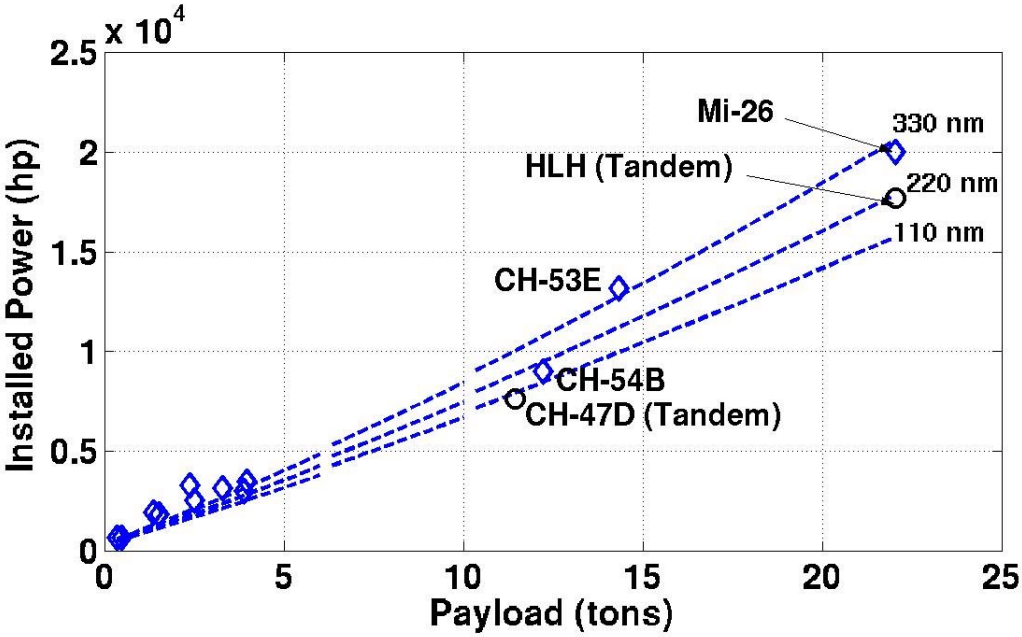

Figure 14: Predicted power requirements versus payload for single rotor helicopters.

the Boeing CH-47 and HLH are shown here for reference.

Figures 15 through 18 show some predicted component weights for the conventional single rotor helicopter. Figure 15 shows the predicted total blade weight versus payload. Blade weight is driven by blade area, which increases with rotor radius (Fig. 11). Blade weight is also determined by the need to increase chord and/or the number of blades to maintain reasonably low values of C_T/σ to retain sufficient stall margins that are necessary to meet forward flight and maneuver requirements. Overall, the predictions were found to be in good agreement with historical data. Notice that the 8-bladed Mi-26 comes in slightly heavier than the 8-blades of the HLH (a tandem with two four bladed rotors – see Ref. 21). This is partly because of the different types of assumed blade construction (conventional metallic versus advanced composites).

Figure 16 shows results for the rotor hub weight. Again, the agreement of the predictions with historical data is considered good. Hub weight is driven by centrifugal forces on the blades, so inevitably hub weight grows quite rapidly with blade weight and with the overall size of the helicopter. In this case it is interesting to note that the results for the Mi-26 and HLH (sum of both rotor hub weights) are in good agreement, even though the machines are of different configurations.

Figure 17 shows predictions of the overall transmission weight, including the main rotor and

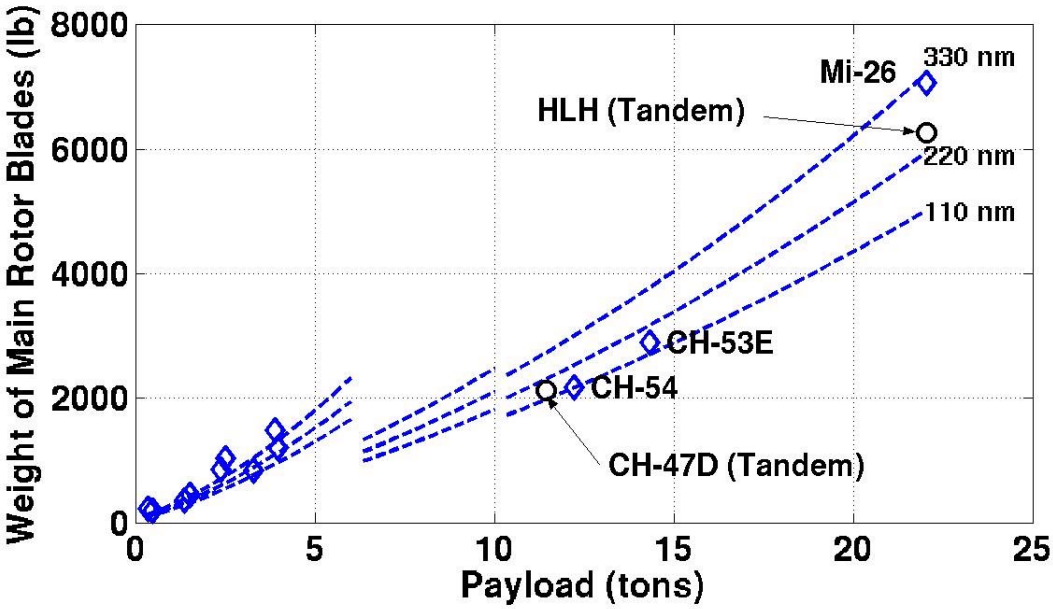

Figure 15: Predicted blade weights versus payload for single rotor helicopters.

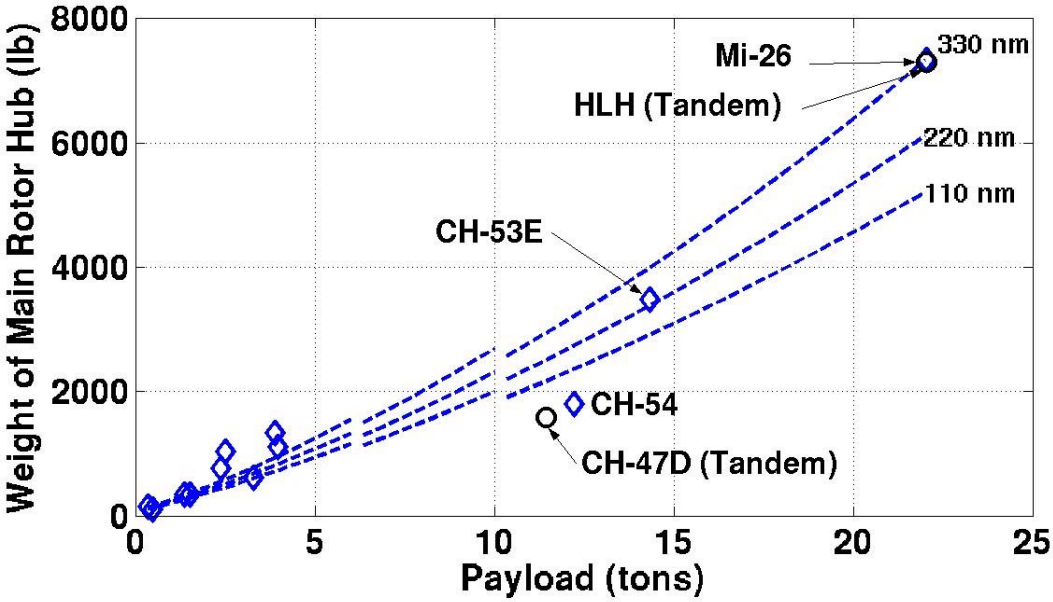

Figure 16: Predicted hub weights versus payload for single rotor helicopters.

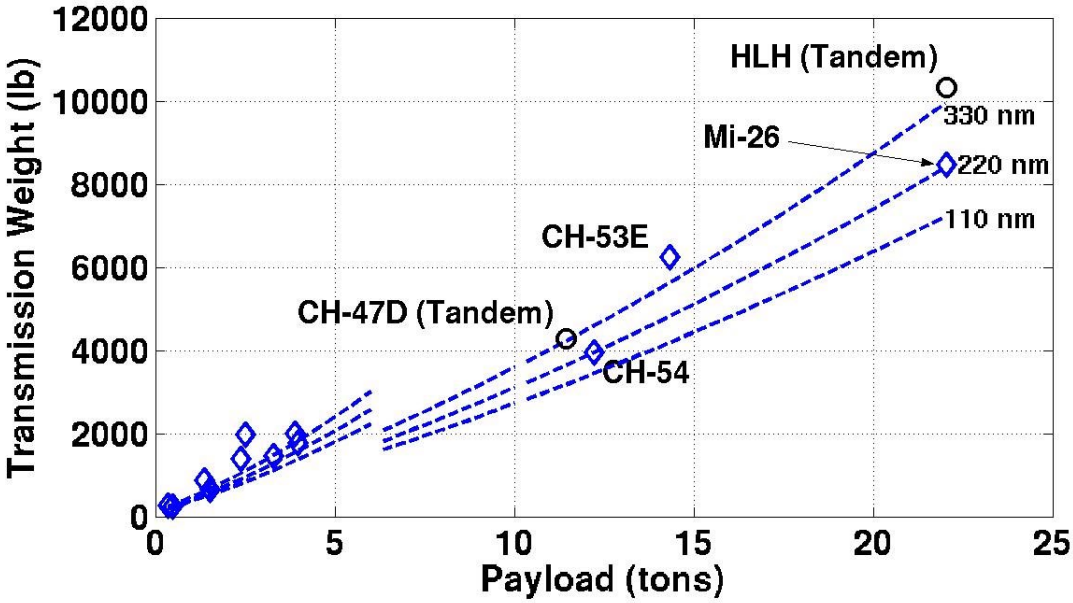

Figure 17: Predicted transmission weights versus payload for single rotor helicopters.

tail rotor transmissions. Transmission weight is driven by overall main rotor torque requirements. The Mi-26 and HLH (Ref. 22) have the biggest transmissions ever designed for helicopters (Ref. 23). Of some interest is that the transmission weight for the HLH comes in about 20% higher than for the Mi-26. This is because the Mi-26 is a split torque design compared to the spiral bevel design on the HLH, and also reflects the need for the interconnect drive shafts with a tandem design. This is despite the fact that the Mi-26 has a very large tail rotor and a long interconnect drive with a secondary gearbox. This point is considered again in the next section in regard to the design of the coaxial rotor helicopter and the MTR.

Figure 18 shows the engine weight versus payload. Overall, good correlations are shown but the analysis tends to slightly over-predict engine weights for the CH-54 and CH-53E, and under-predict the engine weight for the large Mi-26 helicopter. The latter can be explained by the fact that, historically at least, engines designed in the West have shown better power-to-weight ratios. It would be expected that the present results for engine weights are on the pessimistic side overall and further work is planned to examine and improve upon these particular sets of parametric equations.

Figure 19 shows the predicted fuselage weight versus payload of the single rotor helicopter. The results were found to be in good agreement with historical data, where available. Notice that

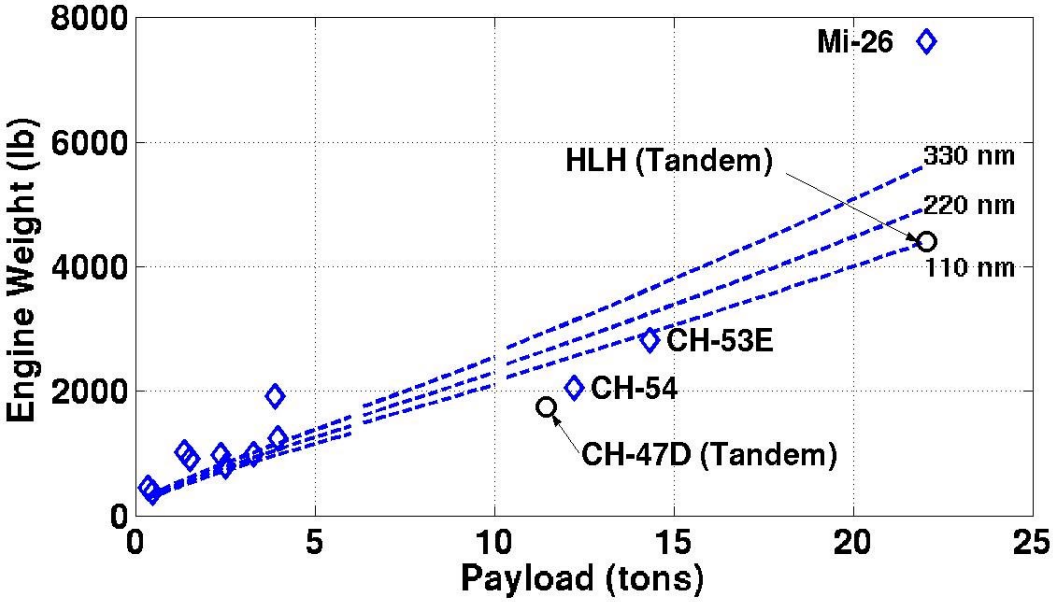

Figure 18: Predicted engine weights versus payload for the single rotor helicopters.

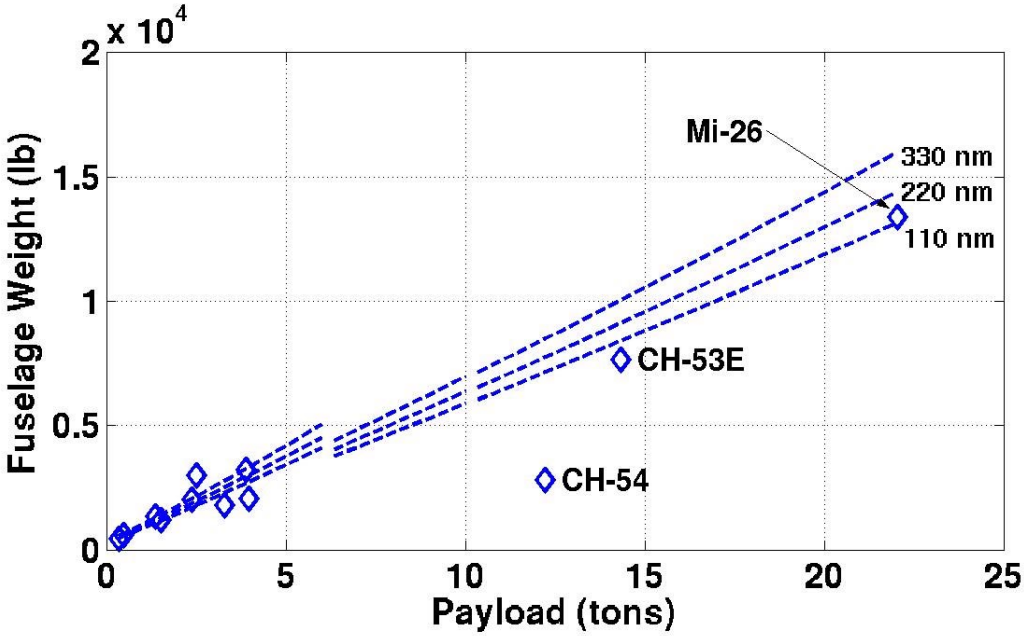

Figure 19: Predicted fuselage weight versus payload for single rotor helicopters.

the CH-54 is a crane design and does not have a conventional fuselage, so this data point sits well below the correlation line.

The overall sizing and component weight correlations obtained for the single rotor helicopter designs is very encouraging, and lends to relatively good confidence levels in the design analysis developed here. While it is apparent that in some cases the correlations could be improved, the results obtained thus far were considered sufficiently good to proceed to the analysis of a coaxial rotor helicopter.

3.2 Coaxial Dual Rotor Helicopter

The design analysis was extended to specifically encompass dual rotor coaxials. This involved several modifications and changes to the parametric equations, including aerodynamic changes to take into account losses that are a consequence of rotor-on-rotor interference, as well as appropriate weight estimates for the coaxial rotor hub and the different type of airframe (no tail boom but larger empennage).

A dual rotor coaxial hub is complicated by the approximate doubling of the number of total blades (but this depends on several factors), the need for a longer (and heavier) main rotor shaft, and for a secondary swashplate with control linkages and bigger and more powerful control actuators. There are also modifications to the parametric equations required to represent the transmission weights. Of course the tail rotor, its transmission and associated gearboxes can be dispensed with on a dual rotor coaxial design. This is a significant weight savings.

To our knowledge there are no existing parametric equations based on historical data that have been derived and published for the design of a dual rotor coaxial system, and this is probably the first time such an analysis has been undertaken outside the helicopter industry. Historical data were obtained for Kamov dual rotor coaxial helicopters (although published data are still relatively limited in scope), and were used to help verify the modified design analysis.

The results for the general sizing of the coaxial helicopters are shown in Figs. 20 through 23. Good correlations were obtained against the results for the Kamov helicopters, where historical data were available. There have been no large dual rotor coaxial helicopters designed with payloads more than 5 tons, and so there are no historical data available in this range to compare with. In this case, the design analysis proceeded on the basis of adjusted trends for large single rotor systems

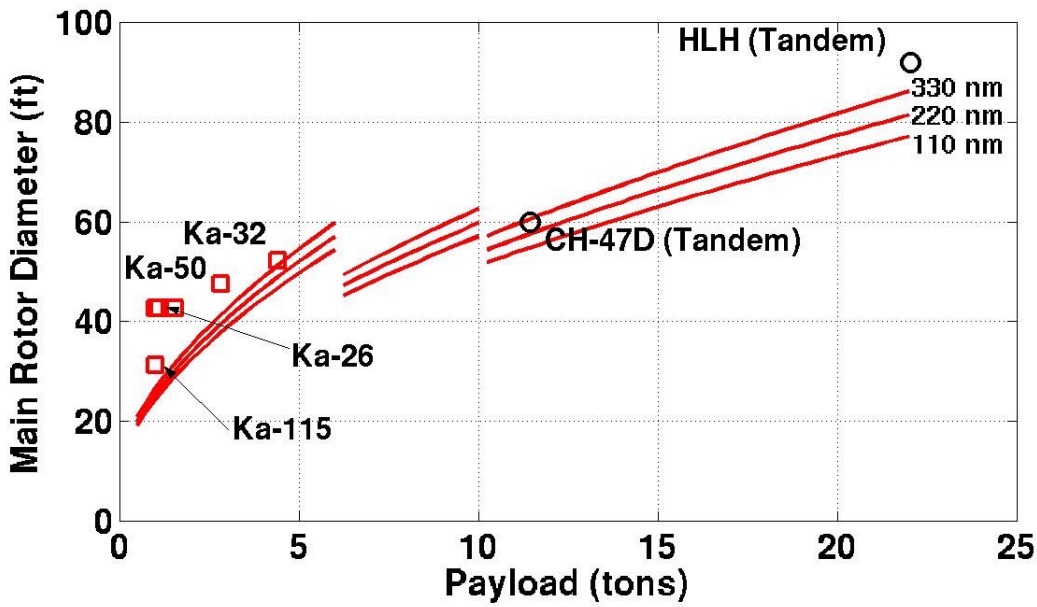

Figure 20: Predicted rotor diameter versus payload for coaxial dual rotor helicopters.

with further adjustments of the estimated weights and aerodynamic losses extrapolated based on results for the smaller, dual rotor coaxial helicopters.

Figure 20 shows the rotor diameter versus payload for the coaxial designs. These results basically follow the square-cube law in a manner similar to that found for the single rotor machines (Fig. 11). However, in this case the rotor is about 25% smaller than an equivalent single rotor machine when carrying the same payload over the same range. Nevertheless, for large payloads of 20 tons or more the rotor diameter exceeds 80 ft, which is not a small rotor by any standard.

For the lighter payloads, the predictions of rotor size were found to be in good agreement with historical data for the Kamov machines. For the heavier payloads no historical data exist for coaxials, but data points for the tandem rotor CH-47 and HLH machines are shown as a reference. There is good agreement. Notice again the breaks in the correlation curves correspond to predicted discrete changes in the number of blades per rotor as the machine grows in size.

Figure 21 shows the predicted relationship between gross takeoff weight and payload for the coaxial machines. There are very little differences here between those found for the single rotor machines (Fig. 12). The corresponding empty weight results are shown in Fig. 22, where it is apparent that these too are comparable to single rotor machines. Therefore, the results suggest that

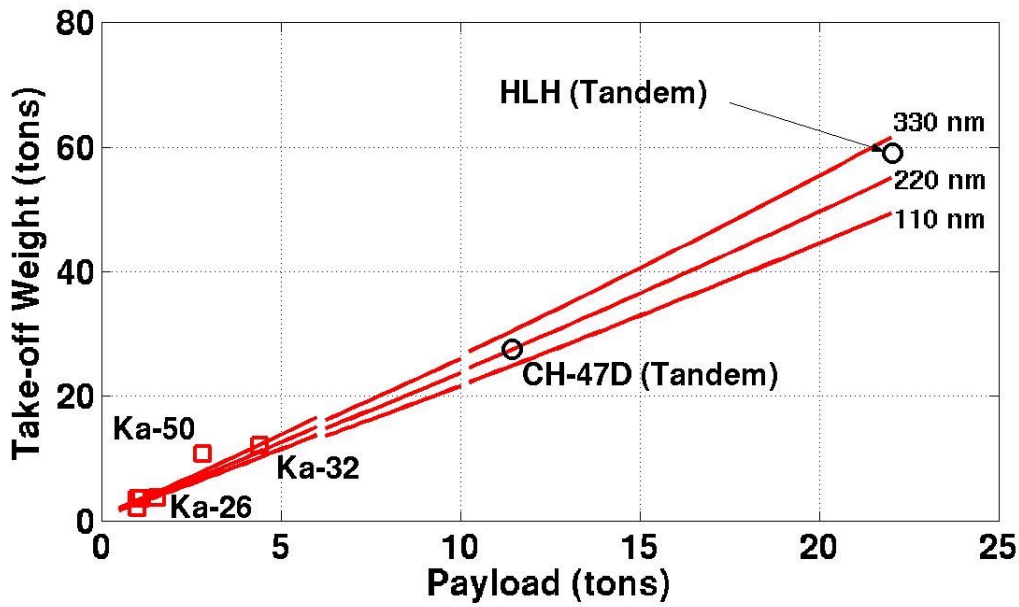

Figure 21: Predicted gross takeoff weight versus payload for coaxial dual rotor helicopters.

even with the advantages of a smaller rotor a conventional coaxial helicopter concept offers very little weight saving advantage over a single rotor machine when carrying the same payload.

The net installed power requirements of the coaxial machines are shown in Fig. 23. These were noted to be marginally higher than for an equivalent single rotor machine. This is mainly because of the loss of aerodynamic efficiency resulting from rotor-on-rotor interference, despite the absence of a tail rotor. Again, the overall results suggest few advantages in the coaxial design over the single rotor machine, other than the smaller rotor.

There are few component weight data that have been published for the Kamov machines, and without historical data points covering a range of conditions and for several different machines it was felt inappropriate to show ad hoc points less inappropriate correlation coefficients be obtained and misleading conclusions be drawn. Instead, where empirical data are unknown, the coefficients in the parametric equations used for the single rotor machines have been used. However, for reference, the results for the CH-47 and HLH machines have been included in the various plots, but recognizing again, of course, that these are tandem rotor machines and not coaxials.

The predicted weight of the rotor blades are shown in Fig. 24. Despite the larger number of blades typical of a coaxial rotor system, the net blade weight is comparable to the single rotor

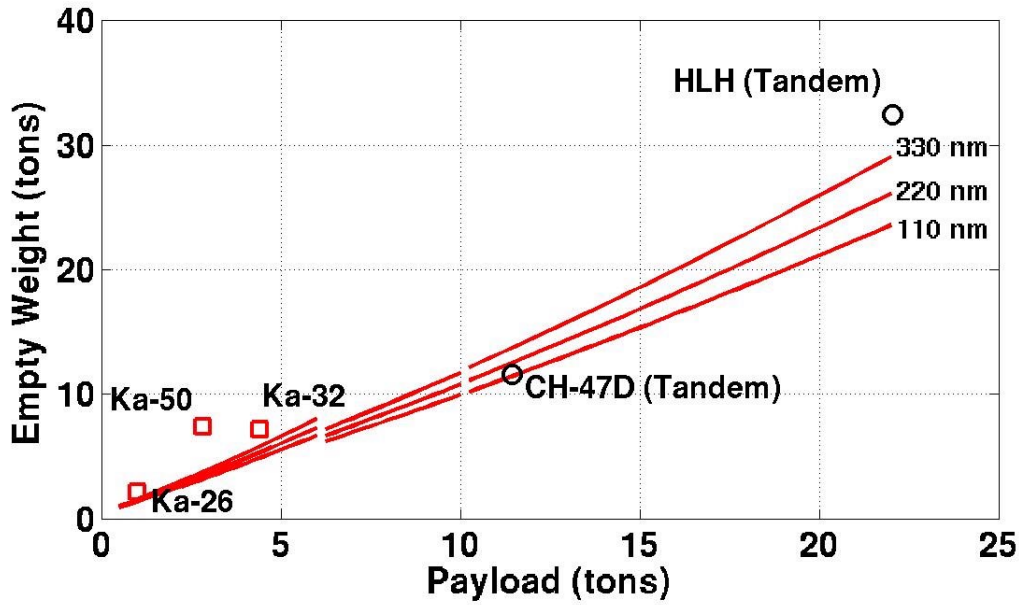

Figure 22: Predicted empty weight versus payload for coaxial dual rotor helicopters.

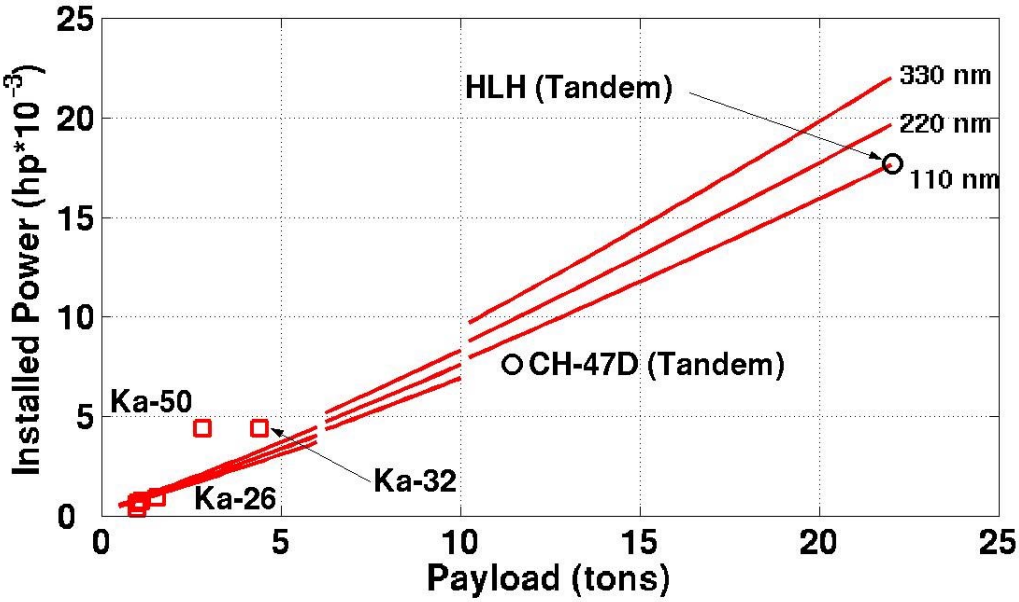

Figure 23: Predicted power requirements versus payload for coaxial dual rotor helicopters.

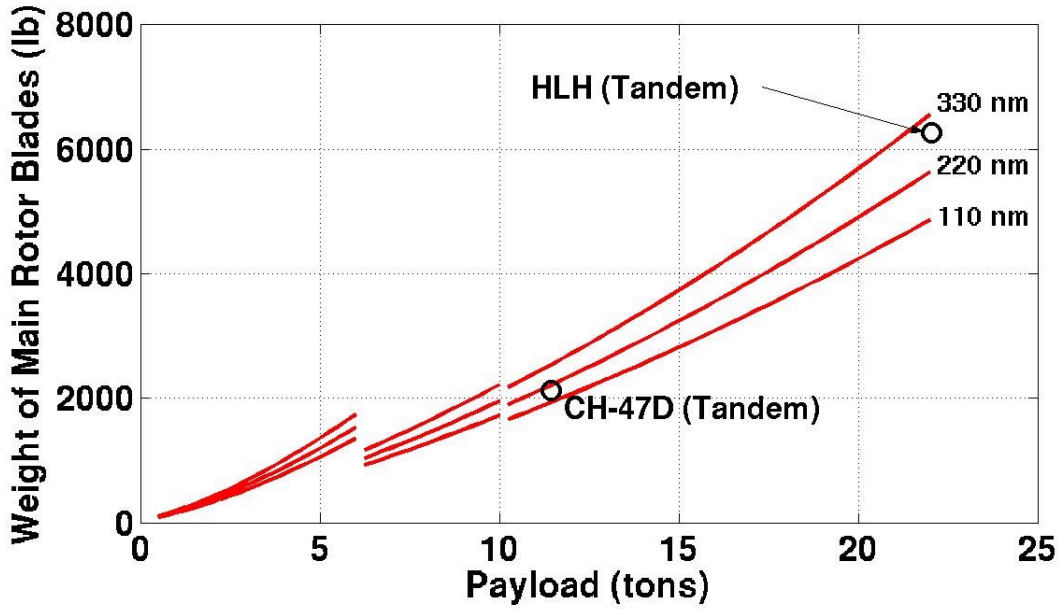

Figure 24: Predicted blade weights versus payload for the coaxial dual rotor helicopters.

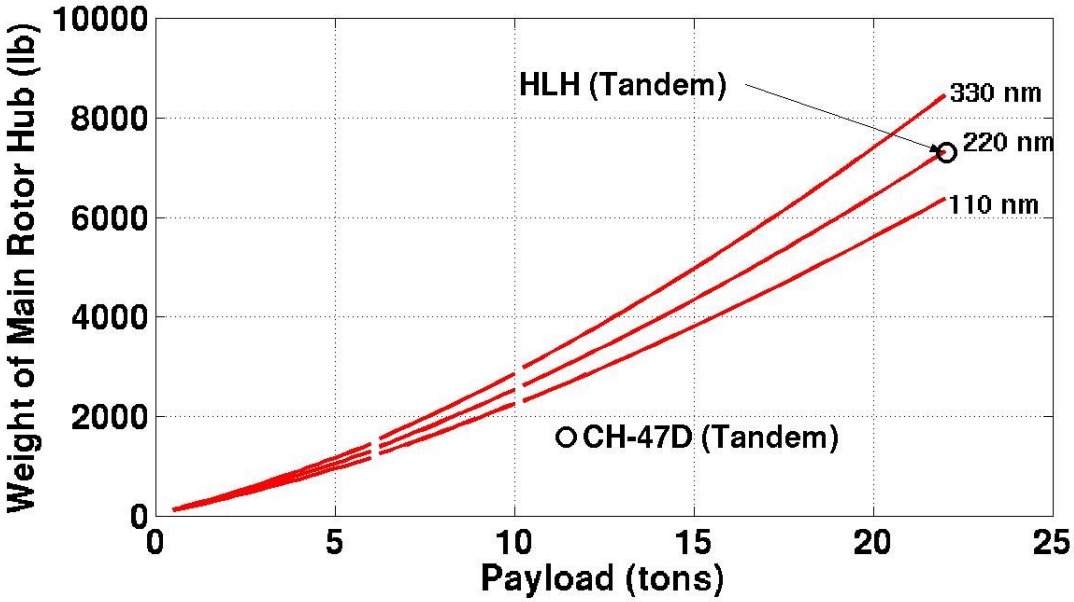

Figure 25: Predicted hub weights versus payload for the coaxial dual rotor helicopters.

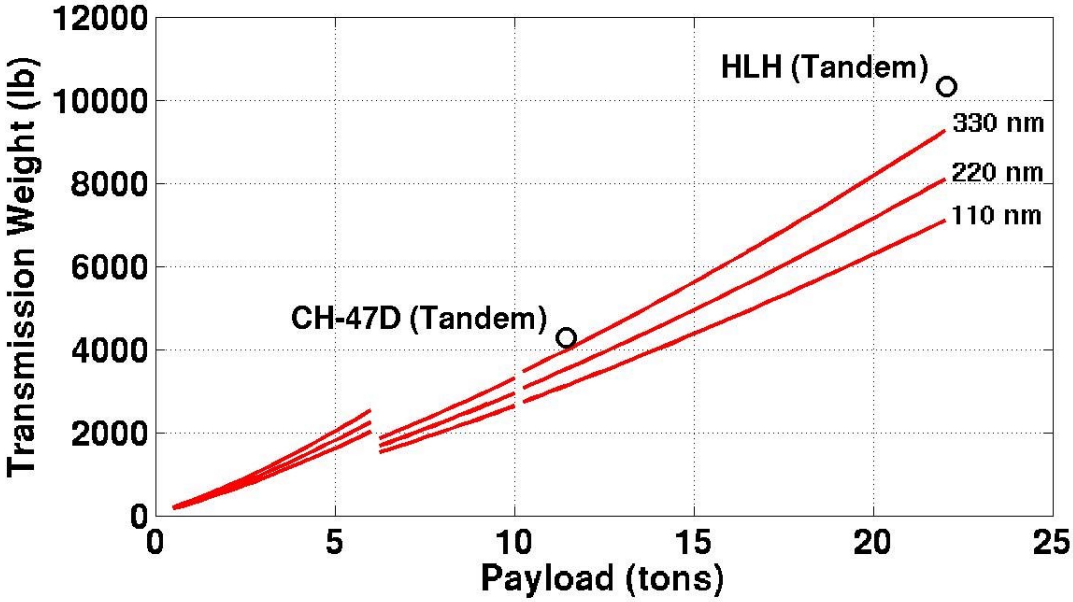

Figure 26: Predicted transmission weights versus payload for the coaxial dual rotor helicopters.

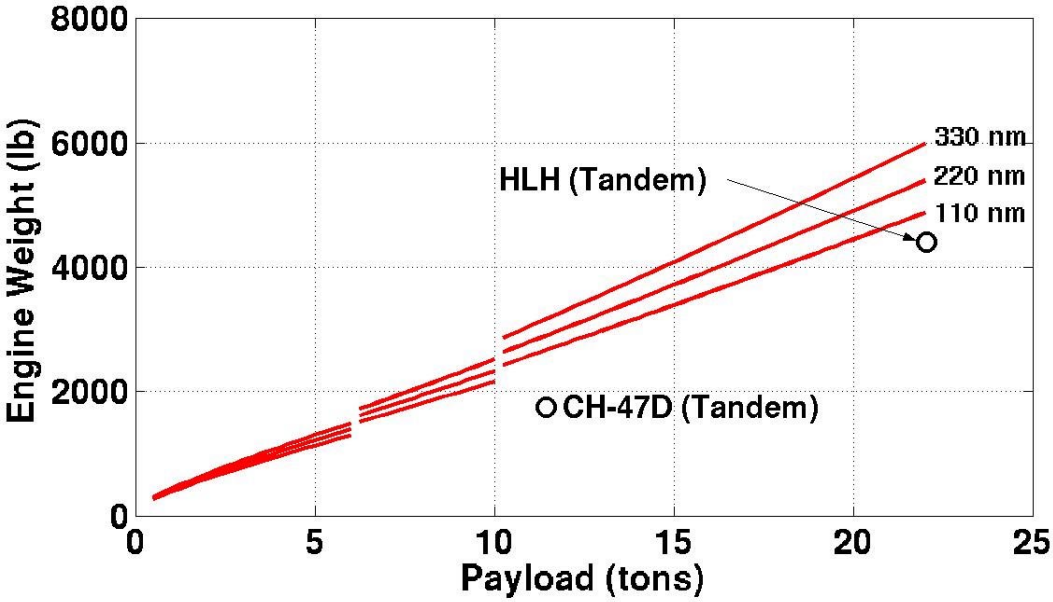

Figure 27: Predicted engine weights versus payload for the coaxial dual rotor helicopters.

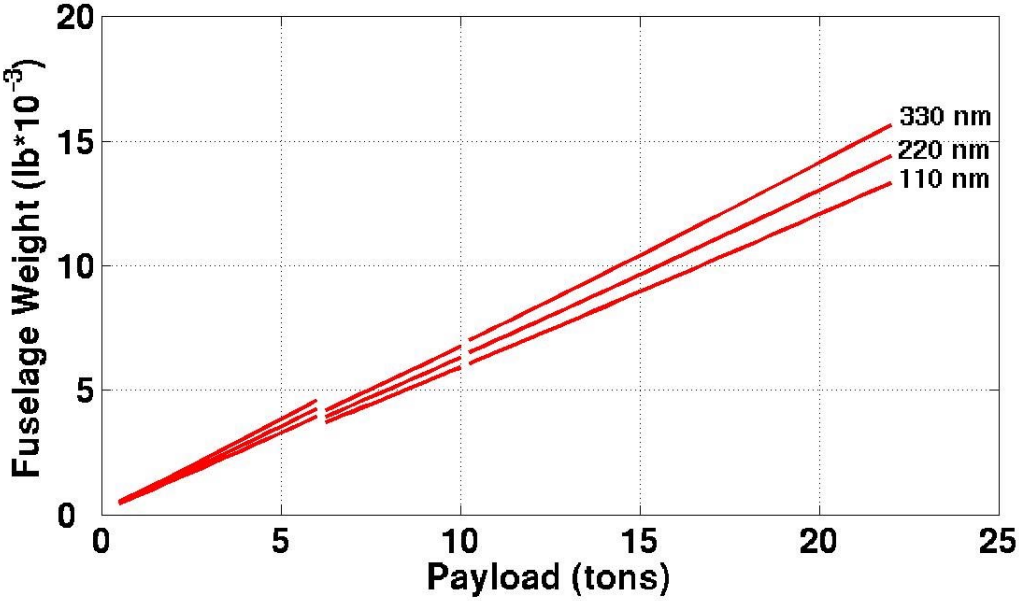

Figure 28: Predicted fuselage weight versus payload for coaxial dual rotor helicopters.

system (Fig. 15). This is a consequence of the lower blade radius, which offsets the increase in weight associated with the larger number of blades. However, the hub weights shown in Fig. 25 are notably larger than for a single rotor machine. This is because of two factors. First, the hub weight is driven by the strength requirements to react the net centrifugal effects on the blades, this being higher for a coaxial rotor system than an equivalent single rotor system. Second, there is a weight penalty associated with the extra shaft length on a coaxial rotor system.

This higher hub weight, however, is offset by the lower transmission weight but engine weight is higher, as shown in Figs. 26 and 27 and can be compared with the results of Figs. 17 and 18 for the single rotor helicopters. The fuselage weight (Fig. 28) is slightly higher than for a conventional single rotor helicopter. Based on the previously shown results obtained for the single rotor helicopter, the performance predictions for the coaxial machines have been assigned relatively good confidence levels.

3.3 Ultra-Long Range Heavy-Lift Helicopter

A requirement that motivated, in part, the design of the MTR was to meet a military goal that a vertical-lift aircraft be able to carry at least a 20 ton useful payload efficiently and economically

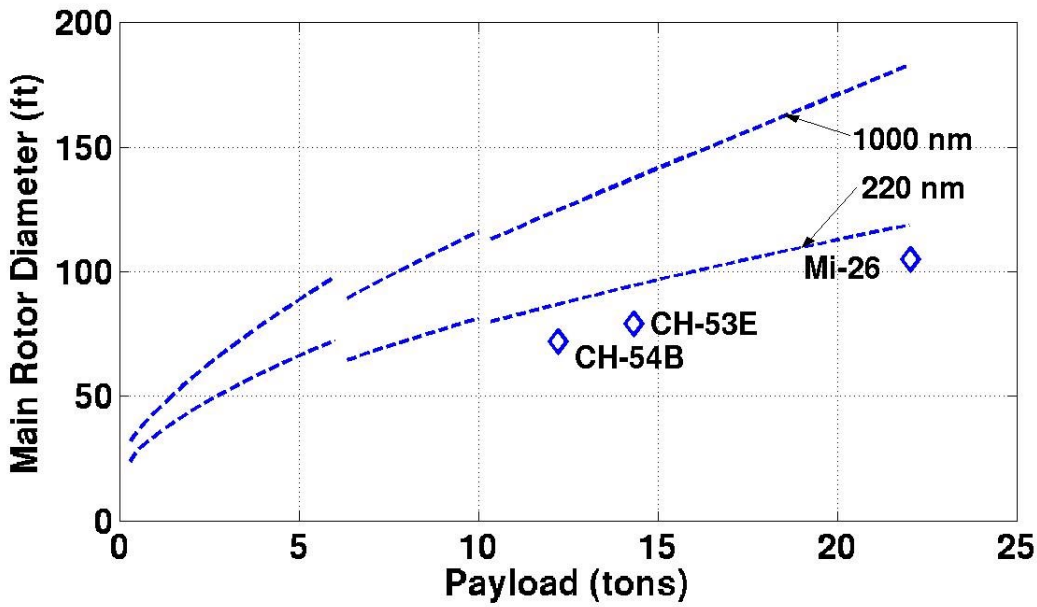

Figure 29: Predicted rotor size versus payload for a single rotor helicopter with ranges of 220 nm and 1,000 nm.

over an unrefueled distance of 1,000 nautical miles. This is an unprecedented range for a conventional helicopter. To examine the possible hypothetical designs that might result from attempting to meet such a requirement, a design analysis was undertaken to meet a 1,000 nm unrefueled range specification with a range of payloads from as little as one ton to just over 20 tons.

The results in Fig. 29 show the predicted size (rotor diameter) of the single rotor helicopter versus payload to meet both 220 nm and 1,000 nm range goals. Notice that the machines become extremely large in size for larger payloads, and especially so when longer ranges are required. To meet the 20 ton useful payload over 1,000 nm goal, a rotor diameter approaching 170 ft would be required. This is too large to be practical, especially when viewed in context that the world's largest helicopter currently in service, the Mi-26, has a rotor diameter of 105 feet The results for a coaxial machine (shown in the next section) suggested that a 125 ft diameter rotor would be necessary, but this too is extremely large and probably infeasible to build with sufficient blade stiffness.

The corresponding takeoff weights for the designs are shown in Fig. 30. While for lower ranges (typically 220 nm) the net (gross) takeoff weight is roughly proportional to payload, to meet the 1,000 nm range requirement the machine becomes very heavy when required to carry a

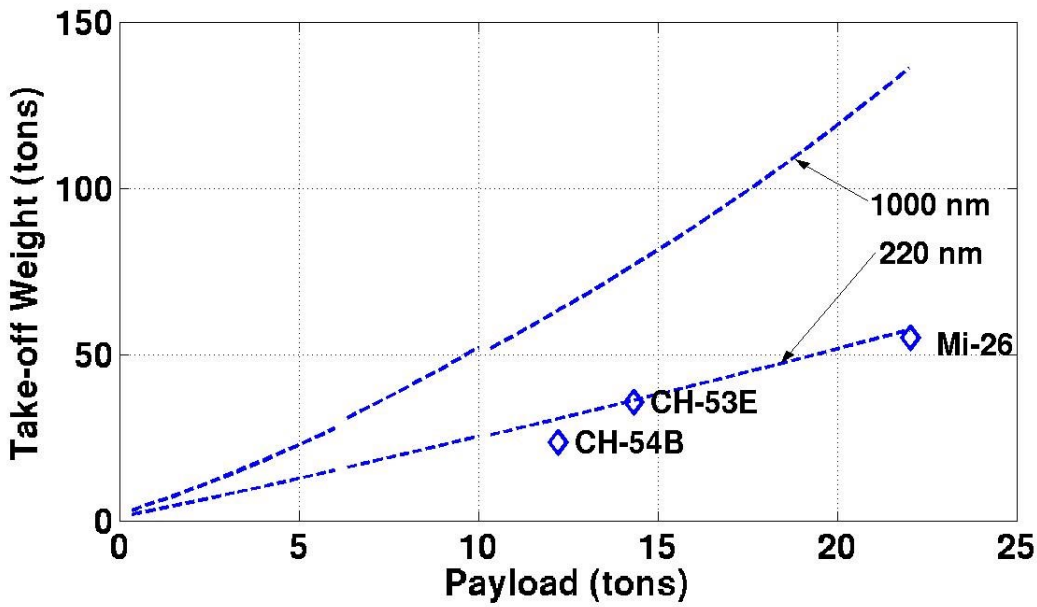

Figure 30: Predicted takeoff weight versus payload for a single rotor helicopter with ranges of 220 nm and 1,000 nm.

large payload over 10 tons. Most of this extra takeoff weight is fuel, which is shown in Fig. 31 as a function of payload, although empty weight also increases rapidly because of the extra structure required to carry this fuel. This result reflects the relative inefficiency of the conventional helicopter when required to fly over long ranges exceeding about 400 nm.

Based on the amount of power required (about 35,000 hp) as shown in Fig. 32 and the corresponding amount of torque that must be transmitted to the rotor through the gearbox, it would seem unrealistic that a conventional helicopter could be built to meet these large payload and long-range requirements.

3.4 Performance of MTR Architecture

The characteristics of the MTR have been previously described, and it has been proposed (in part) as a vertical-lift vehicle that can provide heavy-lift capability over considerable flight ranges. The MTR is basically a compound concept, morphing its flight configuration to combine some of the attributes of a dual rotor coaxial helicopter and a fixed-wing aircraft. Like all compound rotorcraft, however, the MTR is a compromise. Yet the unique characteristics of the MTR, if technically

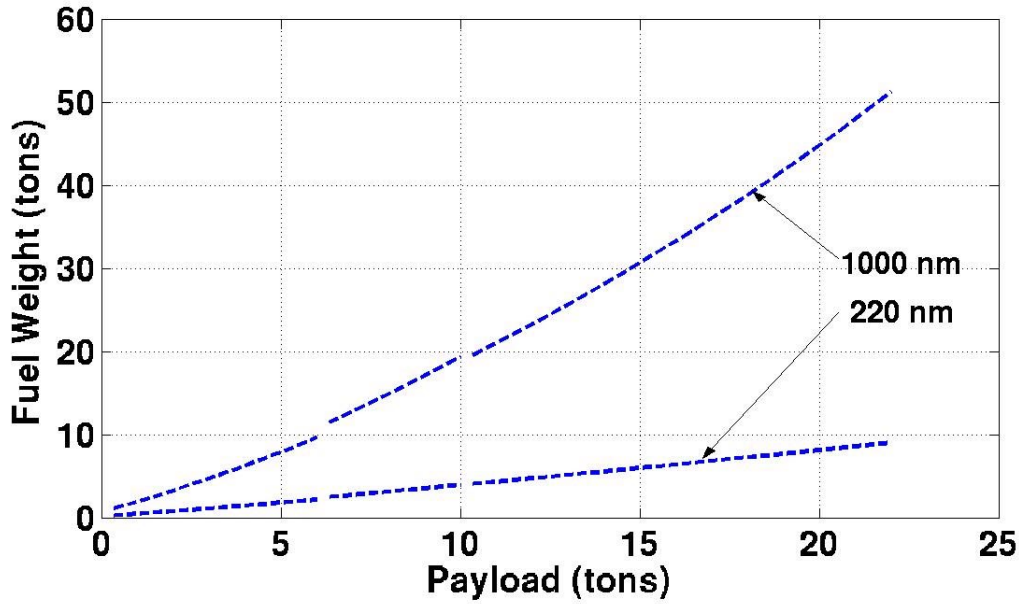

Figure 31: Predicted fuel weight versus payload for a single rotor helicopter with ranges of 220 nm and 1,000 nm.

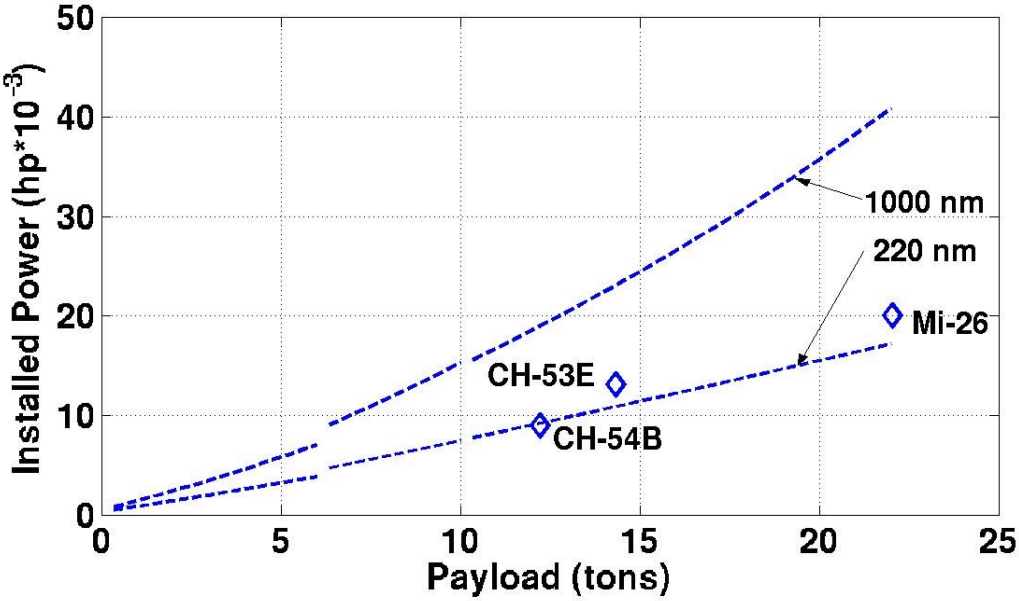

Figure 32: Predicted power requirements versus payload for a single rotor helicopter with ranges of 220 nm and 1,000 nm.

realized, could make it more suitable for long-range, heavy-lift applications.

The specific equations governing the performance and component weight characteristics of the MTR concept have already been described. The various parametric equations describing the operation of the MTR both in helicopter and airplane mode were integrated together in the design analysis. The mission profile for the MTR was also incorporated so that the future design process and trade studies can proceed under the assumption of a series of flexible mission profiles, which is examined in the latter part of this report. This focuses primarily on radius of action mission profiles, which can be conducted in both helicopter and airplane mode, or just as a pure helicopter.

In the present report, the results focus mainly on the heavy-lift, 1,000 nm longer-range mission where the MTR meets a limited 20 minute hover time requirement and cruises in airplane mode for the remainder of the mission. A 20 minute reserve time in each of helicopter and airplane flight mode were also factored into the design.

The disk loading of the MTR's rotor design was constrained to be representative of a helicopter (not of a conventional tiltrotor) so as to maintain relatively low downwash velocities for cargo loading and unloading, and also for operations in austere environments. As a first approximation, propulsive efficiency of a fixed geometry rotor in airplane mode was estimated to be no less than 0.6, although this result is a function of several parameters including disk loading, tip speed and cruise speed (Ref. 24). It would seem realistic to assume that in practice the cruise efficiencies of at least 70% could be obtained, even without a highly optimized rotor design.

Cruise L/D can be estimated in comparison to fixed-wing aircraft. The container handling system was presumed to envelope and fully streamline the container for minimal drag, thus having performance similar to a streamlined fuselage holding a container. Furthermore, the MTR's high aspect ratio wing has a substantially positive impact on L/D. By comparison, conventional tiltrotors have cruise L/D's of about 9, whereas the C-130 has a cruise L/D of about 15. As a first approximation, MTR cruise L/D is estimated at 10, which is 9% better than conventional tiltrotors in consideration of the wing with significantly larger aspect ratio, offset by perhaps a larger profile drag contribution from the container handling system. While the integration of the container handling system presents an intriguing engineering challenge, this performance analysis holds for any inherently streamlined payloads such as a fuel deployment pod or a conventional payload fuselage.

Calculated results for the MTR concept are shown in Figs. 33 through 39 using the previously

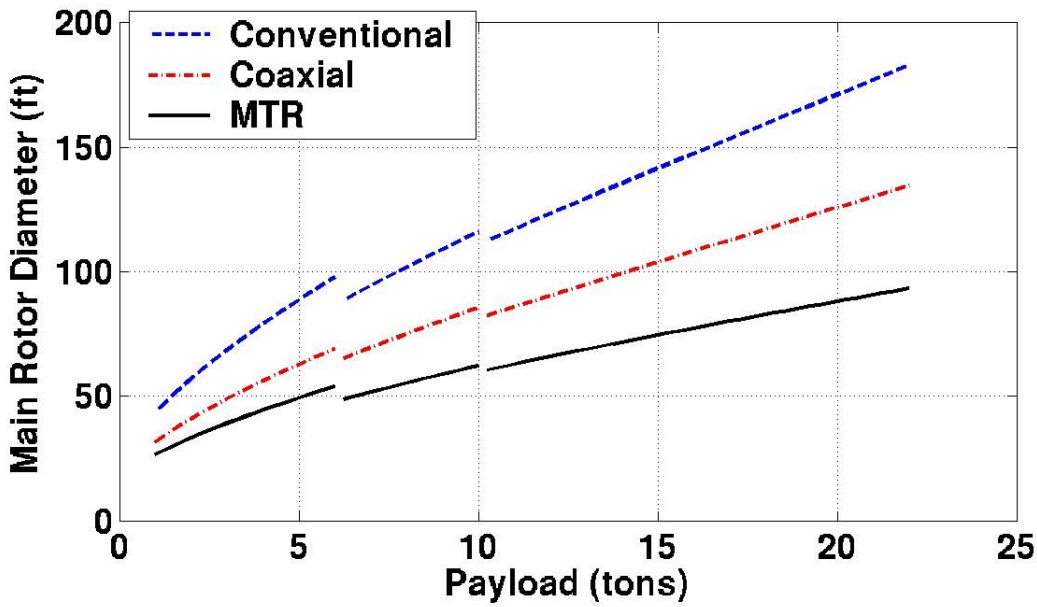

Figure 33: Predicted rotor size (diameter) for the MTR architecture to meet a 1,000 nm range requirement versus hypothetical conventional (single) and coaxial rotor helicopters.

stated assumptions. Overall, the results suggest that if the MTR concept were to be technically realized then it could be up to 50% smaller (see Fig. 33) with a 50% lighter gross takeoff weight (see Fig. 34) compared to a conventional helicopter when carrying the same useful payload over the same distance. The 20 ton/1,000 nm payload/range requirement could be met with a MTR vehicle that has about an 85 ft diameter rotor with a gross takeoff weight of 64 tons. Figure 34 shows that the gross takeoff weight of the machine is about half of what a conventional helicopter would be. The MTR's empty weight as shown in Fig. 35 is 65% less than a conventional helicopter for the same payload and range. This is in comparison to the results shown in Fig. 13 (single) and Fig. 22 (coaxial).

Hovering efficiency of the MTR is maintained by the requirement that rotor disk loading be held at values comparable to a helicopter (Fig. 36). While this compromises somewhat the propulsive efficiency of the machine in airplane mode, the need for good hovering efficiency and low downwash velocities in hover was considered more important because a coaxial operated at the same equivalent disk loading as a single rotor machine will have a higher wake slipstream velocity. This is an important operational issue that can subtract from the value of a coaxial rotor

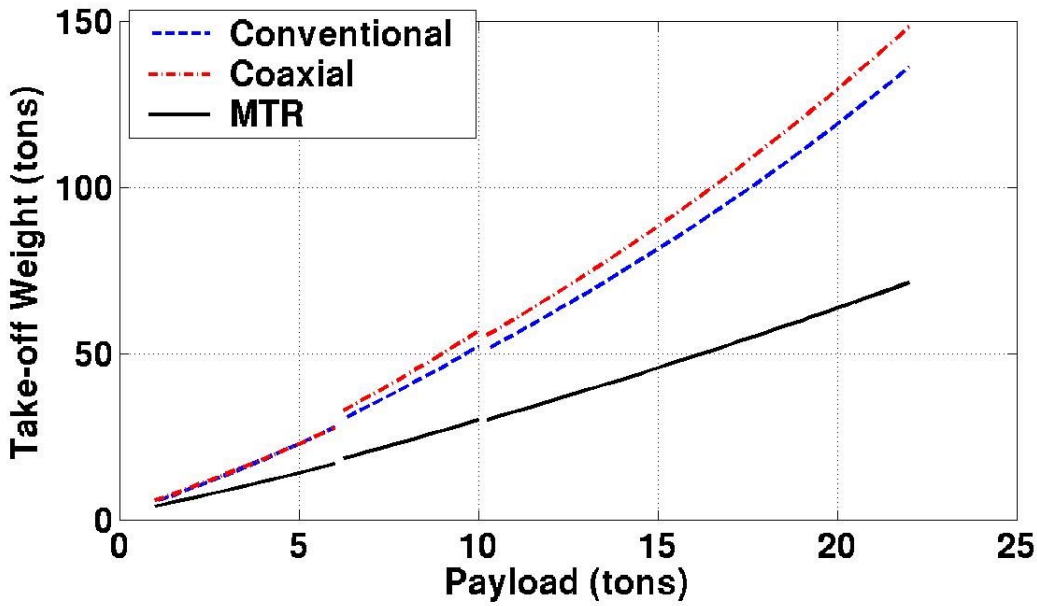

Figure 34: Predicted gross takeoff weight for the MTR architecture to meet a 1,000 nm range requirement versus payload compared with hypothetical conventional (single) and coaxial rotor helicopters.

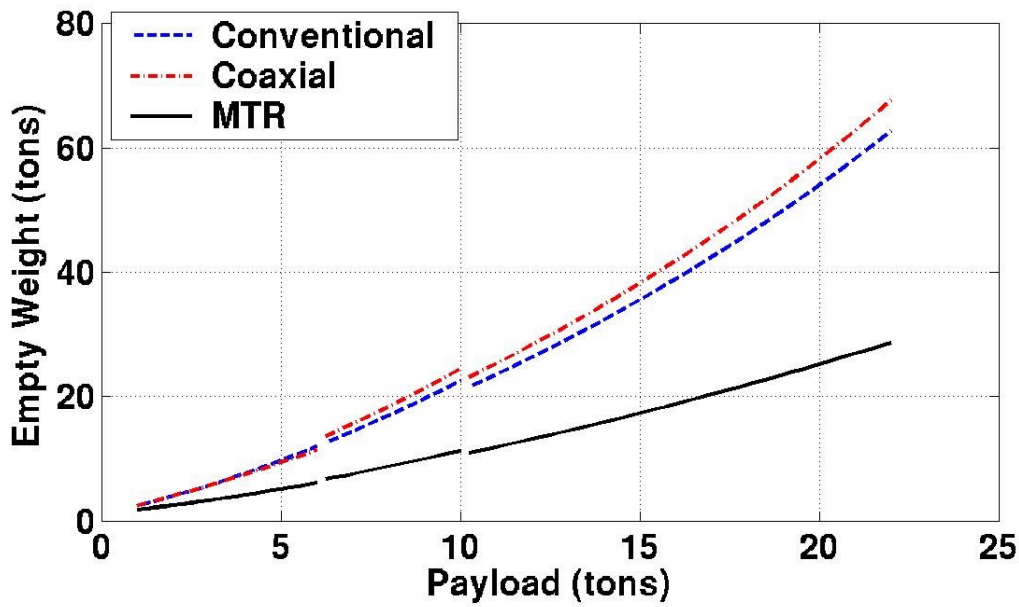

Figure 35: Predicted empty weight for the MTR architecture to meet a 1,000 nm range requirement versus payload compared with hypothetical conventional (single) and coaxial rotor helicopters.

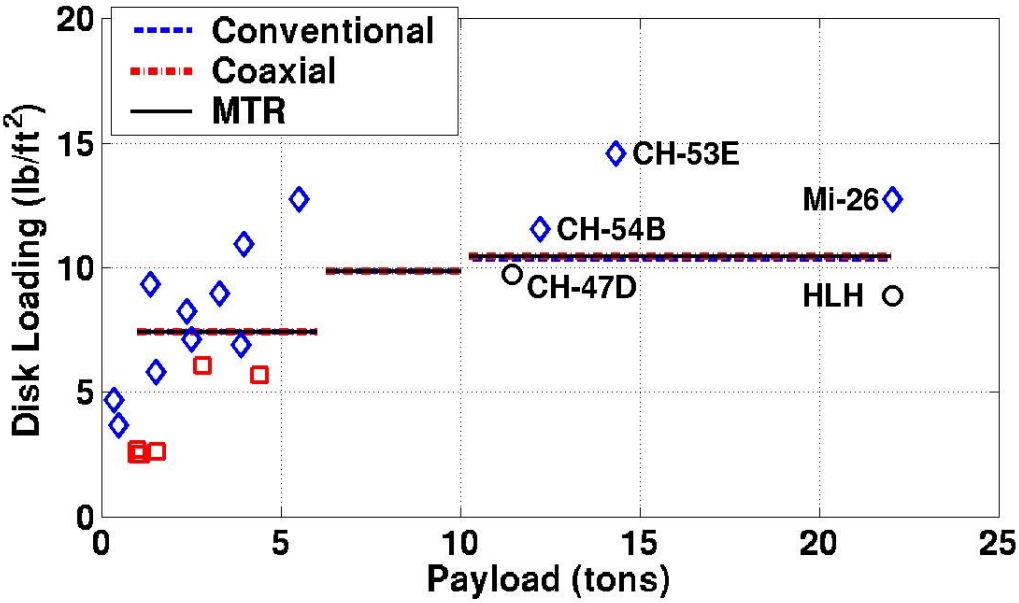

Figure 36: Predicted disk loading of the MTR architecture versus historical data for conventional (single) and coaxial rotor helicopters.

configuration, but is offset somewhat on the MTR because of the higher position of the rotor relative to the ground.

Because the MTR machine is smaller and lighter than a conventional helicopter, Fig. 37 shows that less installed engine power is required for flight; this serves to contain net empty vehicle weight and also the fuel load required. In fact, the MTR's power requirements are still relatively large ($\approx$ 20,000 hp), but they are more realistically achievable than the 35,000+ hp net installed power that would be required to meet the same goals using a conventional helicopter configuration.

The MTR has a higher weight efficiency (lower empty weight fraction) than a conventional helicopter, in part because of its minimal "crane" type of airframe design, even when including the deployable wings and cargo suspension unit. This is driven in part by the results shown in Fig. 38, where the MTR fuselage weight is shown as a function of useful payload. Recall from the weight equations that MTR fuselage weight is defined as the sum of suspension structure, cargo handling system, and crew compartment weights. MTR fuselage weight is 1/20 of net empty weight (Fig. 35), and supports only the payload and fuselage, which together comprises 1/3 of the gross weight. This correlates to the CH-54 Skycrane where the fuselage weight is 1/8 of empty

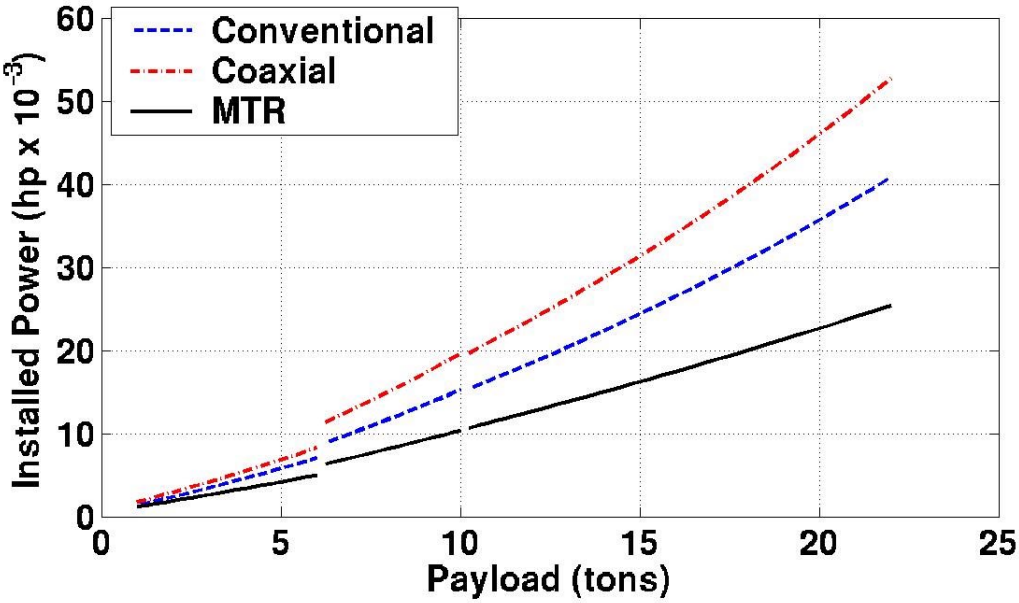

Figure 37: Predicted power requirements for the MTR architecture to meet a 1,000 nm range requirement versus payload compared with hypothetical conventional (single) and coaxial rotor helicopters.

weight (Figs. 13 and 19), but supports the full gross weight of the vehicle.

The MTR has a smaller (Fig. 33) and lighter rotor than the helicopter designs, as shown in Fig. 39. Of significance also in this design study is that a coaxial rotor system can (in theory) be designed that is smaller and lighter than an equivalent single rotor system. However, because of the size and weight of the airframe and the large amount of fuel required to perform the long-range, heavy-lift mission of 1,000 nm and 20 tons, the rotor of a coaxial helicopter is still very large ($D_{\mathrm{MR}} \approx 125$ ft). The practical difficulties in building a coaxial rotor of this size are unknown, but must be expected to be considerable. While the MTR uses a coaxial rotor, it is about 25% smaller than this and the feasibility of successful construction of an 85 ft diameter rotor is more likely, but certainly not without its issues. The relative size of the rotors for the single, coaxial and MTR are compared in Fig. 40, where it is apparent that the difference in rotor diameter and disk area is dramatic.

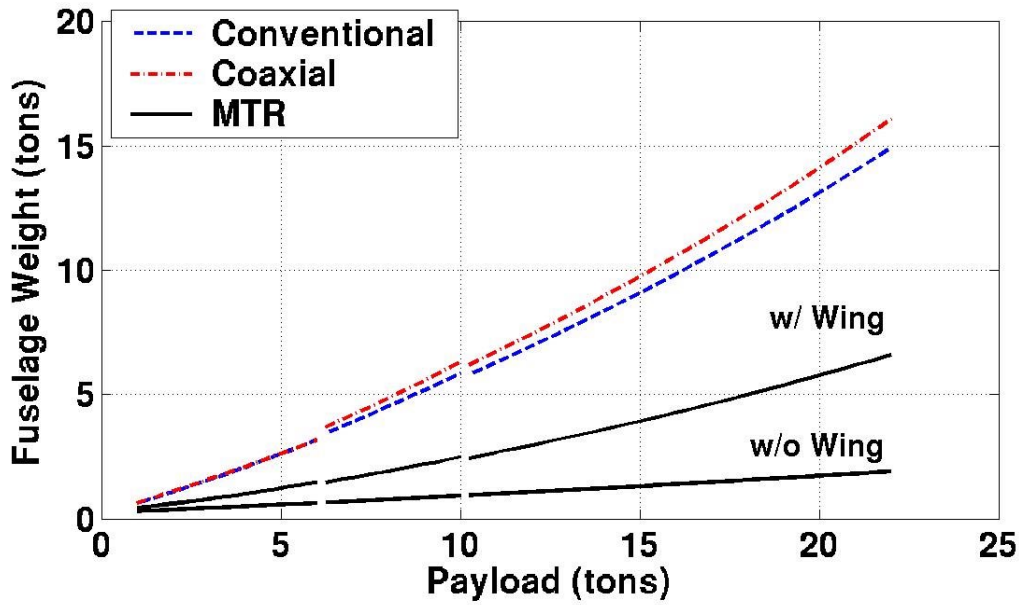

Figure 38: Predicted fuselage weight for the MTR architecture to meet a 1,000 nm range requirement versus payload compared with hypothetical conventional (single) and coaxial rotor helicopters.

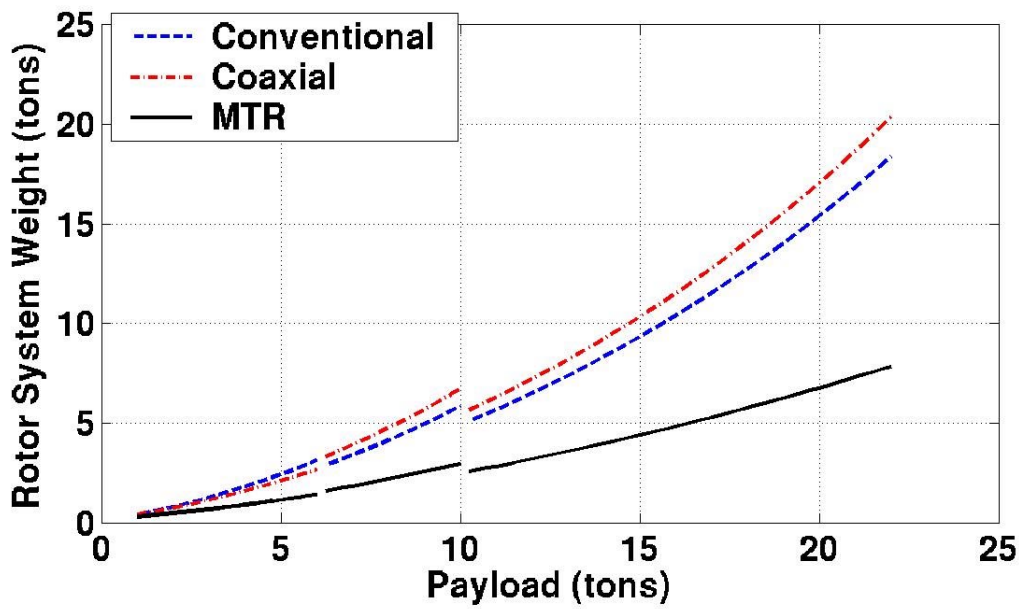

Figure 39: Predicted rotor system weight for the MTR architecture to meet a 1,000 nm range requirement versus payload compared with hypothetical conventional (single) and coaxial rotor helicopters.

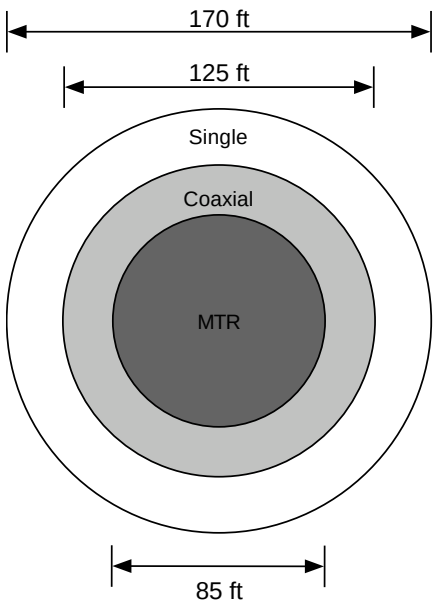

Figure 40: Comparison of rotor diameters for the hypothetical conventional (single) and coaxial rotor helicopters versus the MTR to meet the 1,000 nm range and 20 ton payload requirement.

3.5 Vehicle Efficiency

Several measures of efficiency were selected to assess the value of a long range, heavy-lift transport rotorcraft. First, structural weight efficiency (Eq. 15) measures the proportion of takeoff gross weight dedicated to either fuel or payload. Distance traveled does not factor into this equation, only the efficiency of a structure in lifting a payload vertically. Because the MTR aircraft architecture is proposed mostly as an assemblage of off-the-shelf component technologies, it should at best have a weight efficiency comparable to helicopters. Indeed, Fig. 41 shows the MTR to have a weight efficiency that is better than conventional and coaxial helicopters. If the MTR is more structurally efficient, it is because of being dedicated to carrying external loads.

Second, the vehicle energy efficiency suggested by Tishchenko et al. (Ref. 11) can be viewed as another comparative metric. This quantity is defined by

$$E = \frac{(L/D)\,\eta_{\mathrm{PR}}\,\zeta_{\mathrm{cr}}}{C_e} \tag{127}$$

The net energy efficiency for the MTR versus the conventional and coaxial helicopters is shown in Fig. 42 as a function of useful payload. Notice that the net energy efficiency of the MTR is about 60% greater than that of a helicopter. Both the conventional and coaxial rotor helicopters are comparable in vehicle efficiency, although the coaxial has a slightly reduced efficiency because

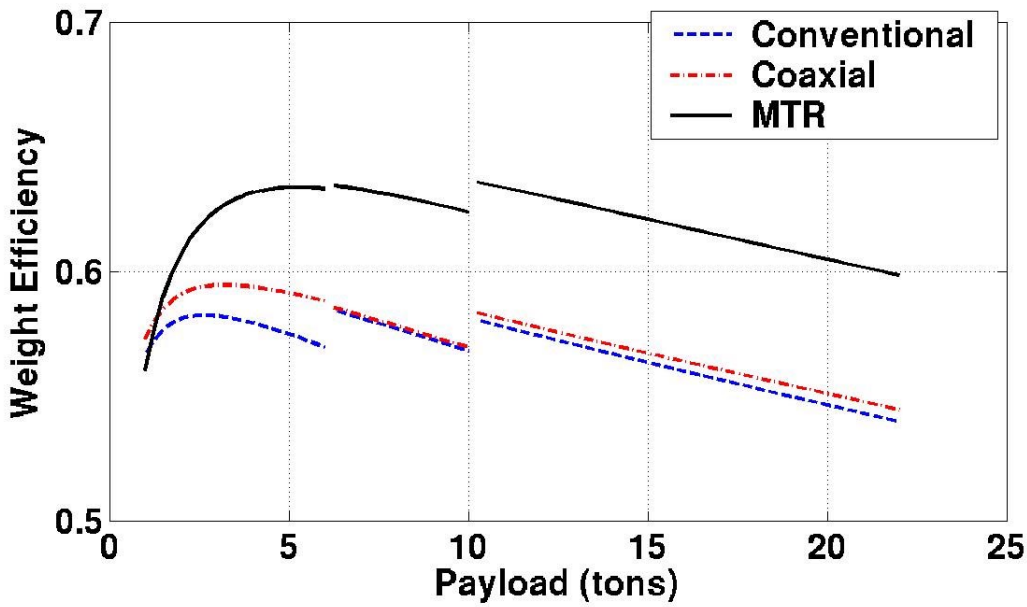

Figure 41: Predicted weight efficiency for the MTR architecture to meet a 1,000 nm range requirement versus payload compared with hypothetical conventional (single) and coaxial rotor helicopters.

of the higher drag of the rotor system and slightly lower effective L/D. In all cases the weight efficiency decreases with increasing payload. The breaks in the curve are a consequence of the design analysis increasing the number of main rotor blades in an attempt to optimize the design in each case.

Finally, a range specific transport efficiency can be defined using

$$E = \frac{W_{\text{PAY}}}{W_{\text{FUEL}}} \tag{128}$$

This quantity measures the payload moved per unit weight of fuel over a specific range. Because the MTR uses a fixed wing for lift generation in cruise flight, it is predicted to have a better cruise efficiency than a conventional helicopter. Furthermore, because of its tilting rotor concept the MTR is also predicted to cruise faster than a helicopter, which based on current estimates is expected to be in the range of 200 to 250 kts. Therefore, the MTR architecture needs to carry much less fuel (see Fig. 43) to meet the 20 ton/1,000 nm payload/range mission requirements. The MTR transports 1.2 pounds of payload per pound of fuel, whereas a helicopter would transport only about 0.5 pounds. This result suggests that the MTR architecture, if technically realized, would be

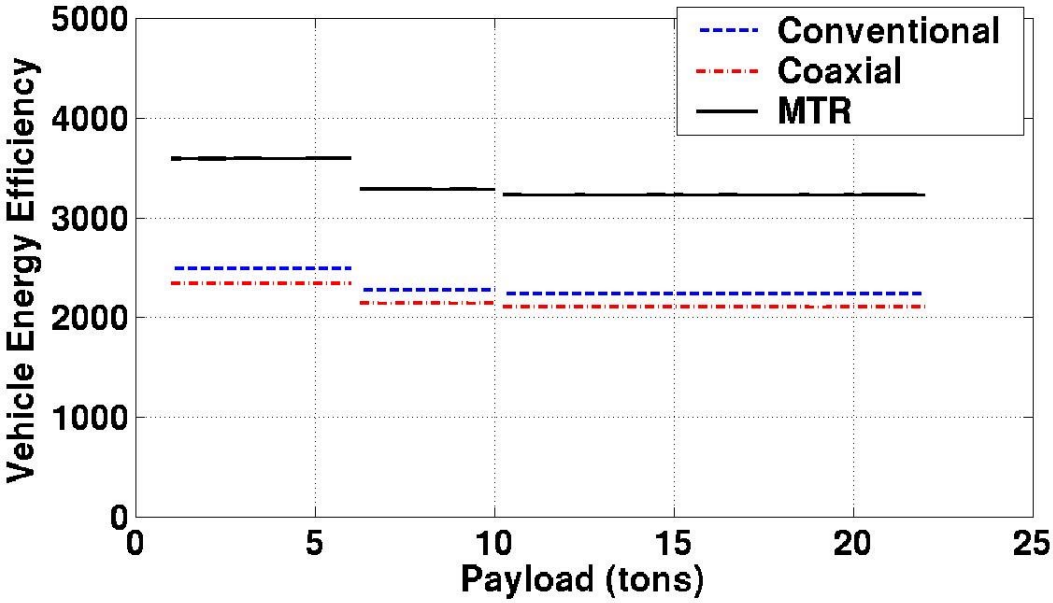

Figure 42: Predicted Tishchenko et al. “energy efficiency” of the MTR versus payload compared with hypothetical conventional (single) and coaxial rotor helicopters.

2.4 times more efficient at transporting payload.

3.6 Payload–Range Performance

Results for the vehicle weight versus distance flown and payload versus range performance of the MTR are shown in Figs. 45 and 46, respectively. The MTR was designed to meet the 20 ton useful payload and 1,000 nm range requirement. Also shown is the result for a conventional single rotor helicopter, but in this case it was designed to meet a more realistic 20 ton payload and 220 nm range goal that would be typical of legacy helicopters such as the Mi-26.

While the gross takeoff weight of the MTR is higher than that of the helicopter, most of this extra weight is fuel. The legacy helicopter has a higher fuel burn per mile and reaches its maximum range at 220 nm. In other words, the legacy helicopter would require at least four refuelings in transit to reach the destination 1,000 nm away. The MTR has a lower fuel burn per mile, as shown by the lower slope of the curve, and reaches the 1,000 nm range target. Notice that the fuel burn rate decreases as the fuel is burnt and net vehicle weight decreases, stretching the range.

Figure 46 shows the predicted payload/range graph for the MTR concept when compared with

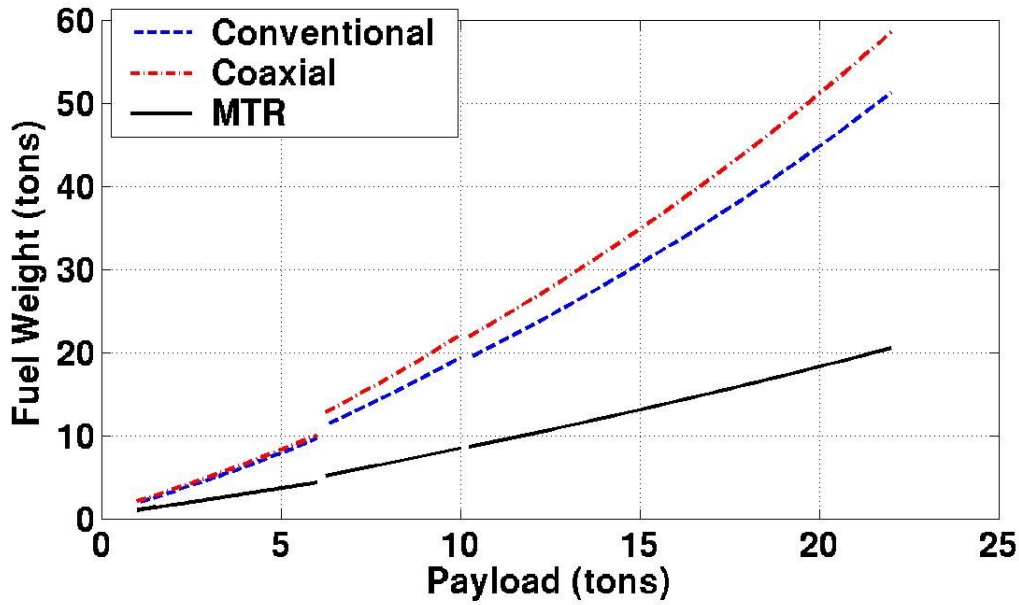

Figure 43: Predicted fuel weight for the MTR architecture to meet a 1,000 nm range requirement versus payload compared with hypothetical conventional (single) and coaxial rotor helicopters.

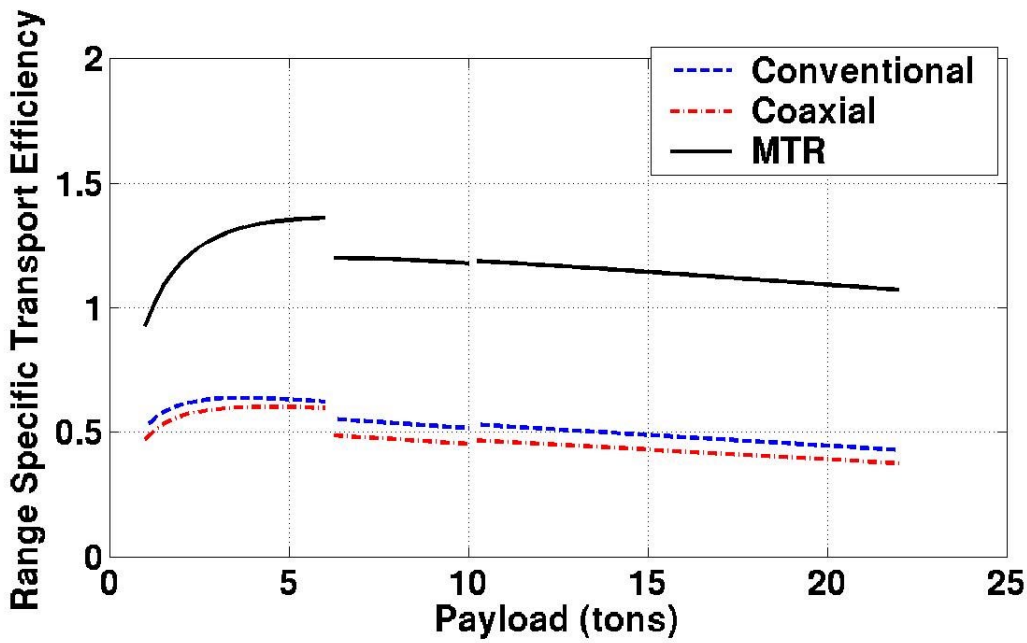

Figure 44: Predicted specific transport efficiency of the MTR versus payload compared with hypothetical conventional (single) and coaxial rotor helicopters.

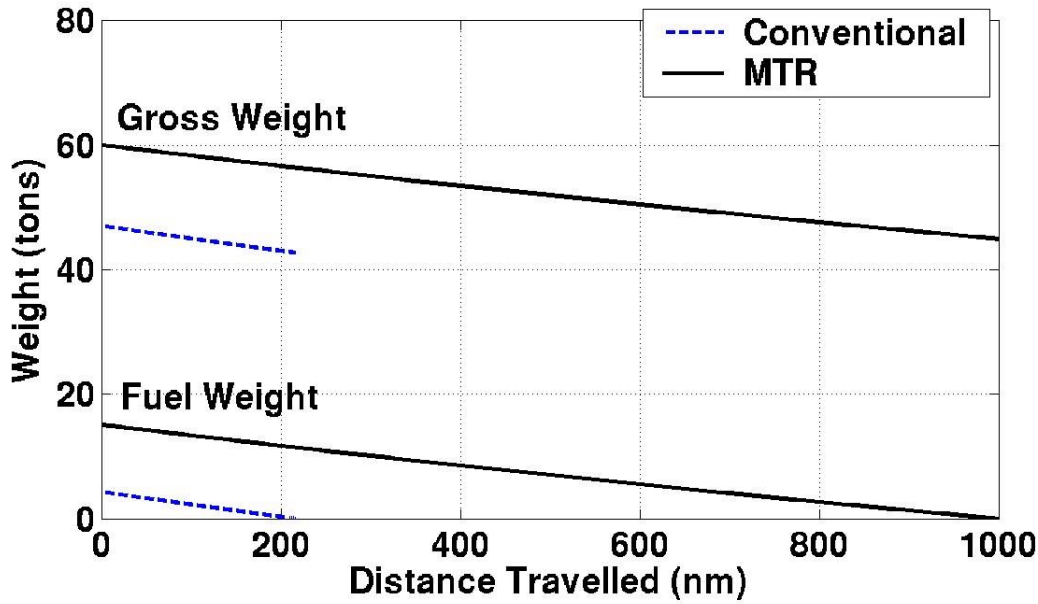

Figure 45: Predicted gross weight and fuel weight versus distance flown for 20 ton useful payload MTR concept versus a legacy helicopter design.

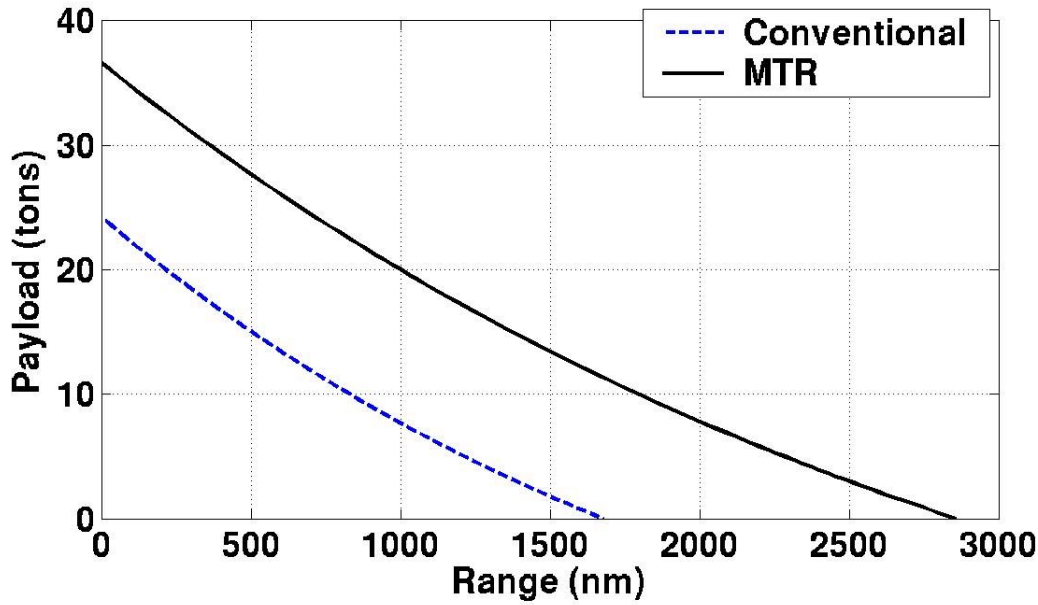

Figure 46: Predicted payload/range graph for the MTR concept when compared with a legacy helicopter design.

a legacy helicopter design. Useful payload can be traded off for fuel and vice-versa, to a point. Notice that the MTR has about a 30 ton useful payload capability for the nominal 220 nm range, although this would be reduced to about 25 tons if the MTR was operated in pure helicopter mode over such relatively short ranges. It is apparent that the MTR can carry a 10 ton payload over about 1700 nm, or 2,500 nm with a 5 ton payload. The self-deploy range of the MTR is about 3,000 nm without payload or using long-range fuel tanks.

4 Refined Aerodynamic Analysis

After these initial validation and comparison trade studies were completed, several improvements were made to the MTR analysis, including a better estimate of the aircraft's lift-to-drag ratio and improvements to the wing sizing methodology. These are discussed in the following sections. Through these improvements, confidence in the MTR design methodology and the breadth of its analytical capabilities have been refined.

In the original design analysis, a notional value of 10 was assumed for the lift-to-drag ratio. To improve confidence in this value and to improve the overall versatility of the MTR design methodology, it was decided to explicitly calculate the lift-to-drag ratio within the calculation steps based, in part, on an estimate of the parasitic drag in terms of an equivalent flat plate area of the aircraft.

The equivalent flat plate area, f_{eq}, was estimated through a standard component drag breakdown for the vehicle in each of its flight modes (helicopter and airplane). After this equivalent flat plate area is obtained, the power required for flight and lift-to-drag ratio of the vehicle as a whole can be calculated using standard methods for both helicopter and aircraft performance.

4.1 Component Drag Breakdown

A component drag breakdown is a standard practice in preliminary aircraft design. It provides a good first estimate of the overall parasitic drag of an aircraft without having to perform costly wind tunnel tests. For each component used on the aircraft, the drag coefficients based on frontal area are estimated based on the shape and Reynolds number of the component. These drag coefficients come primarily from empirical measurements conducted in a wind tunnel, corrected for Reynolds

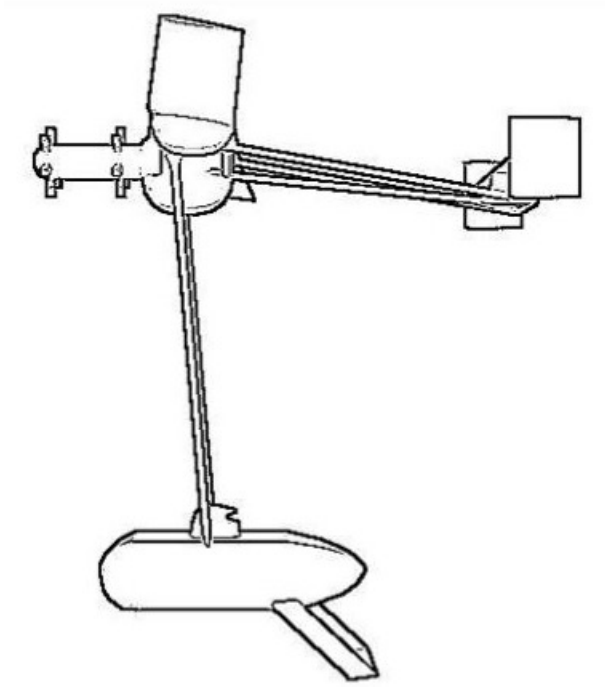

Figure 47: Conceptual design sketch of MTR flying in airplane mode.

number effects. For the present analysis, the results documented in Hoerner (Ref. 25) were used to find the drag of basic geometric shapes and components typical of airplanes. Results documented in Prouty (Ref. 26) were used for the MTR components that were characteristic of helicopters.

For example, the engine nacelle in airplane mode was modeled as an ellipsoid with a length to diameter ratio, l/d, of 1.1 based on dimensioned drawings of the updated heavy-lift MTR – see sketch shown in Fig. 47. According to Hoerner, this ellipsoid combination yields a drag coefficient, C_{D_0}, of approximately 0.09. The frontal area, A_f, for each component was calculated based on the dimensioned drawings of the MTR provided by BTC. The equivalent flat plate area, f_{eq}, was then calculated for each component and finally synthesized to find the total equivalent flat plate area for the MTR in each flight mode using

$$f_{\text{eq}} = \sum_{i=1}^{n} C_{D_{0_i}} A_{f_i} \tag{129}$$

The component drag breakdowns for the MTR in airplane and helicopter mode are given in Tables 1 and 2, respectively. An interference factor was added to the net drag to account for component interference effects, miscellaneous items, and any surface irregularities. This value was assumed

Component	Characteristic Length (ft)	Re	l/d	C_{D_0}	A_f (ft^2)	f (ft^2)
Wings	9.2	2.6×10^7	8.3	0.045	86.7	3.9
Nacelle	12	3.4×10^7	1.1	0.09	94.3	8.5
Fuel Pods	7	2.0×10^7	1.57	0.09	38.5	3.5
Tail Boom	33	9.4×10^7	-	0.05	4.1	0.2
Horiz Stab	6.5	1.9×10^7	8.3	0.045	20.3	0.9
Vert Stab	9	2.6×10^7	8.3	0.045	10.8	0.5
M/R Shaft	5	1.4×10^7	-	0.04	19.6	0.8
Struts	1.2	3.4×10^6	3	0.1	17.6	1.8
Cargo Handling	10	2.8×10^7	2	0.1	100	10
Crew Comp	4.5	1.3×10^7	1.6	0.06	8.0	0.5
Interference	-	-	-	-	-	6.0
Total, f_{air}						**36.6**

Table 1: MTR component drag breakdown in airplane mode.

to be 20% of the sum of the component flat plate areas.

For airplane mode, it is shown from the results in Table 1 that the components that have the most significant contributions to the vehicle net drag are the engine nacelles, the fuel pods, the suspension struts and the cargo handling unit. The total equivalent flat plate area of the MTR configuration in airplane mode, f_{air}, was estimated to be 36.6ft^2. The relatively low drag of the MTR in airplane mode depends heavily on the streamlined design of the cargo handling system. It

Component	Characteristic Length (ft)	Re	l/d	C_{D_0}	A_f (ft^2)	f (ft^2)
Wings	9.2	1.4×10^7	8.3	0.045	86.7	3.9
Nacelle	13	1.9×10^7	0.4	0.2	122.5	24.5
Fuel Pods	7	1.0×10^7	1.57	0.09	38.5	3.5
Tail Boom	33	4.9×10^7	-	0.05	4.1	0.2
Horiz Stab	6.5	9.6×10^6	8.3	0.045	20.3	0.9
Vert Stab	9	1.3×10^7	8.3	0.045	10.8	0.5
M/R Hubs	-	-	-	0.6	40	24
M/R Shaft	5	5.6×10^5	-	0.3	90	27
Struts	1.2	1.8×10^6	3	0.1	17.6	1.8
Cargo Handling	10	1.5×10^7	2	0.1	100	10
Crew Comp	4.5	6.6×10^7	1.6	0.06	8.0	0.5
Interference	-	-	-	-	-	19.3
Total, f_{hel}						**116.1**

Table 2: MTR component drag breakdown in helicopter mode.

is known that an untreated MILVAN container carried as a slung load can have an equivalent flat plate area of up to 100 ft^2. However, the current MTR design includes an enveloped, streamlined container, as can be seen in Fig. 47. Through the use of fore and afterbodies with a rounding radius along the sides of the container, the drag can be reduced by a factor of 10, as shown by the results in Hoerner (Ref. 25).

Table 2 shows that the MTR in helicopter mode has a much higher equivalent flat plate area than in airplane mode. This is mainly a consequence of the vertical orientation of the main rotor shaft, which leads to large increases in the parasitic drag of the hub, shaft and engine nacelle. The coaxial hub of the MTR in helicopter mode was modeled as being equivalent to two CH-53 hubs, for which drag data has been given by Prouty (Ref. 26). The helicopter flat plate area, f_{hel}, of 116.1ft^2 is comparable to that for a large crane helicopter design. While this value is indeed a large amount of equivalent drag, it should be notes that the MTR is not specifically designed for extended cruising flight in helicopter mode.

The values for equivalent flat plate area derived in the component drag analysis pertain only to the particular point design of a large heavy-lift MTR. To use these values in the design methodology, they must be scaled with the aircraft weight. From an examination of flat plate drag data for legacy helicopters and airplanes it can be seen that the equivalent flat plate area can be scaled with the square root of the aircraft gross weight (Ref. 27) – see Fig. 48. Thus, the flat plate area of the MTR in the design analysis was defined using

$$f_{\text{eq}} = k_{\text{eq}}\, W_{\text{TO}}^{1/2} \tag{130}$$

where the value of k_{eq} was calculated based on the values of flat plate area and the takeoff weight of the vehicle at its reference condition.

4.2 Lift-to-Drag Ratio Estimation

With a good estimate of the equivalent flat plate area of the aircraft, it is possible to directly calculate the power requirements for flight and the lift-to-drag ratio of the MTR in cruise for a given airspeed and density altitude. The power requirements for the MTR in airplane mode were estimated using the equation

$$P_{\text{req}_{\text{air}}} = \frac{1}{2}\rho\, V_{\text{air}}^3\, f_{\text{air}} + \frac{1}{2}\rho\, S_{\text{W}}\, V_{\text{air}}^3 \frac{C_L^2}{\pi\, e_{\text{W}}\, AR} \tag{131}$$

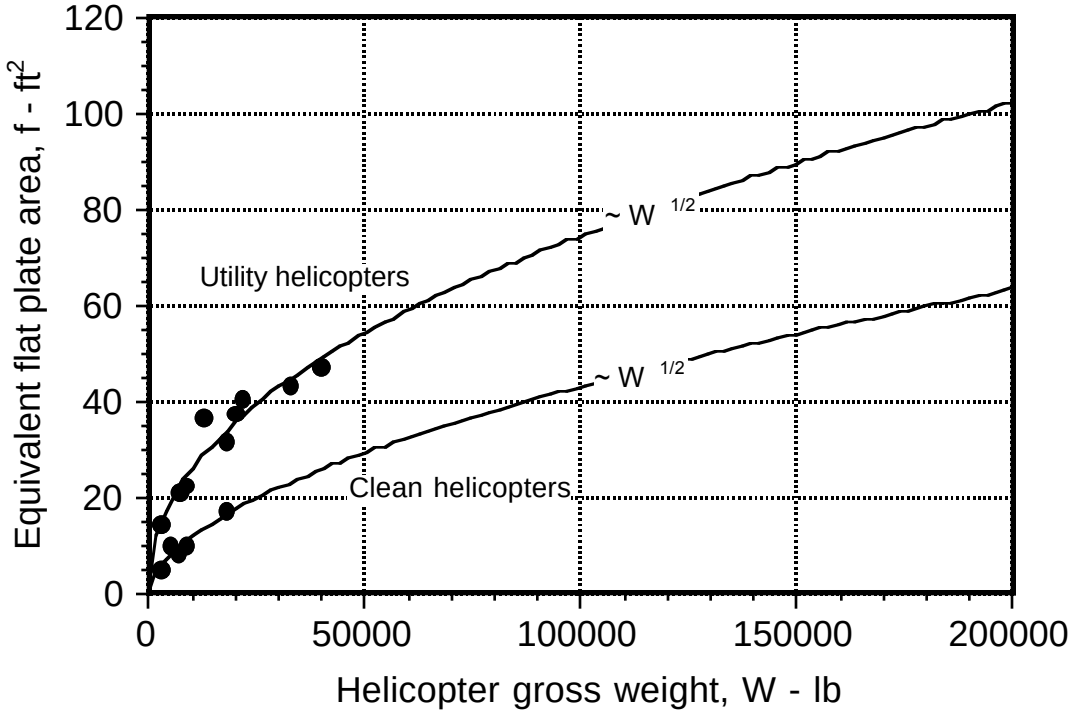

Figure 48: The equivalent flat plate area of a helicopter tends to grow with the square-root of its gross weight. "Crane" and utility helicopters tend to have a much higher drag because of their typically non-streamlined airframe shapes.

where S is the wing area, C_L is the lift coefficient of the wing and e_{W} is Oswald's span efficiency parameter for the wing. The helicopter cruise power requirements can be calculated using

$$P_{\mathrm{req_{hel}}} = \kappa \frac{W_{\mathrm{TO}}^2}{2\rho A_{\mathrm{MR}} V_{\mathrm{hel}}} + \frac{\sigma C_{d_0}}{8}(1+4.65\mu^2)\rho A_{\mathrm{MR}}(\Omega_{\mathrm{MR}} R_{\mathrm{MR}})^3 + \frac{1}{2}\rho\, V_{\mathrm{hel}}^3 f_{\mathrm{hel}} \tag{132}$$

where μ is the advance ratio of the rotor and the induced power requirements have been estimated using Glauert's high-speed approximation to the induced velocity through the rotor. The lift-to-drag ratio, L/D, was then calculated as

$$\frac{L}{D} = \frac{W_{\mathrm{TO}} V_{cr}}{P_{\mathrm{req}}} \tag{133}$$

These calculation steps were performed for the heavy-lift MTR configuration that was designed to carry 20 tons of useful payload over 1,000 nm.

The predicted lift-to-drag ratio of the MTR in both flight modes is shown in Fig. 49 versus airspeed at mean sea level conditions. Notice that in helicopter mode the MTR has a relatively low lift-to-drag ratio that is also reached at a relatively low airspeed. This is comparable to existing helicopter designs. The benefits of conversion to airplane mode can be clearly seen by the large

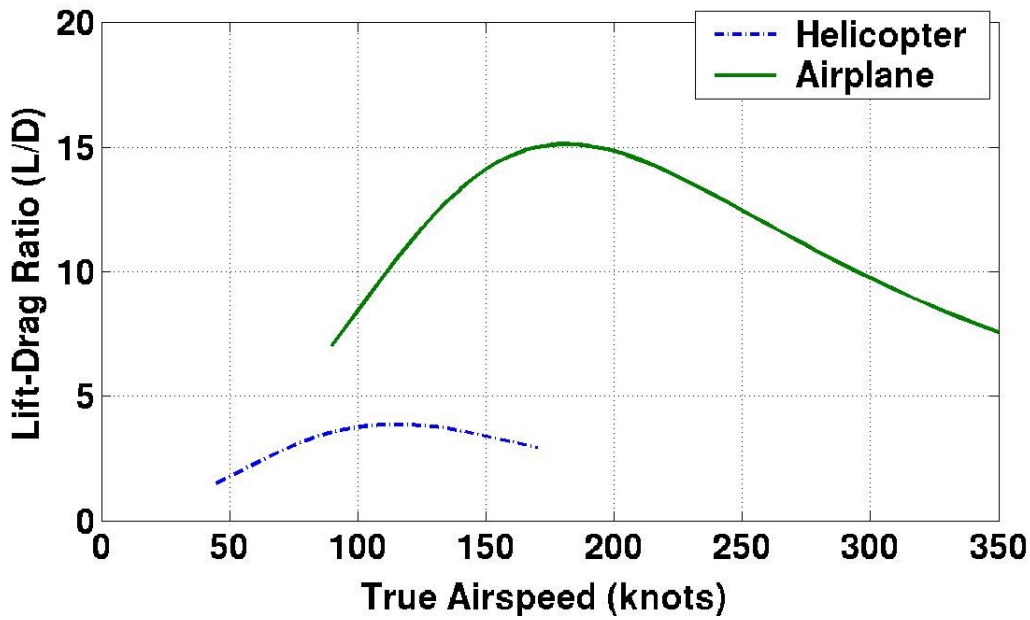

Figure 49: Lift-to-drag ratio of the MTR in both helicopter and airplane modes.

improvements in lift-to-drag ratio, which is reached at about twice the airspeed compared to helicopter mode. Figure 49 also shows that the value of lift-to-drag ratio of 10, which was assumed in the initial studies, was indeed a conservative value, with lift-to-drag ratios of 15 being predicted in airplane mode based on the component drag breakdown for the MTR.

4.3 Revised Wing Sizing Methodology

In the initial wing sizing method, which has been described in Section 2, the span of the wing was set equal to the rotor diameter. This was done to maximize the wing aspect ratio for the given design constraints of the MTR configurations. The wing area was calculated based on an assumed input value for the design cruise lift coefficient, which was initially assumed to be 0.5. The wing aspect ratio was then calculated based on these two values (wing span and design lift coefficient).

After the initial results were calculated, however, one issue encountered with this initial sizing methodology was that the resulting wing area based on a cruise lift coefficient was leading to high stall speeds for the MTR in airplane mode, with values exceeding 150 knots. A high stall speed in airplane mode is obviously undesirable as it creates the need for the MTR to achieve a higher speed in helicopter mode to make a successful conversion. The power requirements to fly a

large helicopter faster than 150 knots would be higher than that desirable from the perspective of transition from helicopter to wing-borne flight.

4.3.1 Determination of Wing Area

The original methodology was revised to determine the required wing area based on a design stall speed using the equation

$$S_{\mathrm{W_{st}}} = \frac{W_{\mathrm{TO}}}{\frac{1}{2}\rho_{\mathrm{TO}} V_{\mathrm{st}}^2 C_{\mathrm{L_{max}}}} \tag{134}$$

where $C_{\mathrm{L_{max}}}$ is the maximum lift coefficient of the wing. This value was assumed to be 2.5, a value that is consistent for a wing with a double-slotted flap, or a plain wing that operates in the energetic slipstream of a rotor. The final wing design of the MTR is expected to combine the benefits of both high-lift devices and wing boundary layer control from the rotor slipstream. The design stall speed, V_{st}, was then determined to be 120 knots at standard sea level conditions, which was considered sufficiently acceptable for such a large aircraft to allow for a safe, efficient conversion corridor.

Notice that the wing was sized for the stall speed at the takeoff density altitude. This means that there will be some design cruise altitude for which the wings (sized based on stall speed at the takeoff altitude) will not have enough area to maintain sufficient stall margins at that altitude for a given cruise speed. Because this result was found to be true for cruise altitudes within the theoretical flight envelope of the MTR, an additional wing area calculation was made that determines the size of the wing based on the need to maintain sufficient stall margins at the cruising altitude. This is given by

$$S_{\mathrm{W_{cr}}} = \frac{W_{\mathrm{TO}}}{\frac{1}{2}\rho_{\mathrm{cr}} V_{\mathrm{cr}}^2 C_{\mathrm{L_{cr}}}} \tag{135}$$

where the value $C_{\mathrm{L_{cr}}}$ is the maximum lift coefficient in cruise to maintain sufficient stall margins. This value was set to $C_{\mathrm{L_{cr}}} = 0.8$ for the present analysis. Once the values $S_{\mathrm{W_{st}}}$ and $S_{\mathrm{W_{cr}}}$ were calculated, the largest of these two values became the required wing area for the design.

4.3.2 Determination of Wing Aspect Ratio

The necessary wing areas obtained in this revised methodology, which is demanded by the need for a lower conversion speed and a high altitude in cruise, were significantly larger than those

previously predicted. Therefore, if the wing span were still limited to the rotor diameter it would lead to a significantly lower wing aspect ratio. This would degrade the cruise lift-to-drag ratio of the MTR and increase the overall fuel requirements and empty weight. While the conceptual design of the MTR originally constrained the wing span to be no larger than the rotor diameter, a wing span over 30% longer can be permitted if the wing pivot point is moved outside of the wing mounted fuel pods, as shown in Fig. 47. This higher wing span allows the MTR design to achieve the required wing area while still maintaining a high wing aspect ratio for low induced drag and efficient cruising flight, thereby reducing the required fuel weight. However, an important point that plays off against this requirement is that a higher aspect ratio wing corresponds to an overall higher wing weight. In fact, it has been found from the parametric studies conducted in the present work that there can be a unique value for wing aspect ratio for a given mission that will lead to a minimum vehicle takeoff weight.

Figure 50 shows the variation in takeoff weight with wing aspect ratio for the MTR aircraft designed for a 500 nm radius of action mission profile with a 20 ton payload being carried on both mission legs, assuming mean sea level conditions at takeoff and landing, 20 minutes of destination hover time, and high altitude cruise. It is shown in Fig. 50 that while a wing aspect ratio of nearly 10 would be feasible, the minimum takeoff weight of the MTR for this mission is achieved using a wing aspect ratio of approximately 7.5. It is also shown that there is a relatively low level of sensitivity to predicted aircraft weight with changes in wing aspect ratio. For example, a wing aspect ratio of 10 could be selected with only a 0.5 ton penalty to the gross weight of the MTR. This is because the increase in wing weight is almost entirely offset by a decrease in the fuel weight.

However, the wing span of the MTR was found to be very sensitive to changes in the wing aspect ratio. The wing span was calculated based on the required wing area and the input wing aspect ratio using the equation

$$b_{\mathrm{W}} = \sqrt{S_{\mathrm{W}}\, AR_{\mathrm{W}}} \tag{136}$$

The variation in wing span with wing aspect ratio for an MTR designed to perform the same radius of action mission is shown in Fig. 51. It is clear that for the heavy-lift mission a wing aspect ratio of 10 will lead to a wing span that is nearly 20 ft larger than a MTR with a wing aspect ratio

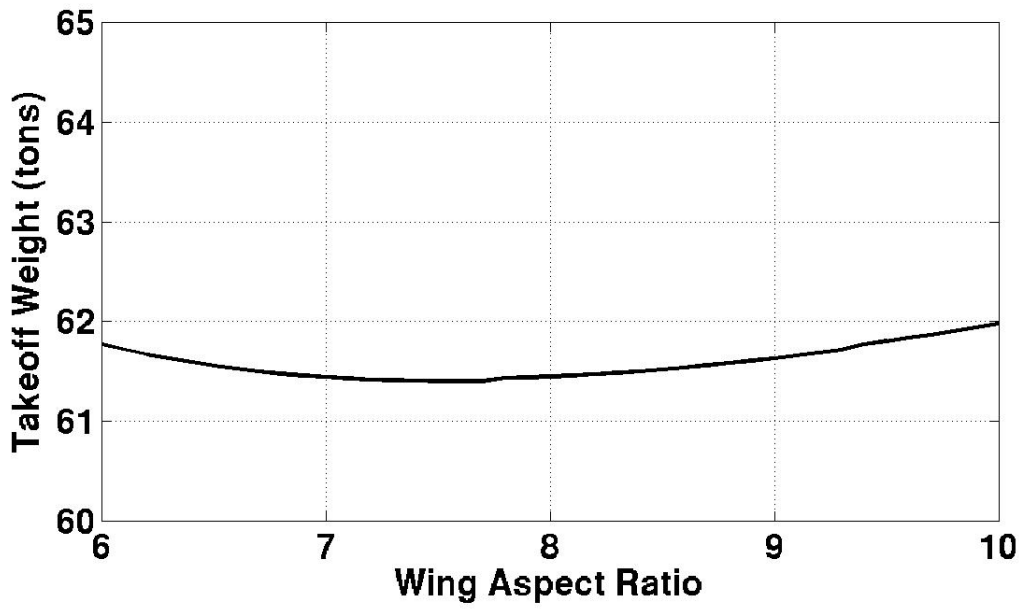

Figure 50: Variation in gross takeoff weight of the MTR with changes in wing aspect ratio.

of 7.5, the latter of which corresponds to minimum takeoff weight and rotor size. Therefore, to minimize takeoff weight, rotor size and wing span, a design wing aspect ratio of 7.5 would be a good compromise for heavy-lift, long-range missions.

5 Mission Profile Trade Studies

Several trade studies were initiated to determine the effects of changing certain mission parameters on the overall design of the MTR. The studies detailed in this report include the variation in destination hover time, takeoff density altitude, and cruise density altitude. The default mission for these studies is a 500nm radius of action goal, in which the MTR deploys and returns with a payload. In the default case, the MTR cruises at 10,000 ft at 240 knots and hovers for 20 minutes at the destination. The takeoff, landing and destination sites were all considered to be at mean sea level conditions in the default case. A constant disk loading of approximately 10.5 lb ft^{-2} was assumed for all MTR designs.

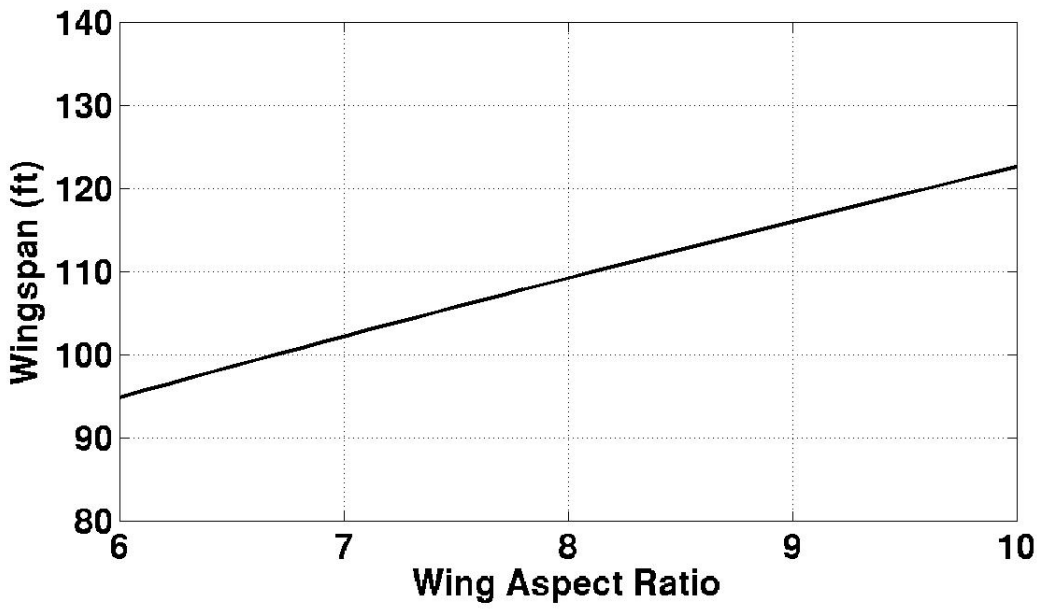

Figure 51: Variation in wing span of the MTR with changes in wing aspect ratio.

5.1 Destination Hover Time

The first study examined the effects of changes in the destination hover time on the overall design. While the MTR features rapid container deployment and acquisition capability, certain mission may require longer hover times than are necessary for a routine payload deployment. Figure 52 shows the effect of increasing the destination hover time on the takeoff weight of the MTR for various mission payloads. Increases in destination hover time tends to increase the takeoff weight of the MTR substantially for large payloads. For a 20-ton payload, the gross takeoff weight was increased from 60 to 65 tons when increasing the hover time at the destination from 20 minutes to 40 minutes. An additional 20 minutes of hover time increased the takeoff weight to over 70 tons.

Figure 53 shows the variation in MTR rotor size with payload and destination hover time. Increases in destination hover time also lead to marked growth in the main rotor. It is apparent that for a 20-ton payload, increasing the destination hover time to 60 minutes can cause about a 6 ft increase in the required rotor diameter.

These large increases in overall size are a result of the high power and fuel requirements in the hover condition for a large hovering vehicle. The effects on the fuel requirements of the MTR with variation in payload and hover time are shown in Fig. 54. It is shown that the fuel weight increases

dramatically with hover time, making this parameter the clear driver for the overall size increases. Therefore, for missions with high hover time demands it will either require a significantly larger aircraft to achieve them or a reduction in the payload and/or range capabilities for that mission.

5.2 Takeoff Density Altitude

The next study regarded the influence of the takeoff density altitude on the overall vehicle size. There are many situations in which an aircraft may be required to takeoff from density altitudes above mean sea level. If the aircraft is taking off from a higher altitude or on a hot day, the aircraft will have less power available making takeoff and hovering flight much more difficult. The effects of changes in the takeoff density altitude on the MTR gross takeoff weight and rotor size are shown in Figs. 55 and 56, respectively. It is shown that the size of the MTR required to perform the same mission while taking off at a density altitude of 6,000 ft is much larger relative to an aircraft designed to takeoff at mean sea level. For a 20 ton payload, this would require an aircraft that is over 15 tons heavier with a rotor over 10 ft larger in diameter.

The main driver for this substantial size difference in the aircraft is the increase in the engine power requirements to take off under these conditions, as shown in Fig. 57. The growth in the

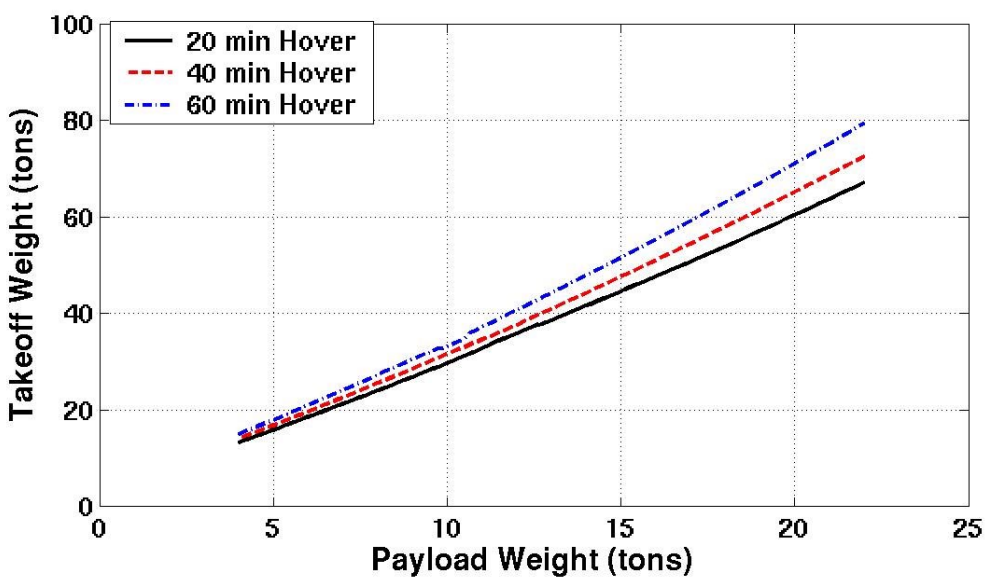

Figure 52: MTR takeoff weight versus payload and destination hover time.

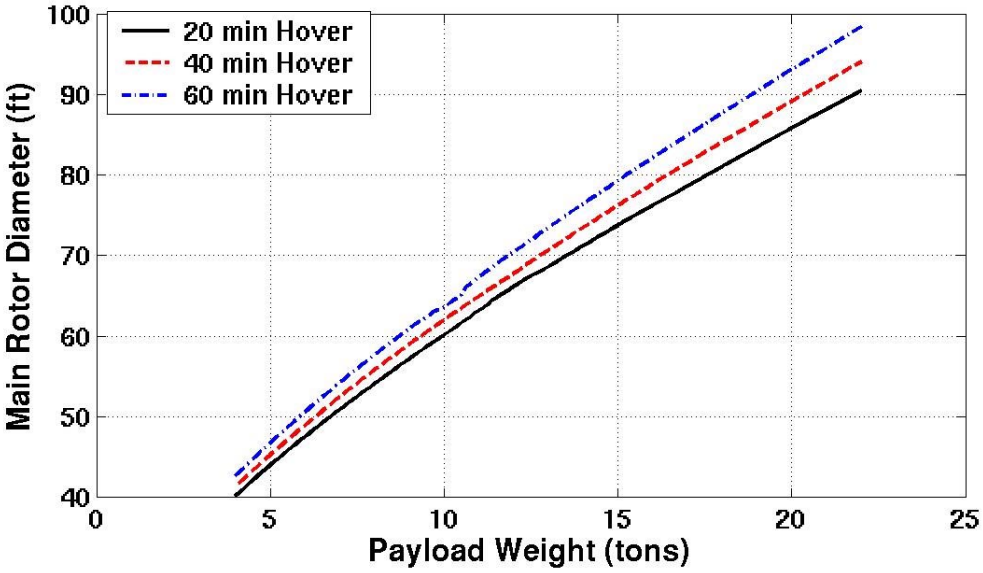

Figure 53: MTR rotor diameter versus payload and destination hover time.

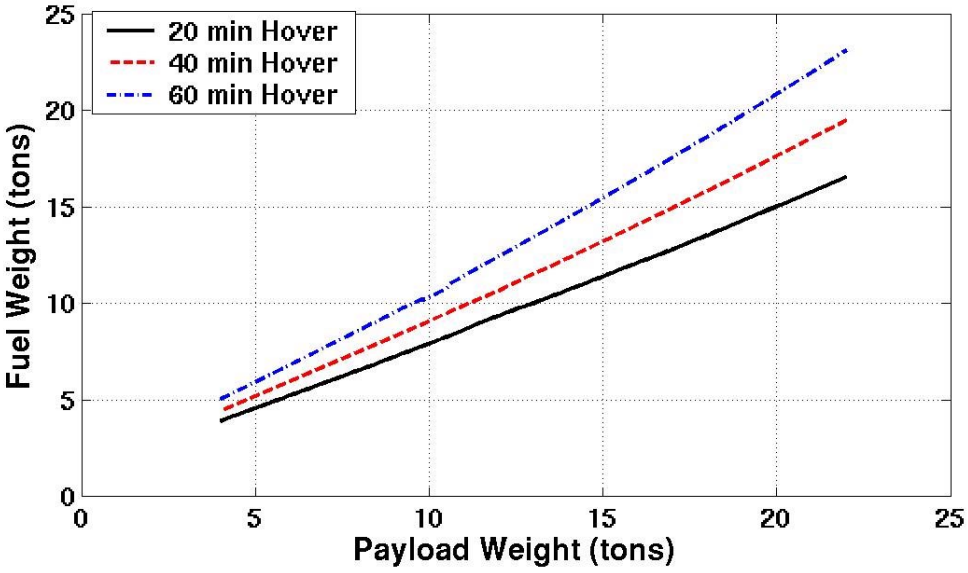

Figure 54: MTR required fuel weight versus payload and destination hover time.

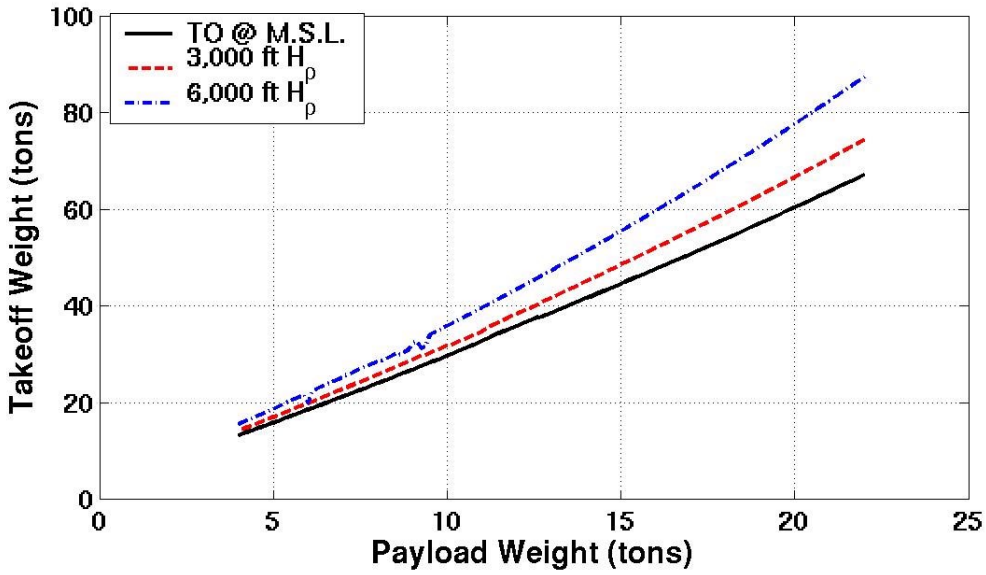

Figure 55: MTR gross takeoff weight versus payload and takeoff density altitude.

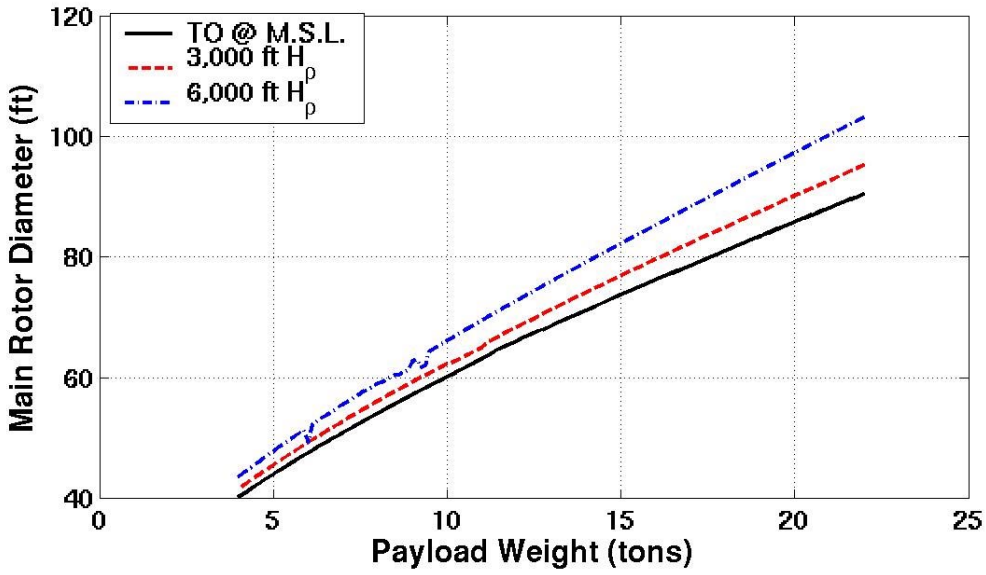

Figure 56: MTR rotor diameter versus payload and takeoff density altitude.

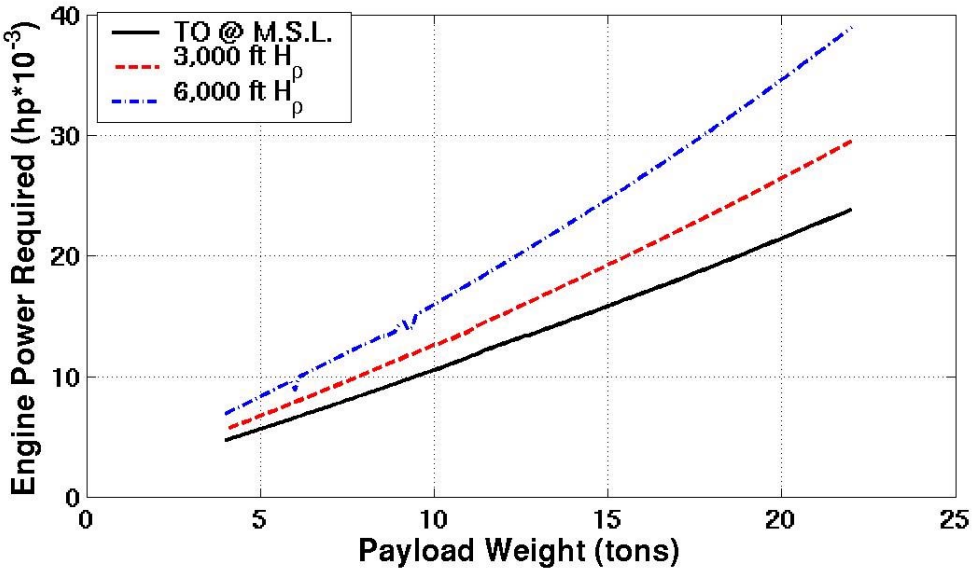

Figure 57: MTR engine power required versus payload and takeoff density altitude.

engine power requirement leads to an increased engine weight, an increase in empty weight and ultimately large increases in the overall vehicle size. The engine power requirements are seen to increase by over 50% for a takeoff at a density altitude of 6,000 feet. Clearly in such "hot and high" conditions, which are required for many types of military missions, less payload can be carried or less range can be achieved if the design is to remain fixed. This is shown in Figs. 55 – 57, where an MTR designed to carry a 20 ton payload taking off at mean sea level is approximately the same size as an MTR designed to carry a 15 ton payload taking off at 6,000 ft density altitude.

5.3 Cruise Density Altitude

Another important study performed investigated the effects of varying the design cruise altitude on the overall MTR design. There are certain benefits of cruising at higher altitudes, including reduced drag because of lower air density, which leads to a higher lift-to-drag ratio and ultimately lower fuel requirements. However, the power available decreases with increasing altitude. Lifting capability is also decreased at high altitudes because of the lower air density, which tends to increase both the required rotor and wing area. For this study, the same default mission was used except that only the heavy-lift, 20 ton payload case was examined.

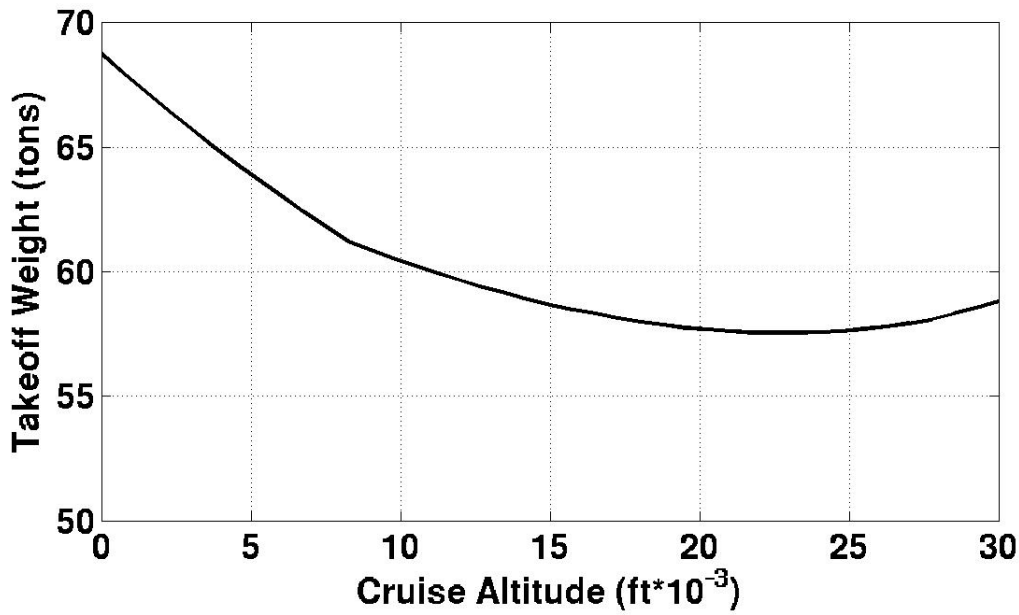

Figure 58: MTR gross takeoff weight versus design cruise density altitude.

Figures 58 and 59 show the effects of varying the design cruise altitude on the MTR gross takeoff weight and main rotor diameter, respectively. It is shown that there exists some unique cruise altitude in which both the takeoff weight and rotor size reach a minimum. For this payload requirement, this condition falls at approximately 23,000 ft density altitude. The initial decrease in size is a result of the increase in lift-to-drag ratio at the higher altitudes (which manifests as a reduction in the fuel requirements), which is shown in Fig. 60. For example, the fuel requirements for a design cruise altitude of 23,000 ft are shown to be just over 50% of the fuel requirements for design cruise at mean sea level. As shown in Figs. 58 and 59, this results in net size decreases in the MTR of 10 tons in terms of gross weight with an 8 ft increase in the main rotor diameter.

However, the required wing size tends to increase rapidly with design cruise altitude, which is shown in Fig. 61. A “shift” in the curves can be seen for Figs. 58 – 61 at around 8,000 feet. This is because of the revised wing sizing methodology. Before this shift point, the wings are being sized based on the stall condition at the takeoff density altitude (Eq. 134) and after the shift, the wings are sized based on the need to maintain sufficient stall margins in the cruise condition (Eq. 135). This is shown clearly in Fig. 61, where the required wing size actually decreases with increasing cruise altitude at low altitudes as the overall size of the aircraft decreases. Once the analysis predicts that

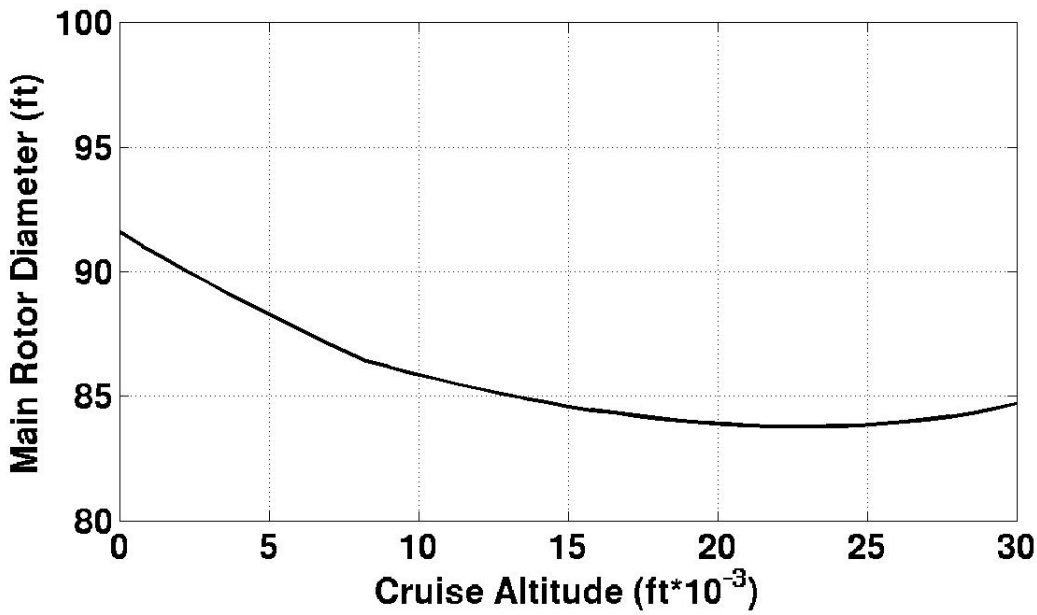

Figure 59: MTR rotor diameter versus design cruise density altitude.

larger wings are required based on the cruise condition, the shift is seen and the wing size begins to rapidly increase with altitude. Because of this rapid increase in wing size, the selection of a design cruise altitude becomes more complicated. For a good compromise between minimizing the takeoff weight, rotor size and wingspan, a design cruise altitude of 20,000 ft is recommended.

6 MTR Design Optimization & Performance

Because there has been significant work in tailoring the MTR design for heavy-lift, long-range missions it was decided to present a somewhat optimized point design specifically to meet this requirement, and to examine the overall size of the MTR and make an assessment of its performance capabilities. Elements of the preliminary MTR design have already been optimized based on the work of previous sections. A cruise altitude of 20,000 ft was selected for heavy lift missions. A wing aspect ratio of 7.5 was selected for heavy-lift, high altitude missions. Further optimization was attempted in terms of the design cruise speed and tailoring the MTR design for a modern, off-the-shelf engine package.

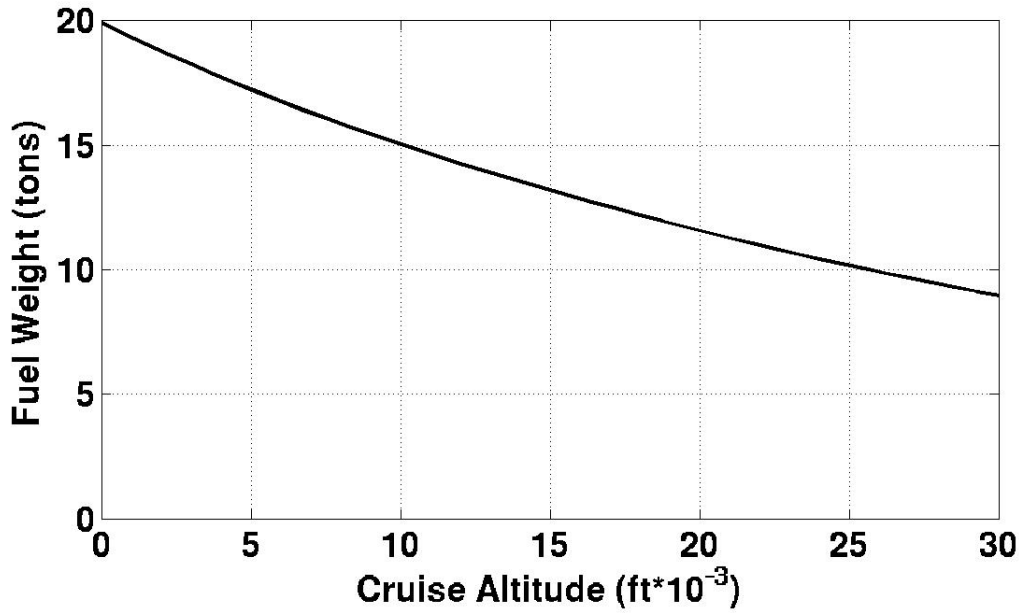

Figure 60: MTR required fuel weight versus design cruise density altitude.

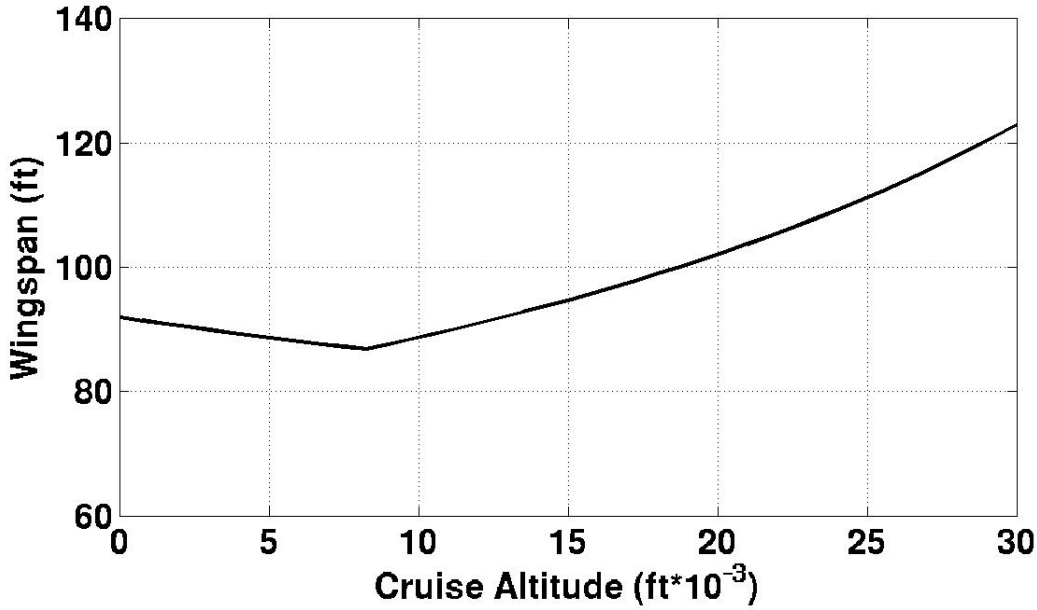

Figure 61: MTR wingspan versus design cruise density altitude.

6.1 Determination of Cruise Speed

For the previous work, the design cruise speed was estimated to be approximately 240 knots, which was a value that did not take into account optimum performance at a high design cruise altitude. Typically, the best cruise speed for a given altitude is just below the speed for maximum range, V_{mr}, which usually corresponds to the airspeed with maximum lift-to-drag ratio. The maximum range speed is an airspeed that corresponds to the maximum range potential for a given quantity of fuel. Thus, flying at this airspeed would be optimal in minimizing fuel for a long-range mission. The value of V_{mr} can be found using the power required curves versus true airspeed at altitude corresponding to the point where P/V is a minimum. This is equivalent to drawing a straight line from the origin tangent to the power curve. The point of intersection corresponds to the maximum lift-to-drag ratio and best range speed at that altitude, as shown in Fig. 62. The maximum range speed, V_{MR}, is shown to be approximately 260 knots for the MTR in airplane mode at a cruise altitude of 20,000 feet. This also corresponds to a power setting just below the maximum continuous power rating. Flying at or close to the maximum range speed will lead to significant reduction in the fuel requirements and minimize the overall size of the aircraft, as shown in the following sections.

6.2 Engine Selection

Previously, the engine sizing was based on the idea of a "rubber engine." This means that a hypothetical engine was created for each design output based on the predicted power requirements and values of power-to-weight ratio comparable to legacy turboshaft engines. For the heavy-lift, long range (20-ton, 500 nm radius of action) MTR design, the decision was made to focus the design around the already existing Allison AE 1107C engine, which is used in the V-22 Osprey. This engine is already designed for tiltrotor operation and has a superior power to weight ratio (P/W = 6.3 shp/lb) over legacy rotorcraft turboshaft engines. The engine power requirements of the heavy-lift, long-range MTR exceed 20,000 shp, requiring the use of four engines, for a total of 24,600 shp takeoff power available at mean sea level conditions.

With the design analysis updated for the selections of design cruise speed, cruise altitude, and engine weight, it was found that the power available exceeded the power required to takeoff by a

significant margin. It is important for the aircraft to be designed in such a way that it uses all of the power that is given by the engines selected. Otherwise, there are significant degradations in specific fuel consumption, which decreases with lower power settings relative to available power (see Eq. 107). Additionally, the surplus power in the design allows the opportunity to increase the disk loading of the aircraft, thereby decreasing the size of the main rotor without significant weight penalty. To take full advantage of the powerplant, the disk loading and rotor solidity of the aircraft were increased iteratively until the power required to takeoff approached the power available. This had the effect of significantly reducing the size of the main rotor. The disk loading was increased from 10.4 to 12lb/ft^2, which is still comparable to legacy heavy-lift helicopters. The main rotor solidity was increased from 0.11 to 0.13, which reduced the predicted main rotor diameter to approximately 79 feet. The resulting sizing and component weights of the MTR preliminary design are given in the following section.

6.3 MTR Point Design Summary

What follows is a summary of the preliminary result for an MTR point design to perform the long-range, heavy-lift mission. Table 3 summarizes the key design and mission inputs for this particular

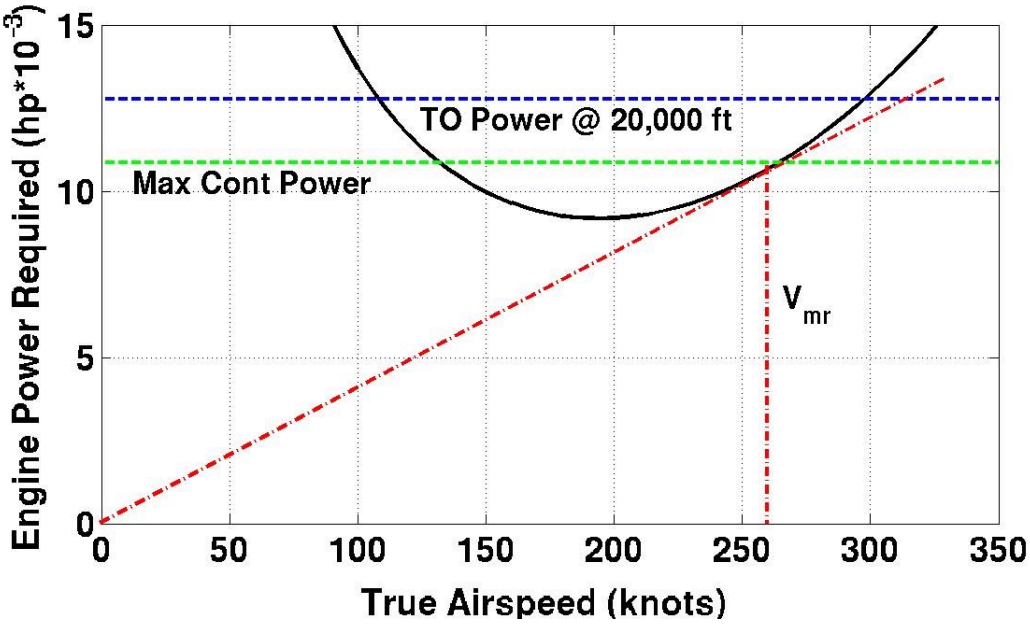

Figure 62: MTR power required versus airspeed at 20,000 feet.

Number of M/R Blades (per rotor)	6
Main Rotor Solidity	0.129
Number of Engines	4
Design Payload (tons)	20
Radius of action (nm)	500
Dest. Hover Time (min)	20
Design Cruise Speed (kts)	260
Design Cruise Altitude (ft)	20,000

Table 3: Key design inputs for heavy-lift MTR point design.

Max Takeoff Weight (lbs)	117,500
Main Rotor Diameter (ft)	78.9
Wingspan (ft)	95
TO Power at MSL (shp)	24,600
Empty Weight (lbs)	52,710
Empty Weight Fraction	0.45
Fuel Weight (lbs)	24,390
Disk Loading (psf)	12
Wing Aspect Ratio	7.5

Table 4: MTR general sizing for heavy-lift point design.

design. The MTR was designed in this case to carry a 20 ton useful payload over a 500 nm radius of action mission with 20 minutes of hover time at the destination.

The general sizing of the resulting preliminary MTR design is summarized in Table 4. It is shown that the maximum takeoff weight has been reduced to under 59 tons and the main rotor is less than 79 ft in diameter. This is a significant size reduction from previous iterations where take-off weights approaching 65 tons and rotor diameters of nearly 90 ft were common. The significant reduction in overall size can be attributed to several factors including the reduction in fuel burn due to flying at optimal cruise speed and altitude and tailoring the aircraft design around the AE 1107C engine, which has a very high power-to-weight ratio. The wingspan is slightly larger than predicted by the original methodology due to the more stringent requirements on the wing size. The empty weight fraction of 0.45 is comparable to that of a conventional crane helicopter. The higher disk loading and main rotor solidity shown may prove very beneficial in the performance of the rotor system in terms of propulsive efficiency, while the smaller rotor size should be ideal for shipboard operations.

MTR Component	Weight (lbs)
Main Rotor Blades (6x2)	5672
Main Rotor Hubs (2)	7431
Main Gear Box	8776
Swashplate	602
Control Hydraulics	188
Automatic Flight Control System	331
Engine Weight (4)	4264
Engine Installation	640
Auxilary Power Unit	162
Fuel System	976
Landing Gear	1938
Electrical System	358
Instrumentation/Avionics/Furnishings	3000
Wing	9416
Vertical Stabilizer	953
Horizontal Stabilizer	2756
Trapeze Struts	264
Cargo Handling System	2000
Tail Boom	629
Tilting Mechanism	1175
Crew Compartment (structure)	500
Tilt Boom	588
Wing Gearing	94

Table 5: MTR component weights for heavy-lift point design.

Table 5 lists the component weights predicted by the design analysis for this heavy-lift, long-range MTR point design. It is shown that the rotor system, gearbox, powerplant and fixed lifting surfaces (wing and tail) are the heaviest aircraft components, along with the cargo handling system, landing gear, tilt mechanism and furnishings also making significant contributions to the total gross weight. The blade and hub weights as designed were found to be comparable to those of the Boeing HLH helicopter, a tandem design that also features dual hubs with similarly sized rotors and gross weight. The transmission weight is also comparable to the HLH although slightly lower because of the longer transmission and secondary gearboxes needed for a tandem helicopter.

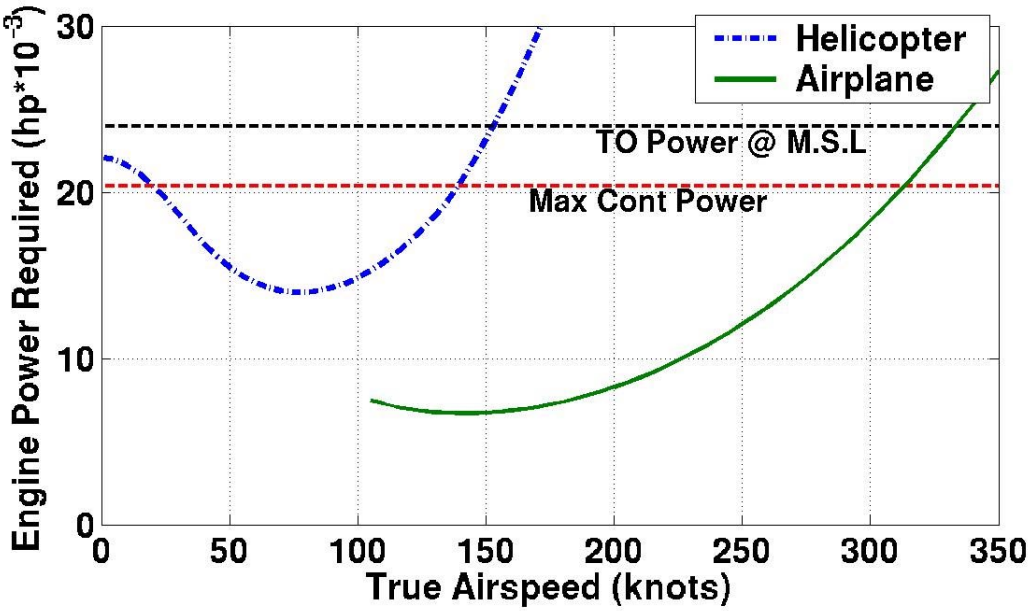

Figure 63: Engine power required versus airspeed at mean sea level conditions for both flight modes.

6.4 MTR Performance

To assess the performance of this particular MTR point design, an important first step is to generate the power required curves as a function of true airspeed. This was done using the methods described in previous sections. The power required curves for both flight modes at mean sea level conditions are shown in Fig. 63. Notice that the power required in helicopter mode reaches the power available at a much lower airspeed than when the MTR is in airplane mode. This is a reflection of the clear airspeed advantage that the airplane possesses over the conventional helicopter. At sea level, the maximum cruise speed is predicted to exceed 300 kts which is comparable to conventional tiltrotor technology. It is shown that if the power curves of the two flight modes were to be connected, there would be some conversion corridor over which the rotor tilts forward gradually from a fully vertical orientation to the axial flight orientation. The stall speed in airplane mode is shown to be nearly 107 kts for this point design which would be the minimum airspeed for the complete conversion to axial flight. The conversion could begin in helicopter mode at airspeed for minimum power, which is shown to be approximately 75 kts. The specifics of this conversion corridor will be further defined and constrained by rotor aeroelastic limitations.

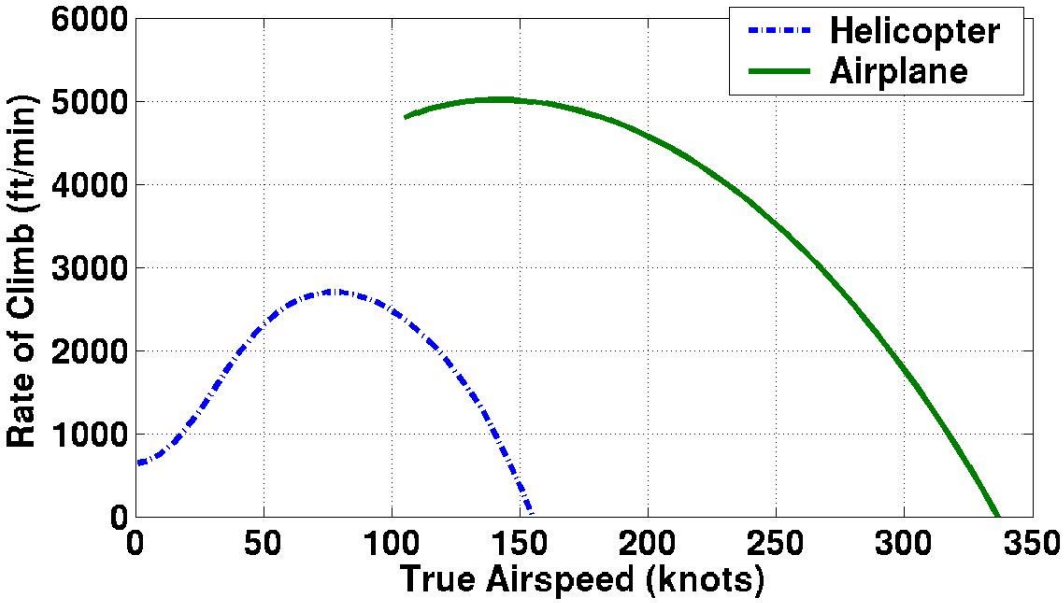

Figure 64: MTR rate of climb capability versus airspeed at mean sea level conditions for both flight modes.

An important parameter in the assessment of aircraft performance is climb capability, particularly the maximum rate of climb. The maximum rate of climb for either flight mode is characterized by the ratio of the excess power to the aircraft gross weight as given by

$$V_{C_{MAX}} = \frac{P_{Avail} - P_{Req}}{W_{TO}} \tag{137}$$

The rate of climb capability versus airspeed is shown in Fig. 64 for both flight modes at mean sea level conditions. Clearly, the rate of climb capability for the MTR in airplane mode far exceeds that of the MTR in helicopter mode, which is a result of the much lower power requirements in airplane cruise for the same available power. The maximum rate of climb of the MTR in helicopter mode is comparable to that of a CH-53 Stallion. The maximum rate of climb of the MTR in airplane mode is high compared to conventional transport airplanes because of the abundance of available power.

The effect of altitude on the maximum rate of climb in airplane mode is shown in Fig. 65. The maximum rate of climb is calculated based on the cruise speed for minimum power, which varies with airspeed. At standard sea level conditions, the true airspeed for minimum power is shown to be approximately 140 kts (see Fig. 63), while at the design cruise altitude of 20,000 feet it is

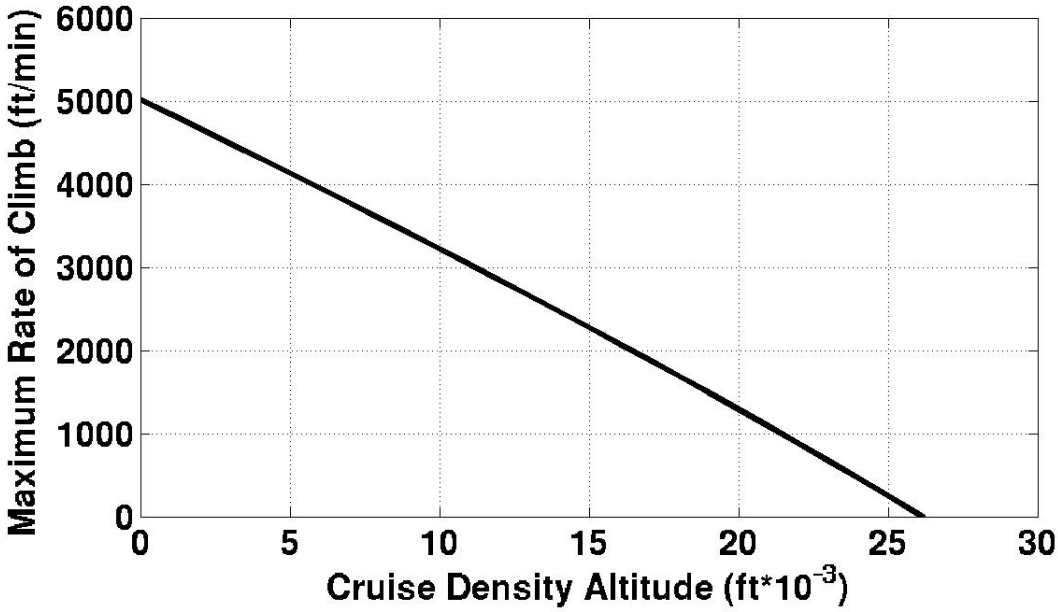

Figure 65: Maximum rate of climb versus altitude for the MTR in airplane mode.

shown to be approximately 190 kts (see Fig. 62). The altitude at which the maximum rate of climb is equal to zero is known as the absolute ceiling. Based on the results in Fig. 65, the absolute ceiling for the MTR point design is approximately 26,000 feet. The service ceiling is defined as the altitude at which the maximum rate of climb is 100 feet/min, which occurs for this point design at over 25,000 feet.

7 Conclusions

The Mono Tilt-rotor (MTR) has been proposed as a vertical-lift aircraft architecture to meet a heavy-lift mission goal of 20 tons of useful payload carried over a range of 1,000 nm. The MTR architecture integrates a coaxial rotor, a folding lifting wing system and an efficient cargo handling system. This paper has reported on a conceptual design study of the MTR architecture that has been conducted to predict its size and weight and to objectively examine its potential performance. Comparative studies of the MTR against legacy helicopter designs show the substantial benefits of the MTR if it were to be technically realized. While it must be recognized that there are many design challenges and potentially several new technology developments that would be necessary to bring the MTR concept to fruition, this conceptual design study assumes that such developments can, in fact, be ultimately realized.

This conceptual analysis of the MTR architecture leads into a more detailed preliminary design phase. To this end, there are still several matters to address in regard to acceptably representative MTR specific performance parameter inputs to the design algorithms. For example, rotor/propeller efficiencies were all estimated based on more detailed analyses not reported here, or were based on nominal data for existing tiltrotor concepts. These values need further study as they apply specifically to the MTR if confidence levels in the MTR as a viable aircraft architecture are to be improved. In addition, the component weights for the tilt boom and additional weight for the tilt actuation system has not yet been determined to acceptable levels of approximation, and this must be rectified before predictive confidence levels can be improved further in a preliminary design phase.

The following specific conclusions have been drawn from this conceptual design study:

1. The design analysis developed in this work was validated against historical sizing and weight data for legacy helicopters, including both single rotor conventional and coaxial dual rotor designs. Overall, the design predictions have shown satisfactory levels of correlation when compared to historical data, both for heavy-lift vehicles and otherwise.

2. The coaxial rotor and the relatively lightweight overall design of the MTR allow a much smaller vehicle with better weight efficiency than a conventional helicopter for any size of

payload. This allows the MTR to carry less fuel and more useful payload over a longer flight range. Overall, the results suggest that if the MTR concept were in fact to be technically realized then it could be up to 50% smaller and up to 65% lighter than a conventional helicopter when carrying the same useful payload over the same distance.

3. The proposed ability to morph the MTR architecture to fixed wing borne flight allows the vehicle to cruise at a substantially better lift-to-drag ratio and cruise speed than could be achieved with a conventional helicopter. This is the key to reducing overall vehicle weight, substantially improving its range, reducing fuel burn and improving overall operational economics.

4. A parametric design sensitivity study was used to address uncertainties in performance estimation and also to show that even with reduced performance, sufficiently attractive payload/range design goals can still be reached with the MTR architecture compared to other vertical lift aircraft designs.

5. It was found that for significant increases in mission parameters such as hover time or takeoff density altitude, the necessary result is either a marked increase in the overall aircraft size or a noteable degradation in the payload or range capabilities of the mission.

6. Optimizing the mission design for the best cruise speed and altitude lead to significant reduction in the required fuel, driving down operating costs as well as the overall size and weight of the aircraft.

7. Tailoring the design of the MTR for the use of modern, off-the-shelf tiltrotor engine systems leads to significant reductions in the overall size. The size of the main rotor is particularly reduced, which would likely improve the propulsive efficiency in airplane mode and enhance the ship basing capability of the aircraft.

8. While this conceptual analysis of the proposed MTR architecture to meet a 20 ton useful payload and 1,000 nm unrefueled range yields an aircraft that is very large and requires a great amount of fuel, the value of having a large transport aircraft with both efficient vertical lift and long-range flight capability may very well outweigh such concerns.

8 Acknowledgements

This work has been supported by the Office of Naval Research (ONR) for the Expeditionary Logistics (ExLog) Future Naval Capability (FNC) Integrated Product Team (IPT). The authors are grateful to many professional colleagues for their advice throughout the course of the study.

References

[1]Gillmore, K. B., Schneider, J. J., "Design Considerations of the Heavy Lift Helicopter," *Journal of the American Helicopter Society*, Vol. 8, No. 1, 1963, pp. 31–37.

[2]Wax, C. M. and Torci, R. C., "Study of the Heavy-Lift Helicopter Rotor Configuration," USAAVLABS Technical Report 66-61, Nov. 1966.

[3]Schneider, J. J., "The Influence of Propulsion Systems on Extremely Large Helicopter Design," Paper No. 334, Proceedings of the 25th Annual National Forum of the American Helicopter Society, Washington DC, May 16—18, 1969. See also the *Journal of the American Helicopter Society*, Vol. 15, No. 1, Jan. 1970.

[4]Schneider, J. J., "The Developing Technology and Economics of Large Helicopters," Paper No. 3, Proceedings of the Sixth European Rotorcraft and Powered Lift Aircraft Forum, Bristol, England, Sept. 16–18, 1980.

[5]Schrage, D.P., Costello, M. F., Mittlevden, D. N., "Design Concepts for an Advanced Cargo Rotorcraft," Paper AIAA-88-4496, Proceedings of the AIAA/AHS/ASEE Aircraft Design, Systems and Operations Meeting, Atlanta, Georgia, Sept. 1988.

[6]Christensen, C. M., "The Innovator's Dilemma," Harvard Business School Press, 1997.

[7]Baldwin, G. D., "Rapid Vertical Deployment Systems," Baldwin Technology Company, LLC. Available from: http://www.baldwintechnology.com. Sept. 2003.

[8]Baldwin, G. D., "Logical Development of the Scalable MTR Aircraft Architecture," Baldwin Technology Company, LLC. Available from: http://www.baldwintechnology.com. Oct. 2003.

[9]Tishchenko, M. N., "Simplified Performance Determination Method – Helicopter Design Lecture Notes," University of Maryland, College Park, 1998.

[10]Tishchenko, M. N., "Helicopter Parameters Optimization at Preliminary Designing – Helicopter Design Lecture Notes," University of Maryland, College Park, 2002.

[11]Tishchenko, M. N., Nagaraj, V. T., and Chopra, I., "Preliminary Design of Transport Helicopters," *Journal of the American Helicopter Society*, Vol. 48, No. 2, April 2003, pp. 71–79.

[12]"Chesapeake Civil Transport Rotorcraft," AHS Student Design Competition Report, University of Maryland, College Park, May 1998. Available on-line from: http://www.enae.umd.edu/AGRC/Design98/chesapeake.html

[13]"CalVert High-Speed Personal V/STOL Personal Transport," AHS Student Design Competition Report, University of Maryland, College Park, June 1999. Available on-line from: http://www.enae.umd.edu/AGRC/Design99/Calvert.html.

[14]"The Martian Autonomous Rotary-Wing Vehicle (MARV)," AHS Student Design Competition Report, University of Maryland, College Park, June 2000. Available on-line from: http://www.enae.umd.edu/AGRC/Design00/MARV.html.

[15]"Raven SAR Rotorcraft Advanced Rotor Control Concept," AHS Student Design Competition Report, University of Maryland, College Park, June 2001. Available on-line from: http://www.enae.umd.edu/AHS/Raven_Design_Proposal.pdf.

[16]"406-UM TerpRanger Light Helicopter Upgrade Program," AHS Student Design Competition Report, University of Maryland, College Park, June 2002. Available on-line from: http://www.glue.umd.edu/ shreyas/ahsdesign2003/TerpRanger.pdf.

[17]"UM-911 Aeneas - The Urban Disaster Response System," AHS Student Design Competition Report, University of Maryland, College Park, June 2003. Available on-line from: http://www.glue.umd.edu/ shreyas/ahsdesign2003/Aeneas.pdf.

[18]Dingeldein, R. C. 1954. "Wind Tunnel Studies of the Performance of a Multirotor Configurations," NACA Technical Note 3236.

[19]Kroo, I. *Aircraft Design: Synthesis and Analysis*, http://adg.stanford.edu/aa241/AircraftDesign.html

[20]Raymer, D. P., and Przemieniecki, J. S., *Aircraft Design: A Conceptual Approach*, AIAA Education Series, 3rd edition, 1999.

[21]Boeing Vertol Company, "Heavy Lift Helicopter – Prototype Technical Summary," USAAVRADCOM-TR-80-D-11, April 1980.

[22]Mack, J. C., "Large Rotorcraft Transmission Technology Development Program," NASA-CR-168120, 1983.

[23]Fries, G. H. and Schneider, J. J., "HLH and Beyond," SAE Paper No. 791086, Presented at the SAE Aerospace Meeting, Los Angeles, CA, Dec. 1979.

[24]Farrell, M. K., "Aerodynamic Design of the V-22 Proprotor," Proceedings of the 45th Annual Forum of the American Helicopter Society, Boston, MA, May 22–24, 1989.

[25]Hoerner, *Fluid Dynamic Drag*, Hoerner Fluid Dynamics" in Vancouver, WA, 1965.

[26]Prouty, R., *Helicopter Performance, Stability and Control*, PWS Engineering Publishing, Boston, MA, 1986.

[27]Leishman, J. G, *Principles of Helicopter Aerodynamics*, Cambridge University Press, New Yok, NY, 2000.

Appendix 1: Correlation Coefficients for Performance Equations (Imperial units)

AR_{HT}	4	
AR_{VT}	1.7	
C_{e_1}	0.198	lb/hp/hr
C_{e_2}	0.22	lb/hp/hr
C_{HT}	1	
C_{pow}	1.1	
C_{VT}	0.09	
$C_{L_{\mathrm{des}}}$	0.5	
$C_{\mathrm{SH_G}}$	1.1	
$(C_T/\sigma)_{\mathrm{MR}}$	0.075	
$(C_T/\sigma)_{\mathrm{MR}}$	0.075	
$(C_T/\sigma)_{\mathrm{TR}}$	0.08	
e_W	0.9	
f_{SH}	1.80	
FM_{MR}	0.72	
FM_{TR}	0.67	
g	32	ft/s^2
(L/D)	4.60	
$(L/D)_{\mathrm{coax}}$	4.20	
$(L/D)_{\mathrm{air}}$	10	
n_{MTR}	5	
n_{SH}	4000	rpm
N_{ult}	6	
P_{DC}	150	hp
t_{RES}	0.33	hr
t_{HOV}	0	hr
t_{MR}	1.02	
t_{TR}	1.06	
$(t/c)_{\mathrm{W}}$	0.12	
$(t/c)_{\mathrm{HT}}$	0.12	
$(t/c)_{\mathrm{VT}}$	0.12	
$V_{\mathrm{CR_{hel}}}$	124	kts
$V_{\mathrm{CR_{air}}}$	240	kts

N_{ENG}	2	
η_{PR}	0.98	
η_{coax}	0.85	
η_{prop}	0.70	
Λ_W	10	deg
Λ_{HT}	0	deg
Λ_{VT}	0	deg
ρ_0	.002377	slugs/ft^3
ρ_{HOGE}	.002377	slugs/ft^3
ρ_{CR}	.002377	slugs/ft^3
$(\Omega R)_{MR}$	722	ft/s
$(\Omega R)_{TR}$	722	ft/s
ζ_{CR}	0.88	
ζ_{MGB}	0.96	
ζ_{MR}	0.94	
ζ_{TR}	0.975	
ζ_{air}	0.92	

Appendix 2: Correlation Coefficients for Weight Equations (Imperial Units)

$k_{MR_{BL}}$	0.94
$k_{TR_{BL}}$	1.25
$k_{1_{APU}}$	0.013
$k_{2_{APU}}$	88.2
$k_{1_{BCS}}$	1.56
$k_{2_{BCS}}$	66.2
$k_{1_{ENG}}$	0.22
$k_{2_{ENG}}$	176.4
$k_{1_{FUS}}$	0.095
$k_{2_{FUS}}$	0.09
$k_{3_{FUS}}$	0.013
$k_{1_{SP}}$	2.87
$k_{2_{SP}}$	119
k_{ES}	0.026

k_{EMP}	2.46
k_{FS}	0.04
k_{IGB}	0.272
k_{LG}	0.025
$k_{\mathrm{MR_{BL}}}$	10.5
$k_{\mathrm{MR_{GB}}}$	0.172
$k_{\mathrm{MR_{HUB}}}$	16.6
k_{CHS}	0.05
k_{PIS}	0.15
k_{SH}	0.0069
k_{GHE}	0.05
k_{SS}	104
$k_{1_{\mathrm{SS}}}$	240646
$k_{2_{\mathrm{SS}}}$	2494.4
k_{TB}	0.005
k_{TM}	0.01
$k_{\mathrm{TR_{BL}}}$	14.0
$k_{\mathrm{TR_{GB}}}$	0.226
$k_{\mathrm{TR_{HUB}}}$	8.27
k_{WTM}	0.01
W_{CREW}	440
W_{MEP}	0